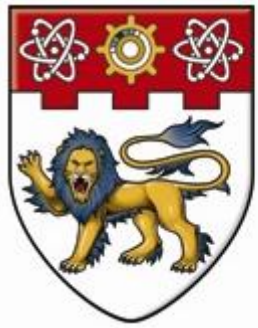

NANYANG TECHNOLOGICAL UNIVERSITY

DESIGN OF IONIC LIQUID INVOLVED HETEROGENEOUS CATALYTIC SYSTEM FOR EFFECTIVE OXIDATIVE TRANSFORMATION

LINLU BAI

SCHOOL OF CHEMICAL AND BIOMEDICAL ENGINEERING

2014

DESIGN OF IONIC LIQUID INVOLVED HETEROGENEOUS CATALYTIC SYSTEM FOR EFFECTIVE OXIDATIVE TRANSFORMATION

LINLU BAI

2014

DESIGN OF IONIC LIQUID INVOLVED HETEROGENEOUS CATALYTIC SYSTEM FOR EFFECTIVE OXIDATIVE TRANSFORMATION

LINLU BAI

SCHOOL OF CHEMICAL AND BIOMEDICAL ENGINEERING

A thesis submitted to the Nanyang Technological University
in partial fulfillment of the requirement for the degree of
Doctor of Philosophy

2014

Abstract

Ionic liquids (ILs), defined as low-melting salts showed great potential in improving the efficiency of catalytic processes due to their unique physicochemical properties. The primary reasons of employing ILs in catalytic processes originated from the facts that ILs have extremely low vapor pressure as well as excellent dissolving capacity, which afforded them promising candidates of green reaction media. ILs have been successfully integrated with an variety of advanced catalytic technologies except for being reaction solvent. Concerning the atom economy and environmental demand, heterogeneous catalysis was preferred as a greener alternative to replace the conventional stoichiometric procedures. Therefore, in this Ph. D. work, taking both the advantages of IL and heterogeneous catalysis, we intended to develop effective and recyclable IL-involved heterogeneous catalytic processes for the oxidative transformation with particular highlights on the specific effects of the involved IL during the reaction process.

Based on the study of the solvent-free aerobic alcohol oxidation over a carbon nanotube supported palladium catalyst, IL 1-ethyl-3-methylimidazolium bis (trifluoromethylsulfonyl) imide ([emim][NTf_2]) was introduced in the reaction mixture as solvent/additive and dramatically improved the catalytic performances. The enhanced catalytic activity was attributed to the stabilization

effect of ILs on the active sites-Pd nanoparticles as well as IL's intrinsic physical-chemical properties, e.g., electronegativity.

In a parallel work, [emim][NTf_2] was applied as a reaction solvent in the alkene epoxidation over vanadium-exchanged faujasite zeolite catalysts (V-X), using *tert*-butyl hydroperoxide (TBHP) as the oxidant. Compared with the conventional organic solvent such as DMF, [emim][NTf_2] significantly improved the catalytic activity, which was elucidated by examining the interaction between IL and the components in the reaction, specifically the hydrogen bonding interaction between IL and *t*-butabol which is one of the by-products.

As indicated above, the combination of heterogeneous catalyst and IL as a reaction solvent has made remarkable progress, while the consumption of a large amount of IL as a solvent is bound to high cost of the process. Therefore from the economic point of view, the strategy of reducing the amounts of IL meanwhile maintaining its unique properties to obtain effective heterogeneous catalysis was urged to be developed. Recent works have shown several strategies to synthesize the heterogeneous catalyst with IL directly integrated, among which the strategy of synthesizing IL-based polyoxometalate (IL-POM) composites by ion exchange method was studied in our work.

A series of IL-POM catalytic materials were successfully synthesized and

found to be able to effectively transform the cellobiose into levulinic acid (LA) and formic acid (FA) in one pot with high selectivities in the presence of oxygen. The IL cation introduced in the hybrid material on one hand acted as the strong Brønsted acidic sites, responsible for their catalytic activity in the hydrolytic degradation of cellobiose. On the other hand afforded the IL-POM catalyst high melting point as well as low solubility in water, which can recrystallize into solid for the ease of recycling catalyst for more runs.

Acknowledgements

Looking back at the four years bearing my youth spent in Singapore, I'm grateful to have encountered the experience and people here. Coinciding the complement of my PhD study, I want to express my heartfelt gratitude to the following people.

Firstly I'm honored to be under the guidance of Professor Yang Yanhui and Professor Lee Jongmin. The opportunity is valuable to come by that to do the research of interdiscipline with two mentors in distinct fields. Thanks for your abortive cultivation both in research and life!

Following I want to show my thank to senior Dr. Hu Shuangquan, Dr. Chen Yuanting, Dr. Xuetong and Dr. Guo Zhen, who lead me to start the research work by teaching me each detailed skill. They affected me by words and deeds. With their help, I successfully finished my first journal article and passed my qualifying examination in my 2nd year.

I'm grateful to the members of Yang's lab and Lee's lab who once helped and encouraged me. They are Dr. Li Kaixin, Dr. Zhou Chunmei, Dr. Chen Zhengjian, Professor Tang Qinghu, Dr. Yan Wenjin, Dr. Wang Ke, Dr. Piyarat Weerachanchai, Dr. Chen Hong, Dr. Lin Haiqiang, Dr. Dai Yihu, Mr. Dam Duc Tai, Ms. Yan Yibo, Mr. Zheng Jianwei, Mr. Yuan Xiang, Mr Yang Zhihong, Mr. Zhao Jun, and Mr Yan Yong.

Moreover, I would like to thank Professor Liu Haichao of Peking University and all the members in Liu's lab, who widen my horizon in research during my exchange for half a year's time in Beijing.

I'm thankful to my peers Dr. Wei Li, Ms. Yan Ya, Mr. Jiang Wenchao and Ms. Zhang Qian etc, who grow and accompany with me.

I also would like to thank School of Chemical and Biomedical Engineering, Nanyang Technological University for the scholarship support.

Finally I want to thank my family and important persons for backing me up to pull through all the challenging times and grow mature!

Table of Contents

Abstract VI

Acknowledgements VI

Table of Contents VI

List of Figures VI

List of Tables VI

List of Schemes VII

Chapter 1 Background and Philosophy 1

1.1 Background and the driving force for applying ionic liquid in heterogeneous selective oxidation 1

1.2 Motivation and outline of this dissertation 2

References 6

Chapter 2 Literature Review 9

2.1 Ionic Liquid 9

2.2 The physical and chemical properties 12

2.2.1 Vapor pressure 12

2.2.2 Melting point 13

2.2.3 Thermal stability 13

2.2.4 Density 14

2.2.5 Viscosity 14

2.2.6 Polarity and Solubility 15

2.2.7 Acidity, basicity and coordination ability 19

2.3 Ionic liquid in catalysis 20

2.3.1 Ionic liquid as solvent 21

2.3.2 Ionic liquid-based hybrid material 25

2.3.2.1 IL modified polyoxometalate 25

2.3.2.2 Supported IL phase catalysis (SILPC) material 27

2.3.2.3 Solid catalysis with ILs (SCIL) material 29

2.3.2.4 Ionogel 30

Reference 33

Chapter 3 Techniques of Characterization, Synthesis, and Catalytic oxidation 41

3.1 Characterization techniques 41

3.1.1 Characterization of catalyst morphologies and structures 41

3.1.2 Characterization of catalyst active sites 44

3.2 Synthesis methodologies 47

3.2.1 Materials 48

3.2.2 Synthesis of V/X 48

3.2.3 Synthesis of Pd/CNT 49

3.2.4 Synthesis of the polyoxometalates (POMs) 49

3.2.5 Synthesis of IL modified POM (IL-POM) 50

3.3 Catalyst evaluation 51

3.3.1 Solvent-free aerobic oxidation of benzyl alcohol 51

3.3.2 Epoxidation of *cis*-cyclooctene with *tert*-butyl hydroperoxide (TBHP) as oxidant 53

3.3.3 One-pot transformation of cellobiose into formic acid and levulinic acid 54

Reference 56

Chapter 4 Palladium-catalyzed aerobic oxidation of 1-phenylethanol with an ionic liquid additive 58

4.1 Catalytic performance of the heterogeneous catalytic system for the aerobic oxidation of 1-phenylethanol with ionic liquid as additive 60

4.2 Intrinsic activity examination of the heterogeneous catalytic system for the aerobic oxidation of 1-phenylethanol with ionic liquid as additive 64

4.3 Recycle of the heterogeneous catalytic system (both Pd catalyst and ionic liquid) 67

4.4 The effect of temperature 68

4.5 The effect of oxygen pressure 69

4.6 The improved catalytic activity due to the nature of ILs 71

4.7 The effect of IL on the Pd/CNT catalyst 72

4.8 Catalytic performance of the heterogeneous catalytic system with [emim][NTf_2] as co-solvent on various alcohols 76

4.9 Comparison of the catalytic performance with the present heterogeneous Pd catalyzed aerobic oxidation of 1-phenylethanol 76

4.10 Conclusion 77

Reference 79

Chapter 5 Catalytic epoxidation of *cis*-cyclooctene over vanadium-exchanged faujasite zeolite catalyst with ionic liquid as co-solvent..... 82

5.1 The catalytic performance of the heterogeneous catalytic system with ionic liquid [emim][NTf_2] involved as co-solvent for the epoxidation of *cis*-cyclooctene 84

5.2 Examination of reaction parameters for *cis*-cyclooctene epoxidation in DMF-[emim][NTf_2] 87

5.3 Recycle of the heterogeneous catalytic system with ionic liquid [emim][NTf_2] as co-solvent 90

5.4 Characterizations of the spent V-X catalyst after reaction..... 91

5.5 Discussion 95

5.6 Catalytic performance of the heterogeneous catalytic system with [emim][NTf_2] as co-solvent on various alkenes 101

5.7 Conclusion 103

Reference 104

Chapter 6 One-pot production of bio-derived chemicals from renewable resources: Transformation of cellobiose into formic acid and levulinic acid over ionic liquid-based polyoxometalate composites 107

6.1 Structure characterization of as-synthesized IL-POM catalysts 111

6.2 One-pot transformation of cellobiose over different IL-POM catalysts 116

6.3 Recovery and reusability of IL-POM catalysts 122

6.4 Exploration of catalytic reaction mechanism 124

6.5 Conclusion 130

Reference 132

Chapter 7 Conclusions and Future Perspectives 136

7.1 Conclusions 136

7.2 Future perspectives 138

Reference 141

Appendix 142

A1 $Co_6(\mu 3\text{-}OH)_6$ cluster based coordination polymer as an effective heterogeneous catalyst for aerobic epoxidation of alkenes 142

A1.1 Experimental 143

A1.1.1 Materials 143

A1.1.2 Synthesis of compound $Co(\mu_3\text{-}OH)(HCOO)_{0.72}(CH3COO)_{0.28}$ (Co_6-CP) 143

A1.1.3 Characterization 144

A1.1.4 Catalytic reaction 145

A1.1.5 Recycle of catalyst 146

A1.2 Results and discussion 146

A1.2.1 Characterization of Co_6-CP 146

A1.2.2 Aeroataic epoxidation activity of Co_6-CP 149

A1.2.3 Examination of reaction parameters 152

A1.2.4 Recyclability and stability of Co_6-CP 156

A1.3 Disscussion 159

A1.4 Conclusion 162

Reference 164

A2 Journal publications and conference presentations 170

Journal publications 170

Conference presentations 172

List of Figures

Fig.4.1 Time-conversion plots of for the aerobic oxidation of 1-phenylethanol. Run conditions: see footnote of Table 4.1.

Fig.4.2 Time course of 1-phenylethanol oxidation in different media. The conversion was connected by the trend line fitted based on the 1st-order kinetic model.

Fig.4.3 Recyclability of Pd/CNT. Run conditions: see footnote of Table 4.1.

Fig.4.4 The effect of temperature. Run conditions: see footnote of Table 4.1.

Fig.4.5 The effect of oxidaiton pressure. Run conditions: see footnote of Table 4.1.

Fig.4.6 XPS spectra: (a) fresh Pd/CNT; (b) Pd/CNT used under solvent-free conditions; (c) Pd/CNT used in [emim][NTf_2]; (d) Pd/CNT used in [bmim]Br ((a)–(d): Pd 3d region); (e) Pd/ CNT used in [emim] [NTf_2] (F 1s region); (f) Pd/CNT us ed in [bmim]Br (Br 3d region).

Fig. 4.7 TEM micrographs and size distribut ions: (a) fresh Pd/CNT; (b) Pd/CNT used under solvent-free condition; (c) Pd/CNT used in [emim][NTf_2]; (d) Pd/CNT used in [bmim]Br.

Fig. 4.8 Raman spectra of fresh and used Pd/CNT catalysts.

Fig.5.1. Kinetic profiles of cis-cyclooctene epoxidation at different reaction time. (a) conversion, (b) selectivity towards epoxide.

Fig.5.2. Kinetic profiles of *cis*-cyclooctene epoxidation at different reaction temperature. (a) conversion, (b) selectivity towards epoxide, reaction condition: see the footnote of Table 1.

Fig.5.3. The recycle of the V-X catalyst in the mixed solvent of DMF and [emim][NTf_2] (the molar ratio of DMF and [emim][NTf_2] is 2:3).

Fig.5.4. XRD patterns of the fresh and spent V-X catalyst after reaction in different solvents.

Fig.5.5. SEM of the V-X catalyst after reaction in different solvents. (a) NaX, (b) V-X, (c) s/V-X/DMF (short for the spent V-X in DMF,), (d) s/V-X/ [emim][NTf_2]

Fig.5.6. (a) UV-vis spectra of the spent V-X catalyst in different solvents; (b) UV-Raman spectra of the spent V-X catalyst in different solvents.

Fig.5.7. The ^{29}Si MAS NMR spectra of the IL-treated NaX with IL.

Fig.5.8. (a) The V $2p_{3/2}$ spectra of V-X; (b) the V $2p_{3/2}$ spectra of the IL-treated V-X; (c)the comparison of N 1s spectra of V-X and the IL-treated V-X; (d) the comparison of F 1s spectra of V-X and the IL-treated V-X.

Fig.6.1 FT-IR spectra of different catalyst (a) $[H_5PV_2Mo_{10}O_{40}$ (b) $[PyBS]_5PV_2Mo_{10}O_{40}$ (c) $[PyBS]_4SiW_{12}O_{40}$ (d) $[PyBS]_6P_2W_{18}O_{62}$ (e) reused $[PyBS]_5PV_2Mo_{10}O_{40}$ after 4 runs

Fig.6.2 XRD patterns of (a) $[PyBS]_4SiW_{12}O_{40}$ (b) $[PyBS]_5PV_2Mo_{10}O_{40}$ (c)

$H_5PV_2Mo_{10}O_{40}$ (d) $H_4SiW_{12}O_{40}$ (e) $H_6P_2W_{18}O_{62}$ (f) $[PyBS]_6P_2W_{18}O_{62}$

Fig.6.3 ^{51}V NMR spectrum of $[PyBS]_5PV_2Mo_{10}O_{40}$ before and after reaction.

Fig.6.4 Cellobiose and cellulose conversion and selectivity for levulinic acid and formic acid for four recycling runs on $[PyBS]_5PV_2Mo_{10}O_{40}$ (Reaction conditions: 0.125 g cellobiose, 423K, 3 MPa O_2,catalyst amount = 5 mol% base on the mole of substrate, 10ml H_2O, 3 h.

List of Tables

Table 2.1. Structures and abbreviations for commonly occurring cations and anions.

Table 2.2 Coordination characteristics of various anions.

Table 4.1 Variation of reaction conditions for the oxidation of 1-phenylethanol to acetophenone over a Pd/CNT catalyst.

Table 4.2. Variation of reaction conditions for the oxidation of 1-phenylethanol to acetophenone over Pd/CNT catalyst-for instrinsic activity examination.

Table 4.3. Oxidation of various alcohols by Pd/CNT in [emim][NTf_2] ionic liquid.

Table 5.1. Epoxidation of *cis*-cyclooctene over V-X catalyst in different solvents.

Table 5.2. Substrate scope of alkene epoxidation over V-X catalyst in mixed solvent.

Table 6.1 Catalytic performances of different IL-POM catalysts in cellobiose degradation in the presence of molecular dioxygen.

Table 6.2 Selectivity of final product in reactions of different sugar intermediates.

List of Schemes

Scheme 2.1 Solvatochromic dye applied to study the ILs' polarity.

Scheme 6.1 Catalytic conversion of cellobiose to formic acid and levulinic acid.

Scheme 6.2 Pathway for the oxidation of glucose to formic acid and carbon dioxide.

Scheme 6.3 Pathway for the rehydration of 5-HMF to formic acid and levulinic acid.

Scheme 7.1 Proposed mechanism for aerobic oxidation of the metal catalyst promoted by imidazolium ILs.

Chapter 1 Background and Philosophy

1.1 Background and the driving force for applying ionic liquid in heterogeneous selective oxidation

The first report of the use of an IL as a catalyst/solvent in Friedel-Crafts acylation was reported in 1986 [1]. However only over the past decade, the IL in catalysis has experienced a tremendous growth, which can be obviously found by the explosion of the papers published [2-6]. A number of catalytic reactions of different types have been successfully performed with IL as a novel reaction media [4, 5, 7, 8]. The primary thought of applying IL as reaction media appeared mainly due to their extremely low vapor as one of the most promising advantages [9]. Nonetheless besides the unique bulk properties such as low vapor pressure, melting point, viscosity and density, the microscopic properties of IL received much attention. ILs which are ionic and highly structured can lead to a distinct chemistry comparing with normal organic solvents [9]. For example some reactions got accelerated in IL, some of which even can't proceed in normal organic solvents. ILs were proposed to play key role in stabilizing relevant reaction intermediates [10]. In addition the ILs showing coordination ability or acidity can significantly affect the catalytic reaction [4, 11]. No matter the bulk or microscopic properties of an IL are actually decided by its chemical nature, which can be easily adjusted by

changing the combination of cation and anion. Basing all above, ILs obviously show great potential to improve the present catalytic technologies.

From the standpoints of atom economy and environmental demand, rapid growing attention has been paid to the development of heterogeneous catalysis as a "greener" alternative. Several apparent advantages, such as high resistance to leaching, simple product isolation, good recyclability, and readily availability from catalyst manufactures in various forms and compositions, make heterogeneous catalysts extremely attractive in designing an environmentally clean process [12].

Oxidation reaction as a major branch of chemical reactions is an important research object in the study of catalysis. Countless organics as important products or intermediates are obtained by the industrial oxidation processes. To enhance the yield and efficiency of valuable oxidative products is the main goal for the development of relevant catalysis.

1.2 Motivation and outline of this dissertation

ILs have been used in oxidative catalysis since 1950s [13]. The studies are dominated by investigations into homogeneous catalytic systems whereby the homogeneous catalyst dissolved in IL to form the catalytic phase. It's once reported that bis(acetylacetonato) nickel(II)/tetra-n-butylammonium tetrafluoroborate salt system can be used in the liquid phase oxidation of ethyl

benzene in air yielding ethylbenzene hydroperoxide at atmospheric pressure [14]. Moreover, bis(acetylacetonato)nickel(II)/(BMI)PF_6 promotes also the oxidation of ethylbenzene at atmospheric pressure, showing that the catalytic ability of the IL involved catalytic systems [15]. Nonetheless, although the advantages of IL got utilized these homogeneous catalytic systems still can't avoid the drawbacks of homogeneous catalysis. By contrast the heterogeneous catalysis takes the advantages in many aspects such as high resistance to leaching, simple product isolation, good recyclability, and readily availability from catalyst manufactures in various forms and compositions [12]. Therefore, to develop effective heterogeneous catalytic systems becomes a superior strategy for utilizing both the advantages of IL and heterogeneous catalysis resulting in obtaining improved the catalytic technologies. Adopting the strategy, the combination of heterogeneous catalyst and IL has been preliminarily studied on several different reaction types [16-25]. Hardacre et al have successfully conducted a series of studies on the selective sulfoxidation of aromatic or aliphatic thioethers catalyzed by mesoporous metal catalysts in ILs [18, 26-28]. The advantage of ILs over normal organic, solvents in these reactions were ascribed to their instrinsic properties, such as the acidity of the imidazolium cation and the capability of forming hydrogen bonding, which directly affect the activity and stability of the solid catalyst. Another heterogeneous catalytic

system consisting of Amberlite IR-120 acidic resin containing an old polymer matrix and IL 1-Butyl-3-methylimidazolium bromide as a solvent effectively catalyzed the oxidation of aromatic alcohols with urea-hydrogen peroxide at 70 ^{o}C [29]. For example when ILs applied as solvent only ambiguous explanations were given concerning the specific effect of ILs, mainly referring to the instrinsic properties of IL which some assumptions without further proven were based on. The large amounts of expensive ILs are needed when they are applied as solvent, which may cause possible toxicological concerns. Recently improved strategies were put up by integrating IL and solid together to synthesize the catalytically effective heterogeneous catalyst, which significantly cut down the using amount of IL. The concept of supported IL phase catalysis (SILPC) therefore emerges. The solid SILPC materials are synthesized by dispersing a small amount of ILs on the surface of a porous solid material and the homogeneous catalyst as the catalytic component is dissolved in the IL phase. Wasserscheid's and Mehnert's groups first demonstrated the feasibility for application of ILs in the concept of SILP catalysis [30-33]. In both their works, a layer of a 1-butyl-2, 3-dimethylimidazolium hexafluorophosphate solution of catalyst coated support materials were synthesized and tested, which show good activities and long-term stabilities. In the current stage, in the terms of the design and the following the investigation of the IL involved

heterogeneous catalytic systems there exist indeed large space to explore. Therefore our work aims at filling the research gap to investigate novel IL involved heterogeneous catalytic systems effective for important oxidative transformations. The substrates of oxidation are extended to alcohols, alkenes, and biomass. Moreover, besides the instrinsic properties of IL, the emphasis is put on the specific effect of IL on the improved catalytic activity by carefully examining the interaction between IL and the components in the reaction system. In the initial stage, basing on the previous works of heterogeneous oxidations the IL 1-ethyl-3-methylimidazolium bis (trifluoromethylsulfonyl) imide ([emim][NTf_2]) was lead in extra into the used reaction systems as solvent. The physical&chemical properties as well as the synergistic effect between IL and the catalysts was carefully studied and elucidated. Following, IL-based polyoxometalate (IL-POM) composites were synthesized as heterogeneous catalyst by ion exchange method. The chemical structure of the introduced cations decides the catalytic behavior of the IL-POM, which was carefully studied.

References

[1] L.J.A. Boon J. A., Pflug J. I., Wilkes J. S. , J. Org. Chem. 51 (1986) 480.

[2] R.D. Rogers, Ionic liquids: industrial applications for green chemistry American Chemical Society 2002.

[3] T.J.G. P. J. Dyson, Metal catalysed reactions in ionic liquids, Springer Science & Business, 2005.

[4] T. Welton, Coordination Chemistry Reviews 248 (2004) 2459-2477.

[5] C.H. V. I. Parvulescu, Chem. Rev. 107 (2007) 2615.

[6] C. Yue, D. Fang, L. Liu, T.-F. Yi, Journal of Molecular Liquids 163 (2011) 99-121.

[7] D. Betz, P. Altmann, M. Cokoja, W.A. Herrmann, F.E. K ühn, Coordination Chemistry Reviews 255 (2011) 1518-1540.

[8] J. Muzart, Advanced Synthesis & Catalysis 348 (2006) 275-295.

[9] C. Chiappe, D. Pieraccini, Journal of Physical Organic Chemistry 18 (2005) 275-297.

[10] J.Y.S. Ji Woong Lee, Yu Sung Chun, Hyeong Bin Jang, Choong Eui Song, Sang Gi Lee, Accounts of Chemical Research 43 (2010) 985.

[11] D.B.W. Warren J. Oldham, Coordination chemistry and speciation of metal complexes in room temperature ionic liquids 13th International Symposium on Molten Salts, Electrochemical Society Incpennington, 2002.

[12] U. Diebold, Surface Science Reports 48 (2003) 53.

[13] S. W., Angew. Chem., Int. Ed. Engl. 4 (1965) 222.

[14]C.L. Alcántara R., Guilhermo Joao P., José-María Santos, Ignacio Vázquez, Ignacio, Appl. Catal., A 203 (2000) 259 -268.

[15] C.L. Alcántara R., Guilhermo Joao P, Perez-Mendo J.P., 218 (2001) 269 -279.

[16] J.F. R. T. Carlin, Chem. Commun. (1997) 1345.

[17] P.G. K. Anderson, C. Hardacre, D. W. Rooney, Green Chem. 5 (2003) 448.

[18] V.I.P. Valentin Cimpeanu, Pedro Amorós, Daniel Beltrán, Jillian M. Thompson, Christopher Hardacre, Chem. Eur. J. 10 (2004) 4640.

[19]J.P.L. X. G. Xie, B. Chen, J. J. Han, X. G. She, X. F. Pan, Tetrahedron Lett. 45 (2004) 809.

[20] M.S. K. Okubo, C. Yokoyama,, Tetrahedron Lett. 43 (2002) 7115.

[21] Y.S. H. Hagiwara, T. Hoshi, T. Suzuki, M. Ando, K. Ohkubo, C. Yokoyama, Tetrahedron Lett. 42 (2001) 4349.

[22] H.Q.N.G. S. A. Forsyth, C. Hardacre, A. McKeown, D. W. Rooney, K. R. Seddon, J. Mol. Catal. A 231 (2005) 61.

[23] S.P.K. C. Hardacre, D. Milroy, P. Nancarrow, D. W. Rooney, J. M. Thompson, J. Catal 227 (2004) 44.

[24] Z.M.A.J. H. Y. Shen, C. B. Chiang, Q. H. Xia, J. Mol. Catal. A 212 (2004)

301.

[25] B.V.S.R. J. S. Yadav, M. S. Reddy, N. Niranjan, J. Mol. Catal. A 210 (2004) 99.

[26] A.N.P. V. Cimpeanu, V.I. Pârvulescu, D.T. On, S. Kaliaguine, J.M. Thompson, C. Hardacre, Journal of Catalysis 232 (2005) 60.

[27] V.P. V. Cimpeanu, V.I. Pârvulescu, J.M. Thompson, C. Hardacre, Catalysis Today 117 (2006) 126.

[28] C.H. V Cimpeanu, V. I. Pârvulescu，Jillian M. Thompson Green Chem. 7 (2005) 326.

[29] K.S. N. Bhati, A. Goswami, Chem. Lett. 37 (2008) 496

[30] R.A.C. C. P. Mehnert, N. C. Dispenziere, M. Afeworki, J.Am. Chem. Soc. 124 (2002) 12932–12933.

[31] E.J.M. C. P. Mehnert, R. A. Cook, Chem. Commun. (2002) 3010–3011.

[32] P.W. A. Riisager, R. Hal and R. Fehrmann, Journal of catalysis 219 (2003) 452–455.

[33]N.S. S. Werner, R. W. Fischer, M. Haumann, P. Wasserscheid, Phys. Chem. Chem. Phys. 11 (2009) 10817–10819.

Chapter 2 Literature Review

2.1 Ionic Liquid

The interest in ILs has been motivated over the last decade [1-4]. Generally they are defined as salts that melt at or below 100 ℃ to afford liquids composed solely of cations and anions. The history of ILs can be traced back to the 19th century [5].

The first room-temperature IL $[EtNH_3][NO_3]$ (m.pt. 12 ℃) was discovered in 1914 [6], but interest did not develop until the discovery of binary IL made from 3-dialkylimidazolium chloride [7].

Generally for most of ILs their cations are organic and anions are inorganic, which is not contained in the definition. The normal cations and anions are listed in Table 2.1 [8]. The cations are generally bulky, asymmetric ammonium or phosphonium salts, or hetero aromatics, with low symmetry, weak intermolecular interactions and low charge densities. The 1, 3-dialkylimidazolium salts remain the most intensively investigated.

Table 2.1. Structures and abbreviations for commonly occurring cations and anions.

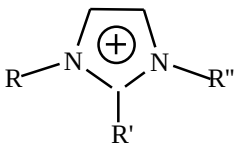

Abbreviation	R	R’	R’’
[Hmim][a]	H	H	Me
[mmim]	Me	H	Me

[emim]	Et	H	Me
[bmim]	*n*-Bu	H	Me
[pmim]	*n*-Pent	H	Me
[hmim]	*n*-Hex	H	Me
[bpim]	*n*-Bu	H	*n*-Pent
[bbim]	*n*-Bu	H	*n*-Bu
[beim]	*n*-Bu	H	Et
[bmim]	*n*-Bu	Me	Me
[hmim]	*n*-Hex	Me	Me
[mPhmim]	Me	Ph	Me
[bPhmim]	*n*-Bu	Ph	Me
[hPhmim]	*n*-Hex	Ph	Me

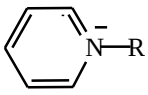

[C_2Py][b]	Et
[C_4Py]	*n*-Bu
[C_5Py]	*n*-Pent
[C_6Py]	*n*-Hex
[$C_3(SO_3H)$Py]	*n*-Pr(SO_3H)

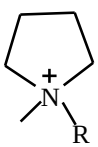

[bmpy][c]	*n*-Bu
[hmpy]	*n*-Hex

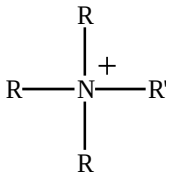	$N_{2,2,2,6}$	Et	*n*-Hex
	$N_{4,4,4,6}$	*n*-Bu	*n*-Hex
	$N_{4,4,4,4}$	*n*-Bu	*n*-Bu
	$N_{6,6,6,6}$	*n*-Hex	*n*-Hex
	$N_{7,7,7,7}$	*n*-Hep	*n*-Hep
	$N_{8,8,8,8}$	*n*-Oct	*n*-Oct
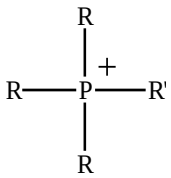	$P_{6,6,6,14}$[d]	*n*-Hex	*n*-Tetradecyl
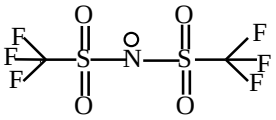	[Tf_2N]		
CH_3COO^-	[AcO]		
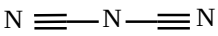	[dca]		

a. Abbreviations for di (or tri) alkylimidazolium cations reflect the first letters of, 3-substituents (and 2 substituents where these are included) followedby ‘im’.

b. Pyridinium cations are designated by C_x, where x is the number of carbonatoms of the alkyl substituent, followed by ‘Py’.

c. Pyrrolidinium cations are designated in similar manner to imidazolium, i.e., first letters of N-substituents followed by 'py'.

d. Tetra-alkylammonium and tetra-alkylphosphonium as N or P, respectively, followed by subscripted numbers indicating the number of C-atoms of the alkyl chains. Anion abbreviations are standard symbols for the ions or as indicated.

Typically, the anions are inorganic including $[PF_6]^-$, $[BF_4]^-$, $[CF_3SO_3]^-$, and $[(CF_3SO_2)_2N_2]^-$. In addition, some organic anions e.g. $[RCO_2]^-$ have also been introduced recently. As development more affordable alternatives of cation and anion will arrive on the scene.

The nature of the cation and anion of IL decides its properties. By changing the structure or the combination of the ions of ILs, their properties can be tuned according to the varied application need.

2.2 The physical and chemical properties

The low volatility of ionic liquids as a green feature is one of the most important reasons making them attractive. Besides it, actually ILs possess many other unique properties, which are reviewed briefly as below.

2.2.1 Vapor pressure

There exists large Coulomb force in the IL. The interaction reaches 100 kJ/mol for the monovalent ions with opposite charges, which is 10 times of that

of water. Therefore, the IL keeps a very low vapor pressure even at a high temperature or vacuum degree.

2.2.2 Melting point

The melting point as an important physical property of IL decides the temperature limit in application. Normally, ILs are low melting liquids. The ILs whose melting point is below room temperature are the most comprehensively applied, as called room-temperature ionic liquid (RTIL). When IL got involved in the reaction, the low melting point can help avoiding the appearance of side reactions, such as decomposition reaction and disproportionated reaction.

As mentioned in the part of *2.1* ILs are designable by adopting the combination of the cation and anion. For imidazolium cation-based ILs increasing the size and asymmetry of cation leads to the decrease of the melting point as experimental examination [9-11]. Further, an increase in the branching on the alkyl chain increases the melting-point. However, in contrast the anion effect is more difficult to rationalize. Recent researchers propose that the hydrogen bonding effect in ILs may explain the melting points and other properties of ILs. Consequently, the mutual fit of the cation and anion, in specific the size, geometry and charge distribution may have a vital influence on the thermo-dynamic properties of ILs [12].

2.2.3 Thermal stability

ILs are mostly highly thermal stable and the decomposition temperatures reported in are generally over 400 ^{o}C. The thermal decomposition temperature decreases as the hydrophilicity of anion increases. The dependence on stability was reported as: $[PF_6]^-$ > $[NTf_2]^-$ > $[BF_4]^-$ > halides [13]. However recent work made some revise on the thermal stability of ILs [14]. The fast thermogravimetric analysis (TGA) scans under a protective atmosphere give the high decomposition temperatures which actually does not exactly reflect ILs' long-term thermal stability. For example, Taking 1-alkyl-3-methylimidazolium hexafluorophosphates for example this IL shows no obvious loss even at 200 ^{o}C after 10h.

2.2.4 Density

Ionic liquids tested so far possess larger density than water. The molar mass of the anion significantly affects the overall density of ILs. With the same cation the ILs with the anion $[Ms_2N]^-$have lower densities than those with the anion $[NTf_2]^-$ [15], which is in agreement with the fact that the molar mass of $[NTf_2]^-$ has a larger molar mass due to the fluorine in the structure. In addition, the density of ILs appreciably decreases as the temperature increases in the low temperature range [16].

2.2.5 Viscosity

ILs normally have higher viscosity than water, which decreases as the temperature increases. The increasing viscosity of ILs is primarily attributed to the increased van der Waals forces [17]. As the carbon atoms in the liner alkyl group increases the viscosities of [Rmim][PF_6] and [Rmim][NTf_2] series ILs get larger [10]. What's more, for 1-alkyl-3-methylimidazolium ILs the branching of the alkyl chain always leads to the reduction of viscosity.

Hydrogen bonding interaction is another important factor which affects the viscosity. Changing the anion of several ILs from [NTf_2]$^-$ to [Ms_2N]$^-$, the viscosities significantly increase. This observation has been attributed to the combination of the decreased anion size, less diffuse charge and large increase in hydrogen bonding [18]. Additionally, the symmetry effect of the has also been considered [9-11] the viscosity decreases in the order Cl^- > [PF_6]$^-$ > [BF_4]$^-$ > [NTf_2]$^-$.

2.2.6 Polarity and Solubility

The feature that how the interaction happens between the solvent and solutes, for the molecular solvents, is commonly recorded as the 'polarity' of the pure liquid. In contrast, the polarity of ILs, however, cannot be judged simply by measuring the dielectric constants as the occasion for molecular solvents. The precise meaning of 'solvent polarity' contains almost all the possible microscopic properties responsible for all the interactions between

solvent and solute molecules (e.g. Coulumbic, directional, inductive, dispersion, hydrogen bonding, electron pair donor and electron pair acceptor forces). So far, the means of solvatochromic probes are mainly applied to study the ILs' polarity. Carmichael and Seddon firstly used a solvatochromic dye (Scheme 2.1), to perform on a series of 1-alkyl-3-methylimidazolium ILs [19].

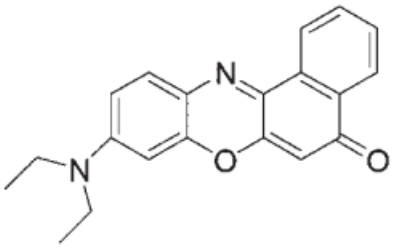

Nile red

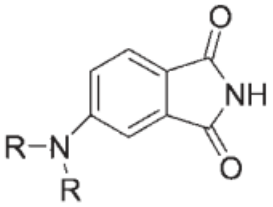

AP: R = H
DAP: R = Me

Scheme 2.1 Solvatochromic dye applied to study the ILs' polarity.

The 1-alkyl-3-methylimidazolium ILs show that the polarity of these ILs is comparable to that of short-chain alcohols [19-21]. The zwitterionic Reichardt's dye is applied to obtain the most widely used Empirical scale of polarity ET (30) scale, where ET (30) = 28 592/λ_{max} (in nm) and λ_{max} is the wavelength maximum of the lowest energy absorption band of the probe. The solvatochromic shift of this probe is strongly affected by the hydrogen-bond donor ability of the solvent, the ET (30) scale is therefore regarded as a measure of hydrogen-bonding acidity the solvent system.

Comparing with the polarity of ILs, the solubility of components in ILs is more comprehensively studied. The interaction between ILs and water is worthy investigating. In one aspect the water content in ILs might affect the rate and selectivity of the reaction performed in the media. In another aspect the solubility of water in ILs is important for their industrial application. The data about the miscibility of alkylimidazolium ILs with water have been extensively obtained. The solubility of these ILs in water depends on the nature of the anion as well as the length of the alkyl chain on the imidazolium cation and temperature. For the ILs with [bmim$^+$] as cation and $[BF_4]^-$, $[CF_3CO_2]^-$, $[NO_3]^-$, $[NMs_2]^-$ and halide as the anions show complete miscibility with water at 25 ^oC. However, upon cooling the [bmim][BF_4]–water solution to 4 ^oC, a water rich-phase separates [9-11].

Moreover, ILs also absorb water from the atmosphere. It has been proposed that when the concentration of water in ILs is in the range of 0.2–1.0 mol/dm^3 , the water molecules hydrogen-bonded with anions, which should mostly exist in symmetrical 1:2 type H-bonded complexes: anion---HOH---anion, observing a “free” state [22].

Recently basing on the voltammetric studies it has been suggested that by adding controlled amounts of water to water-immiscible ILs the nano-inhomogenity can be generated. In the wet ILs the less polar regions could

allow the neutral molecules to reside in while the ionic species in the more polar regions. The wet ILs are still homogeneous and could be regarded as nano-structures with polar and non-polar regions [23].

The solubility of gases in ILs has an important effect on the chemical processes. In many gas−liquid reactions such as alkylation, hydrogenation, aerobic oxidation, hydroformylations, and Diels−Alder addition the gas solubility involves the mass transfer, which might be needed to incorporate into the reaction kinetic equations [24-31]. Blanchard et al firstly measured the solubility data of CO_2 in [Bmim]PF_6 at 298.2 K and pressures up to 40 MPa [32], after which a large amount of solubility data of CO_2 in ILs has been published. The CO_2 solubility is proposed to be associated with the kinds of ILs. It's reported that as the alkyl chain length of the imidazolium cations increases, the CO_2 solubility decreases as the order of [Bmim]BF_4> [hmim]BF_4>[omim]BF_4 [33, 34]

Solubility data of O_2 in ILs for example [Bmim]BF_4, [bmim]PF_6, [bmim]NTf_2, [hmim]NTf_2 and [hmpy]NTf_2 have been measured by many researchers in the past decade. However how the temperature affects the solubility of oxygen is still controversial.

Due to the strong hydrogen bonding interaction between the chloride and the hydroxyl, carboxyl and sulfonyl groups, the cellulose solubility in

[Bmim]Cl reaches 25% under microwave heating [35]. Deng et al has applied [Prmim]Cl to successfully attract the taurine from its mixture with sodium sulfate, affording a novel industrial method to separate the taurine [36].

ILs are also capable of dissolving many metal complexes, meanwhile getting rid of the disturbance of solvation, solvolysis and other side reactions. Therefore, the ILs could be applied comprehensively in the study of 1\7spectroscopy [37, 38]. In a recent work, the thiourea, thioether and urea functional groups for modification are introduced in the alkyl chain of the ILs, which are utilized to extract the transition metal ions [39]. ILs may be the only solvent capable of dissolving the metal hydride (such as NaH and CaH_2), carbide, nitride, kinds of oxide, sulfide and so on [40].

2.2.7 Acidity, basicity and coordination ability

Chloroaluminate ILs have a typical property that their Lewis acidity can be manipulated by altering its composition, since Cl^- is a Lewis base and $[Al_2Cl_7]^-$ and $[Al_3Cl_{10}]^-$ are both Lewis acids.

The Raman spectra of the [Bpy]Cl_2AlCl_3 and [Bmim]Cl_2AlCl_3 [41], along with bthe ^{27}Al NMR spectra [42-45] indicate that when the X ($AlCl_3$)< 0, the anion $[AlCl_4]^-$ and the free Cl^- take the majority, the IL is basic; when X ($AlCl_3$)> 0, there mix the $[Al_2Cl_7]^-$ dimer and $[Al_3Cl_{10}]^-$ trimer, the IL exhibits acidity; when X ($AlCl_3$)= 0.5, the IL is called neutral. The ^{27}Al NMR results

also show that when $X(AlCl_3) \leq 0.67$, there don't exist the $AlCl_3$ or Al_2Cl_6 in the $[bmim]Cl_2AlCl_3$ [42].

Ionic liquids are usually described as innocent, or rather non-coordinating. However, the fact that these so-called non-coordinating ionic liquids very clearly do coordinate to the metal center reveals that the nature of coordination in an ionic liquid in comparison to a molecular solvent that can have profound effects in catalytic chemistry.

Table 2.2 Coordination characteristics of various anions.

Strongly coordinating			Weakly coordinating		Non-coordinating	
Cl^-	Ac^-		$AlCl_4^-$		$Al_2Cl_7^-$	
	NO_3^-		$CuCl_2^-$	SbF_6^-		$Al_3Cl_{10}^-$
		SO_4^{2-}		BF_4^-	$Cu_2Cl_3^-$	
				PF_6^-		$Cu_3Cl_4^-$

The coordination ability is associated with the acidity /basicity, mainly determined by the anion of IL and some common anions are summarized in Table 2.2 [46].

2.3 Ionic liquid in catalysis

Due to the unique physical and chemical properties reviewed in section *2.2*, ILs show great potential for developing the present catalytic technologies. They

are applied in catalysis through various routes, interfering directly the catalysis process or assisting synthesizing the catalysts. In the following I mainly review IL directly interfering catalysis as distinct application ways. The effect of ILs in catalysis is tightly associated with their instrinsic properties.

2.3.1 Ionic liquid as solvent

One of the most promising advantages that ILs have extremely low vapor pressure initially evokes great interest of chemists, making ILs as greener alternatives to volatile organic solvents. The other physical and chemical properties reviewed in section *2.2* also indicate that ILs are superior choice as reaction solvent. An important issue considered for a solvent in catalysis is the solubilities of distinct reaction components in it, such as substrate, product and catalyst and so on. A broad spectrum of inorganic, organic and polymeric materials have adjustable solubilities in ILs, some of which immiscible with numerous organic solvents can dissolve well in ILs. Especially organometallic compounds have excellent solubility in ILs thus catalytic studies in ILs have been dominated by investigations into homogeneous catalytic systems whereby the IL immobilizes the catalyst and affords good separation of the solvent–catalyst system from the products. The first time that ILs applied as solvent for the homogeneous catalysis were reported in 1990 by Chauvin et al. and Wilkes et al. separately. The group of Chauvin reported a nickel catalyst dissolved in

acidic chloroaluminate melts, which catalyzed the dimerization of propene [47]. While for Wilke's group, the same type IL was applied to dissolve the Ziegler-Natta catalyst to catalyze the dimerization of ethylene [48]. Following the synthesis of novel types of ILs opened up a more comprehensive application of ILs as solvent for homogeneous catalysis. What's interesting, although ILs can be regarded as innocent, in some occasions ILs may interact with the catalyst resulting in forming distinct catalytic species compared with the original ones, which is tightly associated with the chemical nature of ILs. The coordination between ILs and the metal center of the catalyst does occur and profoundly affects the catalytic chemistry. The coordination ability as reviewed in section *2.2* is mainly determined by IL's anion. For example Strauss and co-workers once employed NTf_2^- as a weakly, which is a common anion of ionic liquid, coordinating anion in the study of non-classical metal-carbonyl complexes [49]. Moreover, cations of ILs occasionally are able to act as ligand also affect the real catalytic species. The first evidence that the imidazolium based ILs could be generating an entirely new catalyst in situ, came from the observation that the Heck reaction proceeds more efficiently in $[C_4C_1im]Br$ than $[C_4C_1im][BF_4]$ [50]. Xiao and co-workers [50] has isolated the complexes$[PdBr_2/(C_4C_1imy)_2]$ and $[Pd_2(\text{-}Br)_2Br_2(C_4\ C_1imy)_2](C_4C_1imy$: 1-butyl-3-methylimidazolylidene) from the $[C_4C_1im]Br$ solution. The formation

of a mixture of the palladium carbene complexes, as indicated by the characteristic chemical shifts of the olefinic protons of the ylidene ligands in the 1H spectrum and those of the carbene carbons in the ^{13}C NMR spectrum. In sharp contrast, in $[C_4C_1im][BF_4]$ under the same conditions no such carbene species were yielded that were detectable in the ^{1}H NMR spectrum. Indeed the formation of in-situ NHC metal complexes in imidazolium based ionic liquids is possible. This possibility should be considered when the unexpected reactivities or catalyst stabilities are observed. What's more due to the unique properties, IL itself is found to be capable of catalyzing the reaction without the existence of catalyst then they can be regarded meanwhile as a catalyst. Some studies demonstrate that the ILs are capable of being hydrogen donors. Srinivasan et al. proposed the formation of a hydrogen bond between an ionic liquid's cation and the carbonyl group of an anhydride to explain the acetylation of alcohols [51]. MacFarlane et al. have also studied the acetylation of alcohols and proposed that the anion of their ionic liquids is acting as a base catalyst in the acetylation of alcohols, but have not studied the effect of the cations [52]. In some cases IL catalyze the reaction by part of ions. For example the acidic chloroaluminate (III) ionic liquids offers a high concentration of $[Al_2Cl_7]^-$ along with the good solubility of simple arenes, which makes them ideal solvents for electrophilic aromatic substitutions. In a study of the alkylation of benzene with

benzyl chloride in acidic $[C_2C_1im]Cl$-$AlCl_3$ the ionic liquid system was found to be highly active and selective [53].

2.3.1.1 ILs as solvent combined with heterogeneous catalyst

Nonetheless, although the advantages of IL got utilized these homogeneous catalytic systems still can't avoid the drawbacks of homogeneous catalysis. By contrast the heterogeneous catalysis takes the advantages in many aspects such as high resistance to leaching, simple product isolation, good recyclability, and readily availability from catalyst manufactures in various forms and compositions [54]. Therefore, to develop effective heterogeneous catalytic systems becomes a superior strategy for utilizing both the advantages of IL and heterogeneous catalysis resulting in obtaining improved the catalytic technologies. Adopting the strategy, the combination of heterogeneous catalyst and IL has been preliminarily studied on several different reaction types [55-64]. C. Hardacre et al have successfully conducted a series of studies on the selective sulfoxidation of aromatic or aliphatic thioethers catalyzed by mesoporous metal catalysts in ILs [57, 65-67]. The advantage of ILs over normal organic , solvents in these reactions were ascribed to their instrinsic properties, such as the acidity of the imidazolium cation and the capability of forming hydrogen bonding, which directly affect the activity and stability of the solid catalyst. Another heterogeneous catalytic system consisting of Amberlite

IR-120 acidic resin containing an old polymer matrix and IL 1-Butyl-3-methylimidazolium bromide as a solvent effectively catalyzed the oxidation of aromatic alcohols with urea-hydrogen peroxide at 70 ^{o}C [68]. For example when ILs applied as solvent only ambiguous explanations were given concerning the specific effect of ILs, mainly referring to the instrinsic properties of IL which some assumptions without further proven were based on.

2.3.2 Ionic liquid-based hybrid material

2.3.2.1 IL modified polyoxometalate

Bourlinos et al firstly reported a derivative liquid hybrid material of the $H_3PW_{12}O_{40}$ (12-tungstophosphoric acid) by partial exchange of the surface protons of the POM core cluster by a bulky PEG-containing quaternary ammonium cation [69]. The POM salts show several advantages over the corresponding POM such as zero vapor pressure, good thermal stability and higher ionic conductivity. Further, a POM based IL hybrid material was synthesized by pairing of a Keggin or Lindqvist polyoxometalate (POM) anion with an appropriate tetralkylphosphonium cation. The material has lower melting point than ILs meanwhile keeps the unique properties of ILs, such as the good thermal stability and conductivity, on another aspect, also shows the properties of POM [70]. Although relevant works reported were limited, this kind of hybrid material possessing both the advantages of the POM and IL, has

shown application potential in catalysis [71-78]. POMs are a type of intriguing catalysts that can be applied for wide range of technologically relevant applications owing to reasonably high thermal stability, and reversible electron transfer ability under mild conditions. Although homogeneous catalysis provides high catalytic efficiency in m any cases, they suffer from difficult catalyst recovery and separation. Furthermore, one of the major difficulties that largely restrict POMs in industrial application is the severe deactivation of the acid sites by water. Indeed, most solid acids lose their catalytic activity in aqueous solutions. As such, the development of easily recoverable and recyclable POM-based catalysts is required in practical application in industry and so heterogeneous catalysis is preferable. Solidification especially with the assistance of IL is an important strategy to heterognize the POM material in the reaction condition. As reported in some works the solidficated hybrid has another significant feature that it could dissolve at an elevated temperature while separates from the reaction system automatically, which makes the separation of the catalyst facile. Except for the heterogenization of the POM, it's found the hybrid as obtained through the introduction of the IL cation even shows an improved catalytic ability.

It's suggested that the crystal structure of POM is rearranged by introducing the organic IL cation, involving the self-assembly of cations and anions through

the microscopic interaction for example the electrostatic interactions, hydrogen bondings and Vander Waals force. The metal species in the bulk of the hybrid still act as the active centers. On another aspect the cavities developed among cations and anions of this self-assembled macrostructure may allow the permeating of substrates into the bulk of the catalyst structure [79].

Another work reported the enhanced catalytic activity of the the Venturello–Ishii POM $H_3PW_{12}O_{40}$ modified by the imidazolium cation with amimo group comparing with the POM [80], which is mainly attributed to the bonding between the terminal oxygens of PW and amino groups without degrading the intramolecular W–O–W bonds.

2.3.2.2 Supported IL phase catalysis (SILPC) material

Although the homogeneous catalysts in ILs usually present the advantages of high catalytic activity and good selectivity, however, their widespread use in catalytic processes is still hampered by several practical drawbacks, such as product isolation, catalyst recovery. Moreover the homogeneous catalytic process costs large amount of expensive ILs, against economy-practising and green princples. SILPC concept has been established to overcome these drawbacks. The SILPC combines the advantages of ILs and heterogeneous catalysis, such as the designability, good "solubility" of the catalytically active species, ease of handling, separation and recycling. In SILPC materials, a small

amount of ILs is dispersed on the surface of a porous material. Generally, the SILPC materials are composed of three parts including the porous support (alumina, silica or active carbon), the ILs (always a thin layer on the support surface), and the catalyst (nanoparticles or metal complexes). Among the reported studies, Wasserscheid's and Mehnert's groups first demonstrated the feasibility for application of ILs in the concept of SILP catalysis [81-84]. In both their works, a layer of a $[C_4C_1im][PF_6]$ solution of catalyst coated support materials. The catalysts showed high reactivities and good long-term stabilities. Similar SILPC materials have been developed by dipping the porous support in the ILs containing the metal complex. However, the leaching of the ILs and metal-complex urges the strategy that covalent anchoring the IL and the solid support. In a further development, Mehner et al. [85] went on to anchor the cation of the ionic liquid to the support by preparing 1-butyl-3-(3-triethoxysilylpropyl)-4,5-dihydoimidazolium chloride and reacting it with the basic surface of silica gel. As the development of the SILPC, the chemical bonding of the dialkyl imidazolium cation to a solid surface may limit the degrees of freedom of the dialkyl imidazolium cation and even change the physicochemical properties of the ILs. In 2005, a new concept of designing and synthesizing SILPC material was developed for the first time by Deng's group [86]. The physical encapsulation of ILs or ILs containing metal complex into

the pores of the porous silica gels through a sol–gel process. Carbonylation of aniline and nitrobenzene for the synthesis of diphenyl urea, carbonylation of aniline for synthesis of carbamates, and oxime transformation between cyclohex-anone oxime and acetone were used as test reactions for these novel SILPC materials. Catalytic activities were remarkably enhanced with much lower amounts of ILs needed with respect to bulk ionic-liquid catalysts or silica-supported IL catalysts prepared with simple impregnation.

2.3.2.3 Solid catalysis with ILs (SCIL) material

Solid catalyst with ionic liquids (SCILs) is a different concept with Supported IL phase catalysis (SILPC). Solid catalyst uses a free flowing IL to coat the surface of a ready-synthesized solid catalyst. The solid catalyst here is a ready-made heterogeneous catalyst but not an inert support used to immobilize the homogeneous catalyst by the IL. Or rather homogeneous catalyst is not involved in the SCIL concept. The introduction of IL in SCIL is aimed at enhancing the activity/selectivity of the original solid catalyst by the coating of IL. There have been several reports showed the improve effect by leading in IL.

The Mukaiyama-aldol reaction between an aldehyde and a silyl enol ether proceeded very well in water using silica-supported scandium (SiO_2-Sc) coated by a hdrophobic IL, [DBIm]SbF_6, while the reaction proceeded sluggishly using

the catalyst alone without IL coated under the same reaction conditions. The selectivity enhancement was observed in the organic reactions in water catalyzed by a silica-supported sulfonic acid (SiO_2-SO_3H) with a hydrophobic IL, [C_8MIm]NTf_2 [24].

2.3.2.4 Ionogel

For material applications there's a challenging need of immobilizing ILs in solid devices, while keeping their unique properties. Except for the SILC reviewed in part *2.3.4.2*, another novel way of immobilization is to form a three-dimensional network percolating throughout, resulting in obtaining the solid material, which is called ionogel.

Ionogel as a new class of material, hybridizing IL with another component, which may be organic, inorganic or hybrid organic–inorganic. The main properties of ILs except the outflow are preserved, which enlarges the array of their applications. In addition some properties of the IL may be modified due to the confinement; conversely the properties of ILs also influence the building of the solid network.

In 2001 Kimizuka et al. [87] reported the gelation of ether-containing ILs by the addition of L -glutamic acids or carbohydrates such as b-D-glucose, a-cyclodextrin. It was observed that fibrous nano-structures had formed which was attributed to strong interactions between carbohydrates and ether groups.

Shinkai used a cholesterolbased compound known to aggregate by one-dimensional stacking of the cholesterol moieties [88]. Yanagida and co-workers reported ionogels arising from an imidazolium IL and N-benzyloxy-carbonyl-l-isoleucyl aminooctadecane as a gelator [89].

These examples above all applying the low molecular weight gelators as the component exluding the ILs, are firstly reported ionogels. Moreover, some inorganic components are also adopted such as silica particles or carbon nanotubes. The gelation of ILs in the presence of silica nanoparticles was first used by Graetzel to prepare thermally stable quasi-solid electrolytes [90]. Later on, Honma synthesized gels with 10 wt % of [C_4MIm][TFSI] and proved the importance of particle size on gelation [91]. In 2003, Aida and Fukushima [92] found that single walled carbon nanotubes (SWNTs) could be easily dispersed in imidazolium ILs, where heavily entangled bundles of carb on nanotubes were exfoliated to give highly dispersed, much finer bundles. Through the observed phase transition and rheological properties it's suggested that the gels were formed by physical cross-linking of the nanotube bundles, mediated by local ordering of the ILs.

Ionogels enlarge the application potential of ILs in many key areas. The applications range from solid electrolytes to drug release to catalysis, basing on the intrinsic properties of ILs, such as ionic conductivity, drug activity and

solvent ability. By selecting the combination of the anion and cation of ILs the properties of ionogels can be adjusted. The study of solar cells is still in the sustainable development since which has to be faced with the challenge to harvest solar energy with a high yield challenging. The ionogels obtained by mixing silica nanoparticles as "gelator" to solidify IL-based electrolytes resulted in enhanced performances of dye sensitized solar cells (DSSCs). In 2003 such ionogels were applied to DSCCs based on a ruthenium polypyridyl photosensitizer leading to 7% efficiency at AM 1.5 sunlight [93]. Additionally ionogels have also been applied in other energy fields such as Lithium-ion battery and fuel battery.

Except for the application in energy field, it's found that ionogels show potential in catalysis as an alternative nanoreactor system.

Silica based ionogels containing two interpenetrated networks (silica and IL) allows free transport of reactants and products through the liquid phase, while ILs are well confined due to the small pore size of the silica material. Deng et al. synthesized ionogels loaded with $Rh(PPh_3)_3Cl$ and $Pd(PPh_3)_2Cl_2$ as the catalyst which gives enhanced catalytic performance of the carbonylation of aniline into ureas and carbamates [94]. Pd salts were also encapsulated in silica based ionogels and applied as an effective catalytic system without leaching for Heck coupling reaction [95].

References

[1] T.Welton, Chemical reviews 99 (1999) 2071.

[2] P. Wasserscheid, W. Keim, Angewandte Chemie International Edition 39 (2000) 3772-3789.

[3] R. Sheldon, Chemical Communications (2001) 2399-2407.

[4] J.P. Hallett, T. Welton, Chemical reviews 111 (2011) 3508-3576.

[5] J.E. Gordon, Techniques and Methods of Organic and Organometallic Chemistry New York, 1969, p. 51.

[6] P. Walden, Bull. Acad. Imper. Sci. (St. Petersburg) (1914) 1800.

[7] J.S.L. Wilkes, J.A.; Wilson, R.A.; Hussey, C.L. , Inorg. Chem. 21 (1982) 1236-1264. .

[8] S. Chowdhury, R.S. Mohan, J.L. Scott, Tetrahedron 63 (2007) 2363-2389.

[9] V.A. Huddleston JG, Reichert WM, Willauer HD,Broker GA, Rogers RD, Green Chemistry 3 (2001) 156-164.

[10] B.R. Dzyuba S, ChemPhysChem 3 (2002) 161-166.

[11] B.A. Carda-Broch S, Armstrong DW, Anal. Bioanal.Chem. 375 (2003) 191-199.

[12] D.R. Ko ¨lle P, Inorg. Chem. 43 (2004) 2803–2809.

[13] L.K. Ngo HL, Hargens L, McEwen AB, Therm ochim.Acta 357 (2000) 97-102.

[14] G.J. Kosmulski M, Rosenholm JB, Thermochim. Acta 412 (2004) 47–53.

[15] G.J. Pringle JM, Baranyai K, Forsyth CM, Deacon GB,, M.D. Scott JL, New J. Chem. 27 (2003) 1504–1510.

[16] F.S. Holding J, McFarlan D R, Green Chemistry (2002) 223—229.

[17] X. W, W. L-M, N. RA, A. CA, J. Phys. Chem. B 107 (2003) 11749–11756.

[18] G.J. Pringle JM, Baranyai K, Forsyth CM, Deacon GB, Scott JL, MacFarlane DR, New J. Chem. 27 (2003) 1504–1510.

[19] S.K. Charmichael AJ, J. Phys. Org. Chem. 13 (2000) 591–595.

[20] S.M. van de Broeke J, Lutz M, Kooijman H, Spek AL, Deelman B-J, van Koten G, Eur. J. Inorg. Chem. 26 (2003) 2798–2811.

[21] B.R. Dzyuba SV, Tetrahedron Lett. 43 (2002) 4657–4659.

[22] K.S. Cammarata L, Salter PA, Welton T, Phys. Chem.Chem. Phys. 23 (2001) 5192–5200.

[23] d.S.R. Dupont J, Suarez PAZ, Chem.Rev. 102 (2002) 3667–3692.

[24] M.R. Haumann, A, Chem. Rev. 108 (2008).

[25] F.A. Jutz, J. M.; Baiker, A, Chem. Rev. 111 (2011).

[26] J.P.W. Hallett, T. , Chem. Rev. 111 (2011).

[27] P.K. Wasserscheid, W. , Angew. Chem., Int. Ed. 39 (2000).

[28] H.Z. Xu, D.; Xu, P.; Liu, F.; Gao, G. , J. Chem. Eng. Data 50 (2005) 133.

[29] J.L.A. Anthony, J. L.; Maginn, E. J.; Brennecke, J. F., J.Phys. Chem. B 109

(2005).

[30] L.A.G. Blanchard, Z.; Brennecke, J. F., J. Phys. Chem. B 105 (2001).

[31] D.B. Camper, C.; Koval, C.; Noble, R. , Ind.Eng.Chem.Res. 45 (2006).

[32] L.A.H. Blanchard, D.; Beckman, E. J.; Brennecke, J. F., Nature 399 (1999).

[33] M.S.T. Shannon, J. M.; Danielsen, S. P. O.; Hindman, M. S.; Irvin, A. C.; Bara, J. E., Ind. Eng. Chem. Res. 51 (2012).

[34]A.B. Finotello, J. E.; Narayan, S.; Camper, D.; Noble, R. D., J. Phys. Chem. B 112 (2008).

[35] S.S. Swatloski RP, HolbreyJ D, J. Am.Chem. Soc. 124 (2002).

[36] G.Y. Deng YQ, Shi F, 2003.

[37] H.C. Appleby D, Seddon KR, Turp J E, Nature 323 (1986).

[38] H. CL, Pure&Appl.Chem. 60 (1988).

[39] S.R. Visser AE, Reichert WM, Chem.Commun. (2001).

[40] C. Reichardt, Solvents and Solvent effects in Organic Chemistry, Wiley-VCH; Fourth, Updated and Enlarged Edition edition, 2010.

[41] E. F, Phys. Chem. Chem. Phys. 3 (2001).

[42] F.J.S. Wilkes J S, Reynolds GF. , Inorg. Chem. 22 (1983).

[43] G.B.P. Franzen G, Pelzer G, Depauw E, Org.Mass. Spectrum. 21 (1986).

[44] M.G. Gray JL, J. Am. Chem. Soc. 103 (1981).

[45] T.A. Ackermann B L, Allison J, Anal.Chem. 57 (1985).

[46] H.O.-B. V. Chavin, CHEMTECH 25 (1995) 26.

[47] B.G. Y. Chauvin, I. Guibard, J.Chem.Soc.Chem.Commun. (1990) 1715.

[48] R.A.O. R. T. Carlin, Journal of Molecular Catalysis 63 (1990) 125.

[49] W.A.H. D. Betz, F.E. Kühn, Journal of Organometallic Chemistry 694 (2009) 3320-3324.

[50] W.C. L. Xu, J. Xiao, Organometallics 19 (2000).

[51] K.V. A.R. Gholap, T. Daniel, R.J. Lahoti, K.V. Srinivasan,, Green Chemistry 5 (2003).

[52] D.R.M. S.A. Forsyth, R.J. Thompson, M. von Ltzstein, Chem. Commun. (2002).

[53] W.S.A. D.S. Kim, Korean J. Chem. Eng. 20 (2003).

[54] U. Diebold, Surface Science Reports 48 (2003) 53.

[55] J.F. R. T. Carlin, Chem. Commun. (1997) 1345.

[56] P.G. K. Anderson, C. Hardacre, D. W. Rooney, Green Chem. 5 (2003) 448.

[57] V.I.P. Valentin Cimpeanu, Pedro Amorós, Daniel Beltrán, Jillian M. Thompson, Christopher Hardacre, Chem. Eur. J. 10 (2004) 4640.

[58] J.P.L. X. G. Xie, B. Chen, J. J. Han, X. G. She, X. F. Pan, Tetrahedron Lett. 45 (2004) 809.

[59] M.S. K. Okubo, C. Yokoyama,, Tetrahedron Lett. 43 (2002) 7115.

[60]Y.S. H. Hagiwara, T. Hoshi, T. Suzuki, M. Ando, K. Ohkubo, C. Yokoyama, Tetrahedron Lett. 42 (2001) 4349.

[61]H.Q.N.G. S. A. Forsyth, C. Hardacre, A. McKeown, D. W. Rooney, K. R. Seddon, J. Mol. Catal. A 231 (2005) 61.

[62]S.P.K. C. Hardacre, D. Milroy, P. Nancarrow, D. W. Rooney, J. M. Thompson, J. Catal 227 (2004) 44.

[63]Z.M.A.J. H. Y. Shen, C. B. Chiang, Q. H. Xia, J. Mol. Catal. A 212 (2004) 301.

[64]B.V.S.R. J. S. Yadav, M. S. Reddy, N. Niranjan, J. Mol. Catal. A 210 (2004) 99.

[65]A.N.P. V. Cimpeanu, V.I. Pârvulescu, D.T. On, S. Kaliaguine, J.M. Thompson, C. Hardacre, Journal of Catalysis 232 (2005) 60.

[66]V.P. V. Cimpeanu, V.I. Pârvulescu, J.M. Thompson, C. Hardacre, Catalysis Today 117 (2006) 126.

[67]C.H. V Cimpeanu, V. I. Pârvulescu， Jillian M. Thompson Green Chem. 7 (2005) 326.

[68]K.S. N. Bhati, A. Goswami, Chem. Lett. 37 (2008) 496

[69]R.K. Bourlinos AB, Herrera R, Zhang Q, Archer LA, Giannelis EP, J. Am.Chem. Soc. 126 (2004).

[70]P.G. Rickert, M.R. Antonio, M.A. Firestone, K.-A. Kubatko, T. Szreder, J.F.

Wishart, M.L. Dietz, The Journal of Physical Chemistry B 111 (2007) 4685-4692.

[71] C.R. Chhikara BS, Tandon V, Journal of catalysis 230 (2005).

[72] K. A, Catal Commun. 8 (2007).

[73] H.Z. Qiao Y, Li H, Hu Y, Feng B, Wang X, Hua L, Huang Q, Green Chem. 11 (2009).

[74] W.J. Leng Y, Zhu D, Ren X, Ge H, Shen L, Angew Chem Int Ed 48 (2009).

[75] L.W. Wang S, Wan Q, Liu Y, Green Chem. 11 (2009).

[76] H. Li, Y. Qiao, L. Hua, Z. Hou, B. Feng, Z. Pan, Y. Hu, X. Wang, X. Zhao, Y. Yu, ChemCatChem 2 (2010) 1165-1170.

[77] L. Gharnati, O. Walter, U. Arnold, M. Döring, European Journal of Inorganic Chemistry 2011 (2011) 2756-2762.

[78] P. Zhao, M. Zhang, Y. Wu, J. Wang, Industrial & Engineering Chemistry Research 51 (2012) 6641-6647.

[79] P.Z. X. Yan, J. Fei, J. Li, Adv. Mater. 22 (2010) 1283–1287.

[80] Y. Leng, J. Wang, D. Zhu, M. Zhang, P. Zhao, Z. Long, J. Huang, Green Chemistry 13 (2011) 1636.

[81] R.A.C. C. P. Mehnert, N. C. Dispenziere, M. Afeworki, J.Am. Chem. Soc. 124 (2002) 12932–12933.

[82] E.J.M. C. P. Mehnert, R. A. Cook, Chem. Commun. (2002) 3010–3011.

[83] P.W. A. Riisager, R. Hal and R. Fehrmann, Journal of catalysis 219 (2003) 452–455.

[84] N.S. S. Werner, R. W. Fischer, M. Haumann, P. Wasserscheid, Phys. Chem. Chem. Phys. 11 (2009) 10817–10819.

[85] R.A.C. C.P. Mehnert, N.C. Dispenziere, M. Afeworki, J. Am.Chem. Soc. 124 (2002).

[86] Q.Z. F. Shi, D. Li and Y. Deng, Chem.Eur.J. 11 (2005) 5279–5288.

[87] T.N. N. Kimizuka, Langmuir 17 (2001).

[88] K.S. A. Ikeda, M. Ayabe, S. Tamaru, T. Nakashima, N. Kimizuka, S. Shinkai, Chem. Lett. (2001).

[89] S.K. W. Kubo, S. Nakade, T. Kitamura, K. Hanabusa,Y. Wada, S.Yanagida, J. Phys. Chem. B 107 (2003).

[90] S.M.Z. P. Wang, P. Comte, I. Exnar, M. Graetzel, J. Am. Chem. Soc. 125 (2003).

[91] H.Z.a.I.H. S. Shimano, Chem. Mater. 19 (2007).

[92] A.K. T. Fukushima, Y. Ishimura, T. Yamamoto,T. Takigawa, N. Ishii and T. Aida, Science 300 (2003).

[93] S.M.Z. P. Wang, P. Comte, I. Exnar, M. Graetzel, J. Am. Chem. Soc. 125 (2003).

[94] Q.Z. F. Shi, D. Li and Y. Deng, Chem.Eur.J. 11 (2005).

[95] M.G. S. Volland, T. Regnier, L. Viau, O. Lavastre, A. Vioux,, New J. Chem. 3 (2009).

Chapter 3 Techniques of Characterization, Synthesis, and Catalytic oxidation

In the research of catalysis, characterization techniques are indispensable to investigate the physical and chemical properties of catalysts, such as bulk and local structure, morphology, and chemical compositions, which directly effects the catalytic behaviors. Characterizing the catalysts on a molecular/atomic level before and after the reaction may reveal the catalytic process, which further illustrates the catalytic mechanism. In addition the design and modification of catalyst or the catalytic system with improved performance can be conducted more rationally and readily. Therefore understanding the fundamental concepts of the characterization techniques is absolutely necessary to appropriately take their advantage, which will be briefly described in this chapter as well as the synthesis methodologies of catalysts in this thesis.

3.1 Characterization techniques

3.1.1 Characterization of catalyst morphologies and structures

X-ray diffraction (XRD) basing on the elastic scattering of X-rays from the electron clouds of the individual atoms in the system, can afford the information helping to identify and characterize the crystallographic structure, crystallite size (grain size), and preferred orientation in polycrystalline (e.g., metal crystallites [1]) or powdered solid samples with ordered structure (e.g.

zeolites [2] and polyoxometalate [3]). The position (corresponding to lattice spacing) and the relative intensity of the distinctive diffraction pattern indicate a particular phase and material, providing a "fingerprint" for comparison.

In this thesis, powder XRD measurements were conducted on a Bruker AXS D8 X-ray diffractometer (Cu Kα, λ=1.5406 Å, 40 kV, 30 mA) under ambient conditions. Diffraction data were collected with a resolution of 0.02º (2θ) in the angle range 5-40 º. Prior to test, samples were dried at 373 K overnight.

Scanning electron microscope (SEM) is applied to directly observe the catalyst morphologies and structures. In this PhD work, the SEM image was obtained on a JEOL Field Emission Scanning Electron Microscope (JSM-6700F-FESEM). Prior to the measurements, the samples were deposited on a sample holder using an adhesive carbon tape and then decorated with gold through sputtering.

Transmission electron microscopy (TEM) enables the direct observations on the aggregation state, size, morphology and structures, which are the first concerns of nanosized materials. Metal nanoparticles, especially those consisting of noble metal elements, give high contrast after dispersed on thin carbon films. Owing to a rapid improvement in high-voltage electron beam technique, high resolution TEM (HRTEM) can now provide information not only on the particle size and shape but also on the crystallography of mono- and

bi-metallic nanoparticles, giving the atom arrangement and atomic-scale defects in the specimen. In this thesis, TEM was performed on a JEOL JEM-2010, operated at 200 kV. The samples were suspended in ethanol and dried on holey carbon-coated Cu grids. The mean particle diameter was calculated from the mean frequency distribution by counting ca. 200 particles according to: $d = \frac{\sum n_i \cdot d_i}{\sum n_i}$ where Σ is the sum of *i* over the entire sample, n_i is the number of particles with particle diameter d_i in a certain range. The corresponding root mean square error σ was determined using the following statistical expression: $\sigma(d) = \sqrt{\frac{\sum n_i (d - d_i)^2}{\sum n_i - 1}}$.

Solid-state NMR (SSNMR) spectroscopy is a kind of nuclear magnetic resonance (NMR) spectroscopy, characterized by the presence of anisotropic (directionally dependent) interactions. As the supplementary technique of XRD, the solid NMR is capable of revealing the structure change of those undissovable solid samples. For the zeolites it's difficult to study the structure by conventional techniques since as microcrystalline they typically contain four 10-electron atomic species (Si^{4+}, Al^{3+}, O^{2-}, and Na^{+}). While the solid NMR technique zeolite is applied as a powerful structural tool to monitor all elemental components of such frameworks [4].

In this PhD work, 29Si MAS NMR spectra were recorded on a 400 MHz

Bruker spectrometer. Prior to the measurements the catalysts were carefully dehydrated at 373 K in vacuum and filled into the NMR rotors under dry nitrogen gas in a glove box.

3.1.2 Characterization of catalyst active sites

Inductively Coupled Plasma (ICP) technique was applied to determine the metal contents. The samples containing metal components (both organic mixture and the solid samples), an appropriate amount of sample is taken then digested with nitric acid (69 %) at 120 ^{o}C overnight before the ICP test. The Perkin-Elmer Dual-view Optima 5300 DV ICP-OES (Optical Emission Spectrometry) system is applied in this work.

Basing on the phenomenon that a molecule will undergo electronic transitions when it absorbs or reflect light in the ultraviolet (UV) and visible (vis) ranges, the UV-vis spectroscopy has been comprehensively applied, such as determination of the oxidation state of a metal center [5], detection of eluting components in high performance liquid chromatography (HPLC) [6], or determination of the maximum absorbance of a compound prior to a photochemical reaction [7]. A UV-vis spectrum is obtained by plotting the absorbance of energy against the wavelength. The reflection mode of UV-vis spectroscopy has been proved to be the simplest but a powerful method for characterizing metal supported zeolites catalysts [8] [9].

In this PhD work, to examine the local environment of metal incorporated into the framework of zeolite, diffuse reflectance UV-vis spectroscopy was used and recorded on a VARIAN 5000 UV-vis-NIR spectrophotometer with a diffuse reflectance accessory. The spectra were recorded in the range of 200-800 nm at room temperature with $BaSO_4$ as a reference. All samples were dried at 373 K overnight before performing the test.

X-ray photoelectron spectroscopy (XPS) is a powerful tool in the quantitative and qualitative analysis of the surface composition and structures of catalysts, which are indispensable to elucidate the catalytic properties. In this thesis, XPS measurements were performed on a VG Escalab 250 spectrometer equipped with an Al anode (Al Ka = 1486.6 eV). The background pressure in the analysis chamber was lower than 1×10^{-7} Pa. Measurements were performed using 20 eV pass energy, 0.1 eV step, and 0.15 min dwelling time. The correction of the binding energies (BE) used the C_{1s} peak of adventitious C at 284.6 eV. The background contribution caused by inelastic process was obtained by Shirley method and subtracted. The curve fitting was done with a Gaussian–Lorentzian function to deconvolute the overlapped peaks.

Vibrational spectroscopy such as Raman has often been used to probe the molecular structures of supported metal oxides; a large amount of information has been obtained for the supported metal oxide catalysts. Ultraviolet Raman

spectroscopy has been proved to be a powerful technique for the study of catalysts and other solids [10, 11], especially for the identification of isolated transition metal atoms substituted in the framework of molecular sieves [12]. In this thesis, the supported zeolite catalysts were studied by Raman spectroscopy in order to identify the structure of the metal incorporated into the silica framework. Raman spectra were collected on a Renishawin Via Raman system with a 325 nm laser as the excitation source. A laser output of 30 mW was employed and the maximum incident power at the sample was approximately 6 mW [13].

Fourier Transform Infrared (FTIR) Spectroscopy is of the most useful for identifying types of chemical bonds (organic/inorganic), and quantitatively determining the components or consistency of a mixture. In FTIR measurement, an IR spectrum of absorption, emission, photoconductivity or Raman scattering of a solid, liquid or gas molecular is obtained when IR radiation is passed through, creating a unique molecular fingerprint of the sample. Moreover, the surface chemistry of catalyst can be studied by introduction of adsorbed small molecules, particularly carbon monoxide (CO), which can be easily adsorbed on metals. The wavenumber and adsorption mode of adsorbed CO primarily depend on the metal and surface structure. For bimetallic nanoparticles, the surface micro-structure can also be elucidated.

In this thesis, FTIR spectra were recorded on a PerkinElmer Spectrum One FT-IR spectrometer at room temperature (4000-450 cm^{-1}, resolution of 1 cm^{-1}). The sample was pressed into pellet with KBr and placed into an in situ IR cell with CaF_2 windows. After alignment, the sample compartment was subjected to a thermal pretreatment under a helium atmosphere at 393 K for 2h to remove the moisture. The data was collected at room temperature (resolution of 1 cm^{-1}). Diffuse Raman Supported metal oxide catalysts consist of a two-dimensional, active surface metal oxide phase that is fully dispersed and chemisorbed onto the surfaces of high surface area oxide supports (e.g. alumina, titania, silica, etc.).

Nuclear magnetic resonance (NMR) is a physical phenomenon in which nuclei in a magnetic field absorb and re-emit electromagnetic radiation. This energy is at a specific resonance frequency which depends on the strength of the magnetic field and the magnetic properties of the isotope of the atoms. The NMR techniques are comprehensively applied in the characterization of the catalyst which can be dissolved and kept unchanged in the structure.

In this thesis, ^{1}H NMR spectra were obtained at Bruker AV300, using D_2O as solvent.The ^{51}V NMR spectra were recorded on a JEOL ECX-400 MHz using dimethyl sulfoxide-d_6(DMSO-d_6) and$CDCl_3$ as solvents.

3.2 Synthesis methodologies

3.2.1 Materials

Multi-walled carbon nanotubes (MWCNT) was purchased from Cnano Technology Ltd (purity: 97.1%, SBET : 241 m^2/g, bulk density: 0.05 g/cm^3). $PdCl_2$ (99%), HNO3 (69%), HCl (36%), H_2SO_4 (98%), diethyl ether (>99%), 1-phenylethanol (98%) and dodecane (≥ 99.8%) were provided by Sigma-Aldrich.

Ionic liquids 1-ethyl-3-methylimidazolium bis (trifluoromethylsulfonyl)imide [emim][NTf_2], 1-butyl-3-methylimidazolium bromide [bmim]Br and Nafion solution (5 wt.% in isopropanol) were purchased from Regent Chemicals Pte Ltd. All chemicals were used as received without further purification.

cis-Cyclooctene (95% stabilized, Acros Organic), dimethylformamide (A.C.S. Reagent, J.T. Baker), *tert*-butyl hydroperoxide (70% in water, Fluka), were employed as received without further purifications. ILs, [emim][NTf_2] and [bmpy][NTf_2] were purchased from Merck.

All chemicals including pyridine (99%), triethylamine (99%), 1-methylimidazole (99%), 1, 4-butane sultone (99%), silicotungstic acid (AR), phosphotungstic acid (AR) and phosphomolybdic acid (AR) were purchased from Sigma-Aldrich or Fluka and used without further purification.

3.2.2 Synthesis of V/X

Firstly, two grams of NaX faujasite zeolite was weighted and put into a flask and 50ml DI water was added in to the flask which was around pH=11. Next, a measured amount of 3 wt.% vanadyl sulfate (basing on NaX faujasite zeolite) was dropped into the flask. Keep stirring overnight, the mixture was filtered and dried in 403K. Then, the vanadium ion exchanged NaX zeolite were synthesized and named as V-X with the vanadium loading of 2.66 wt.%.

3.2.3 Synthesis of Pd/CNT

The pristine MWCNT was pretreated with concentrated HNO_3 at 120 ^oC for 2 h to remove the amorphous carbonaceous and metallic impurities as well as to introduce surface oxygen functional groups. Palladium catalyst supported on MWCNT was prepared by an adsorption-reduction method with a Pd loading of 1 wt.%: 375.9 μL of H_2PdCl_4 (0.05 M) aqueous solution was added to 0.2g of acid-pretreated MWCNT suspended in 20 ml of DI water, followed by vigorous stirring at 80 ^oC for 5 h. The catalyst, donated as Pd/CNT, was obtained by filtering, washing with DI water, and drying at 60 ^oC overnight. The catalyst was activated in a H_2 flow of 20 ml/min at 400 ^oC for 2 h.

3.2.4 Synthesis of the polyoxometalates (POMs)

$H_6P_2W_{18}O_{62}.nH_2O$.: Na_2WO_4 $2H_2O$ was first dissolved in hot deionized water and then mixed with a 85 wt% H_3PO_4 solution under vigorous stirring for 6 h at 413 K. After cooling to RT, the resultant mixture was acidized with

adequate 37 w% hydrochloric acid. Product extraction by using adequate diethyl ether as extraction solvent lasted for no less than 5 h until the liquid was obviously stratified. The bottom part was then carefully separated out and heated to remove diethyl ether solvent to yield the yellow solid product. Further purification via aqueous dissolution and distillation at 393 K was also performed to remove hydrophilic residues.

$H_5PMo_{10}V_2O_{40}$. nH_2O: $H_5PMo_{10}V_2O_{40}$. nH_2O abbreviated was prepared as the reference [14]. MoO_3 (0.10 mol) and V_2O_5 (0.01 mol) were dissolved in DI water (250 ml); then the solution was heated up to 393K under vigorously stirring with a water-cooled condenser. H_3PO_4 (85% aqueous solution, 0.01 mol) was added to the above mixture with the temperature kept at 393K. After stirred for 24h, the product was cooled to room temperature and dried at 323K in vacuum for 24h. The resulting orange fine powder was then dissolved in deionized water and subjected tore-crystallization for further purification.

3.2.5 Synthesis of IL modified POM (IL-POM)

For the SO_3H-functionalized ionic liquid (IL) was synthesized as the procedures: the prydine (0.11 mol) and 1,4-butane sulfone (0.10 mol) were dissolved in 20 ml toluene and the mixture was continuously stirred for 24 h at 313 K under the protection of nitrogen atmosphere. The obtained white precipitate (denoted as PyBS) was then filtered, washed with diethyl ether three

times and dried in vacuum at room temperature. PyBS (0.06 mol) was added into an aqueous solution containing $H_3PW_{12}O_{40}$ (0.02 mol) in a round-bottomed flask, followed with vigorous stirring at room temperature for 24 h. Continuous evacuation at room temperature was conducted to remove the water moisture and the final solid product was carefully collected and denoted as $[PyBS]_3PW_{12}O_{40}$. Other IL-POMs were synthesized as similar procedures.

3.3 Catalyst evaluation

3.3.1 Solvent-free aerobic oxidation of benzyl alcohol

The solvent-free aerobic oxidation of benzyl alcohol with molecular O_2 was carried out using a bath-type reactor operated under atmospheric condition.

Experiments were conducted using a three-necked glass flask (capacity: 25 ml) pre-charged with certain amount of benzyl alcohol and catalyst. The mixture was stirred using a magnetic stirrer and heated in a silicon oil bath. The system as equipped with a thermocouple to control the temperature and a reflux condenser. In each reaction run, the mixture was heated to 433 K under vigorous stirring. Oxygen flow was bubbled into the mixture to initiate the reaction once the reaction temperature was reached. After the allowed reaction time, the mixture was quickly quenched for further extraction. The solid catalyst was filtered off and the liquid organic products were analyzed by an Agilent gas chromatograph 6890 equipped with a HP-5 capillary column (30m

long and 0.32 mm in diameter, packed with silica based supel cosil) and flame ionization detector (FID). The injector temperature was 523 K and the spilt is 0.1 μl. The column head pressure of the carrier gas (helium) during the analysis was maintained at 22.57 psi. Temperature program: 373 to 393 K; 20 K min^{-1}; hold for 3min. The conversion of benzyl alcohol, the selectivity towards benzaldehyde and *quasi*-turn over frequency (*q*TOF) are defined as follows:

$$Conversion(\%) = \frac{moles\ of\ reactant\ converted}{moles\ of\ reactant\ in\ feed} \times 100\%$$

$$Selectivity(\%) = \frac{moles\ of\ product\ formed}{moles\ of\ reactant\ converted} \times 100\%$$

$$qTOF(h^{-1}) = \frac{moles\ of\ reactant\ converted}{moles\ of\ total\ active\ sites \times reaction\ time}$$

The by-products were identified by a gas chromatography-mass spectrometry (GC–MS, Agilent, GC 6890N, MS 5973 inert).

To ensure the reliability of the catalytic results (conversion and selectivity), tetradecane (C14) was used as inert external standard for the selective oxidation of benzyl alcohol.

Since this catalytic process is a typical slurry-phase reaction with one liquid reactant, one gaseous reactant and a solid catalyst, for excluding the mass transfer effects, the stirring speed is set to be 1000rpm basing on the examination of the stirring speed effects on this reaction.

3.3.2 Epoxidation of cis-cyclooctene with tert-butyl hydroperoxide (TBHP) as oxidant

The epoxidation of *cis*-cyclooctene with peroxide as oxidant was carried out using a bath-type reactor operated under atmospheric condition.

Experiments were conducted using a three-necked glass flask (capacity: 25 ml) pre-charged with *cis*-cyclooctene and catalyst then the solvent was added in. The peroxide was added into the reaction mixture immediately and the reaction time starts to count. The mixture was stirred using a magnetic stirrer and heated in a silicon oil bath. The system was equipped with a thermocouple to control the temperature and a reflux condenser. In each reaction run, the mixture was heated to desired temperature under vigorous stirring. After the allowed reaction time, the mixture was quickly quenched for further extraction. The catalyst was filtered off. When IL applied as solvent/co-solvent, the liquid organic products need to be extracted with diethyl ether getting rid of the IL which cannot be injected into the gas chromatograph directly. The obtained organic phase was analyzed by an Agilent gas chromatograph 6890 equipped with a HP-5 capillary column (30m long and 0.32 mm in diameter, packed with silica based supel cosil) and flame ionization detector (FID). The injector temperature was 523K and the spilt is 0.1 µl. The column head pressure of the carrier gas (helium) during the analysis

was maintained at 9.15 psi. Temperature program: 323 K; hold for 4 min; 323-433 K; 20 K min^{-1}; hold for 1 min. The conversion of *cis*-cyclootene, the selectivity towards the corresponding:

$$Conversion(\%) = \frac{moles\,of\ reactant\,converted}{moles\,of\ reactant\,in\ feed} \times 100\%$$

$$Selectivity(\%) = \frac{moles\,of\ product\ formed}{moles\,of\ reactant\,converted} \times 100\%$$

$$qTOF(h^{-1}) = \frac{moles\,of\ reactant\,converted}{moles\,of\ total\,active\,sites \times reaction\,time}$$

The by-products were identified by a gas chromatography-mass spectrometry (GC–MS, Agilent, GC 6890N, MS 5973 inert).

To ensure the reliability of the catalytic results (conversion and selectivity), *m*-dichlorobenzene was used as inert external standard for the epoxidation of *cis*-cyclooctene.

3.3.3 One-pot transformation of cellobiose into formic acid and levulinic acid

Catalytic conversion of cellobiose was carried out in a stainless steel autoclave reactor with Teflon liner (Parr 4950, 4843 Controller). Typically, a certain quantity of cellobiose substrate, IL-POM catalyst and deionized water were added into a 50 mL Teflon container. High-purity oxygen was introduced to reach an initial reaction pressure of 3 MPa prior to expelling residue air by pressurizing and releasing oxygen for three times. After catalytic reaction

carried out at 423 K for 3 h, the autoclave containing unreacted reactants, products and catalysts was cooled in an ice-bath for no less than 6 h until the used catalyst emerged at bottom as transparent solid. Especially, for catalyst with Dawson-structured POM anions, a cooling time for complete precipitation exceeded 10 h. The products as well as unreacted reactants were all reserved in liquid phase and could be conveniently separated from solid catalysts by decantation or filtration. The recycled IL-POM catalyst was washed with ethanol solvent for three times, dried in vacuum at 333 K for 8 h and then reused in next catalytic run.

Other products including glucose, sorbitol, fructose and FA were separated by a Hi-Plex H column (300-6.5 mm) using 0.01 M H_2SO_4 buffer as mobile phase. Cellulose conversions were determined by the weight difference of cellulose before and after the reaction. The conversion of cellobiose or sugar intermediate products was calculated from the equation:

$$Conversion(wt\%) = \frac{weight\ of\ reactant\ converted}{weight\ of\ reactant\ in\ feed} \times 100\%$$

$$For\ the\ hydrolysis\ of\ cellulose:$$

$$Selectivity(\%) = \frac{weight\ of\ final\ product\ formed}{weight\ of\ cellulose\ converted} \times 100$$

$$For\ the\ hydrolysis\ of\ cellobiose\ and\ the\ sugar\ intermediates:$$

$$Selectivity(\%) = \frac{moles\ of\ C-atoms\ of\ the\ product}{moles\ of\ C-atoms\ of\ the\ converted\ feedstock} \times 100$$

References

[1] I.A. R.A. Sheldon, A. Dijksman, Catalysis Today 57 (2000) 157.

[2] J.K.K. R.A. Sheldon, Metal-Catalyzed Oxidation of Organic Compounds, Academic Press, 1981.

[3] G.M. Maksimov, Russian Chemical Reviews 64 445.

[4] J. Klinowski, Solid-State NMR Studies of Molecular Sieve Catalysts Chem. Rev. (1991) 1459-1479

[5] T.H. K. Mori, T. Mizugaki, K. Ebitani, K. Kaneda, Journal of the American Chemical Society 126 (2004) 10657-10666.

[6] P.C. A. Abad, A. Corma, H. Garcia, Angewandte Chemie International Edition 44 (2005) 4066-4069.

[7] M.F.-S. W. Liu, Journal of Catalysis 153 (1995) 304-316.

[8] B.M. Montanari T., Resini C. Busca G., Journal of Physical Chemistry B 108 (2004) 2120.

[9] L.K. Warnken M., Wark M. , Physical Chemistry Chemical Physics 5 (2001) 1870.

[10] H.E. Tiitta M., Makkonen J., Root A., Sandelin F., Osterholm H. , Recent Advances in the Science and Technology of Zeolites and Related Materials, Pts A-C, 2004.

[11] L.M.F. Li D.D., Chu Y., Nie H., Shi Y.H. , Catalysis Today 81 (2003) 65.

[12] K.S.G. Goddard S.A., Energ. Fuel. 8 (1994) 147.

[13] W. R.S., Journal of Catalysis 151 (1995) 470.

[14] J.W. Y. Leng, D.R. Zhu, L. Shen, P.P. Zhao, M.J. Zhang, Chem Eng J. 173 (2011) 620-626.

Chapter 4 Palladium-catalyzed aerobic oxidation of 1-phenylethanol with an ionic liquid additive

The selective oxidation of alcohols has been considered as one of the most fundamental organic transformations. The corresponding aldehydes or ketones are employed as high-value intermidiates and components for the pharmaceutical, agrochemical, and perfumery industries [1, 2]. From the viewpoints of atom economy and environmental concern, developing noble metal heterogeneous catalysts and using molecular oxygen or air as the oxidant prevail as an attractive green technology [3]. Numerous palladium catalysts with superior catalytic activities have been developed since its first successful application in the aerobic oxidation of secondary alcohols [4]. Moriet al. reported a hydroxyapatite-supported Pd catalyst highly effective for the aerobic oxidation of benzylic alcohols, particularly giving a TOF of 9800 h^{-1} for 1-phenylethanol [5]. Li et al. showed that zeolite-supported Pd nanoparticles of2.8 nm exhibited an exceptional TOF of 18 800 h^{-1} [6]. More recently, our group has also reported the surface-functionalized TUD-1 supported Pd catalysts with a high TOF of 18571 h^{-1} for benzyl alcohol oxidation [7].

Ionic liquids (ILs) have risen as a focus of research interest and made significant progress in the catalytic processes from a green chemistry perspective since the discovery of second-generation ILs in 1992 [8]. ILs are

generally employed to get involved in the catalytic reactions in two ways: as a supported phase (supported ionic liquid phase catalysts, SILPCs) and as medium or additive in the reaction [9]. Making SILPCs, in which active species are immobilized on an IL-functionalized support, is considered as a facile and economic approach [10, 11]. Nonetheless, many studies are also centered at the use of ILs as effective solvents for "green" chemical reactions. ILs can replace the traditional volatile organic and dipolar aprotic solvents in both laboratory and industry-scale production due to their unique properties, i.e., non-flammable, non-volatile, thermally stable, high solvating, and non-coordinating [12]. Moreover, ILs are regarded as designable solvents because their physic-chemical properties can be precisely tuned by a suitable combination of cations and anions. In addition to a vast number of developments achieved using ILs as reaction media in transition metal-catalyzed hydrogenation, hydroformylation and coupling reactions [13-15].Tthere are several examples of catalytic alcohol oxidation in ILs [16-18]. However, most of them involve homogeneous metal catalysts, which require laborious product isolation and generate large amounts of organic/inorganic waste. Therefore, heterogeneous oxidation in ILs media is preferred as a greener alternative which can also effectively solve the problems involving the decomposition or leaching of active metal centers, poor reactants

and catalyst solubility, low activities and selectivities [19].

In this chapter, we reported the application of [emim][NTf_2], a non-nucleophilic and hydrophobic IL, as the reaction additive for the selective oxidation of 1-phenylethanol over a carbon nanotube-supported Pd catalyst using molecular oxygen as the oxidant.

In this work, the reactivity of the catalytic system was benchmarked against solvent-free conditions and another representative IL [bmim]Br. The effects of IL nature and content as well as various reaction parameters (reaction time,O_2 partial pressure, O_2 total pressure, reaction temperature, recyclibility) on the catalytic activity were examined.

4.1 Catalytic performance of the heterogeneous catalytic system for the aerobic oxidation of 1-phenylethanol with ionic liquid as additive

The catalytic performance of the aerobic oxidation of 1-phenylethanol with ionic liquid as additive was examined and summarized in Table 4.1. In the absence of catalyst and ILs (entry 1), only a small amount of 1-phenylethanol converts due to the non-catalytic oxidation [20]. Good activity is observed over a Pd/CNT catalyst under solvent-free conditions (entry 2), showing a TON of 111000. The reaction time-conversion correlation was studied for 1-phenylethanol oxidation in [emim][NTf_2] and solvent-free conditions (Fig. 4.1).

The reaction time-conversion correlation was studied for1-phenylethanol oxidation in [emim][NTf_2]shows superior catalytic activities to solvent-free conditions.

Noteworthy, [emim][NTf_2] distinctly affects the catalytic performances. The activity increases sharply upon introducing a small amount of [emim][NTf_2] as an additive, and reaches the maximum with 1mL of IL addition, showing an excellent TON of 149000 (entries 3 and 4). The conversion was connected by the trend line fitted based on the 1st-order kinetic model.

Table 4.1 Variation of reaction conditions for the oxidation of 1-phenylethanol to acetophenone over a Pd/CNT catalyst[a].

Entry	Ionic liquid/ catalyst	V_{IL}(mL)	ILmolar fraction (%)	Conv. (%)	Select[b] (%)	TON($\times 10^4$)[c]
1	no IL/no cat.	-	0	11.8	100	-
2	no IL	-	0	67.6	90.8	11.1
3	[emim][NTf_2]	0.5	8.7	77.4	91.8	12.7
4	[emim][NTf_2]	1	16.0	90.6	96.9	14.9
5	[emim][NTf_2]	2	23.7	62.8	95.8	10.3
6	[emim][NTf_2]	3	31.8	59.9	91.6	9.8

7	[emim][NTf_2]	4	38.3	43.2	93.9	7.1
8	[emim][NTf_2]/no cat.	1	16.0	42.8	47.9	-
9	[emim][NTf_2]-reused	1	16.0	82.1	91.7	13.5
10	[bmim]Br	1	19.1	0	0	-
11	cat. recovered in [bmim]Br	-	0	60.8	90.2	10.0

a. Reaction conditions: 25 mmol of 1-phenylethanol, 5 mg of Pd/CNT, 20 mL/min of O_2, 160 ^oC, 1 h. Uncertainties: conv. ± 0.15%, select ± 0.35%, TON ± 0.08%.

b. Ethylbenzene is the only byproduct.

c. TON was calculated based on D_{Pd} determined by the CO-stripping method.

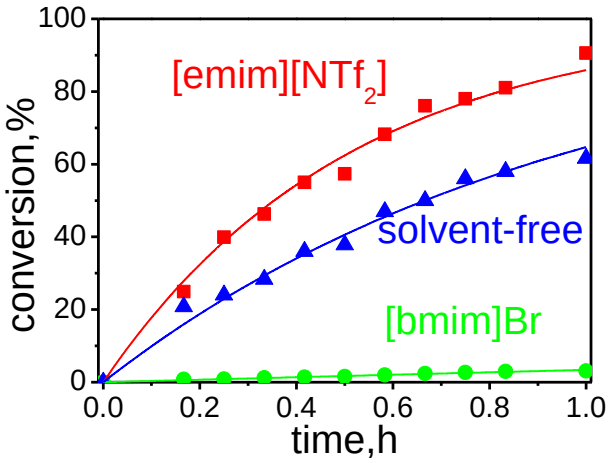

Fig.4.1 Time-conversion plots of for the aerobic oxidation of 1-phenylethanol. Run conditions: see footnote of Table 4.1.

The improvement can be attributed to the enhanced solubility of both alcohol substrate and gaseous O_2 in [emim][NTf_2], leading to a better substrate–

catalyst contact [9].

Further adding [emim][NTf_2] results in a pronounced decline of catalytic performances (entries 5–7), which may be due to either the low concentration of the substrate or the large mass-transfer resistance in the viscous alcohol–IL mixture.

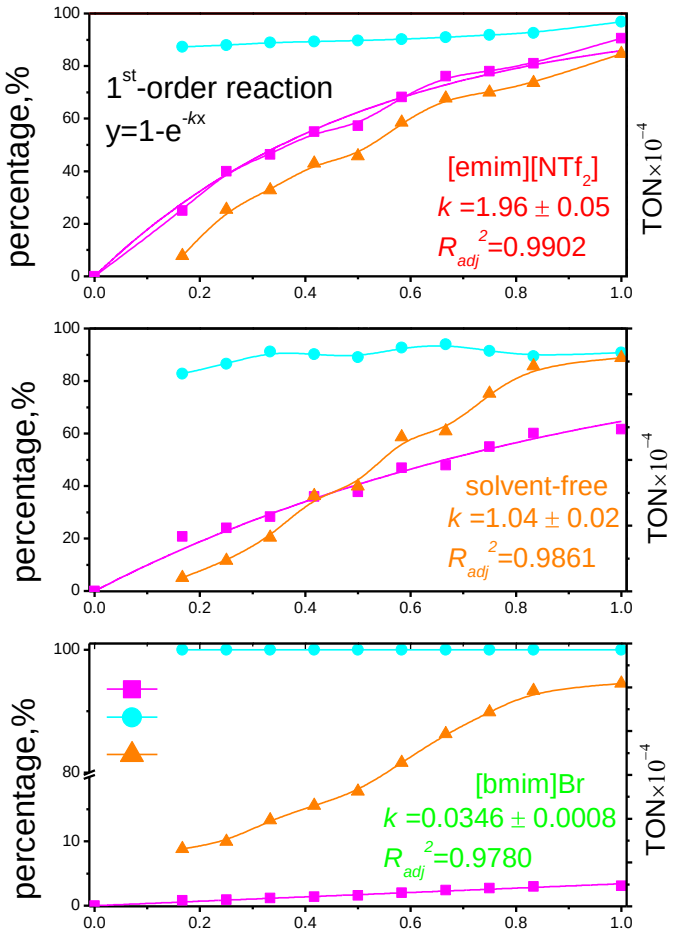

Fig.4.2 Time course of 1-phenylethanol oxidation in different media.

The selectivities toward acetophenone show a similar trend along with

conversions in the presence of [emim][NTf_2],which is higher than that under the solvent-free conditions, accompanied by a trace amount of ethylbenzene as the only detectable byproduct. Another frequently used IL [bmim]Br as also introduced for comparison. Pd/CNT [Bmim]Br is detrimental for the reaction, showing an extremely low conversion of 3.1% (TON of 5120) after reacting for 1h.

The plots were fitted with first-order reaction kinetics; the reaction rate constants k are 1.96 ± 0.05, 0.0346 ± 0.0008, 1.04 ± 0.02 h^{-1} for [emim][NTf_2], [bmim]Br and solvent-free conditions, respectively (Fig. 4.2). Therefore, further investigations on the effects of various reaction parameters will be focused on using [emim][NTf_2] as an additive.

4.2 Intrinsic activity examination of the heterogeneous catalytic system for the aerobic oxidation of 1-phenylethanol with ionic liquid as additive

The steadily increased conversion of 1-phenylethanol in [emim][NTf_2] indicates that the Pd catalyst is stable even at high temperatures. According to Table 4.2. Variation of reaction conditions for the oxidation of 1-phenylethanol to acetophenone over Pd/CNT catalyst-for instrinsic activity examination[a].

Entry	Ionic liquid	V_{IL}(mL)	IL molar fraction (%)	Conv. (%)	Select.[b] (%)	TOF $\times 10^{4}$[c] (h^{-1})

1	-	-	0	7.0	99.9	-
2	-	-	0	13.5	86.6	8.9
3	[emim][NTf_2]	2	8.7	17.3	87.5	11.3
4	[emim][NTf_2]	4	16.0	24.8	94.9	16.3
5	[emim][NTf_2]	8	23.7	20.4	87.7	13.4
6	[emim][NTf_2]	12	31.8	17.6	86.1	11.5
7	[emim][NTf_2]	16	38.3	14.5	85.3	9.5
8	[emim][NTf_2][d]	4	16.0	8.8	50.1	-
9	[emim][NTf_2]	4	16.0	20.7	91.6	13.6
10	[emim][NTf_2][f]	4	16.0	6.2	71.6	4.0
11	[emim][NTf_2][g]	4	16.0	12.4	90.2	8.1

a. reaction conditions: 100 mmol of 1-phenylethanol, 5 mg of Pd/CNT, 40 mL/min of O_2, 160 ^oC, 1h. Uncertainties: conv. ± 0.15%, select. ± 0.35%, TOF (h^{-1}) ± 0.08%. b. Ethylbenzene is the only by-product. c. TOF (h^{-1}) was calculated based on D_{Pd} obtained from CO-stripping (conversion is controlled in the low range, ≤20%) and values are identical with TON. d. no catalyst. IL recovered after the reaction. f. N_2 used. g. air used.

the fitted result, this is a 1st-order reaction respect to 1-phenylethanol (reaction rate constant k =1.96±0.05, R_{adj}^2=0.9902). Nevertheless, the reaction may be in a deactivation region due to the high conversion. To interpret the activity in a

more precise way, we repeated the reactions listed in Table 1 and controlled the substrate conversion at/below 20% by increasing the amount of substrate fourfold while maintaining the catalyst amount and IL molar fraction constant. In these reactions, 100 mmol of 1-phenylethanol, 5 mg of Pd/CNT catalyst and a corresponding amount of [emim][NTf_2] were used.

The catalytic results are shown in Table 4.2 where TOFs are reported to evaluate the intrinsic activity. The low activity in the absence of catalyst and IL (entry 1) is due to the non-catalytic oxidation. The conversion is almost doubled (entry 2) by adding Pd/CNT. Mixture of substrate and IL [emim][NTf_2] shows a moderate activity and rather poor ketone selectivity (entry 8), confirming the essential role of heterogeneous Pd/CNT catalyst. The molar fraction of [emim][NTf_2] remarkably affects the catalytic activities. The TOF increases sharply and then declines in the presence of excess [emim][NTf_2], concomitant with good selectivities (entry 3-7). The best activity is achieved when IL is 16.0 mol% and can be well maintained using recovered IL (entry 9). When using N_2 or air as alternatives, it is distinct that higher O_2 partial pressures contribute to better catalytic activities, implying that sufficient O_2 is crucial to enhance the dehydrogenation and suppress the hydrogenolysis side reaction. Noteworthily, regardless of the variation of reaction conditions and as far as intrinsic activity concerned, TOFs for 100 mmol-scale 1-phenylethanol

oxidation show comparable values of TONs within 1 h reaction to 25 mmol-scale oxidation when using same amounts of Pd/CNT catalyst. The steady catalytic performance, regardless of changing the substrate/catalyst ratio, verifies that reaction is conducted in a kinetic region; dehydrogenation is the rate-limiting step without any mass transfer limitation.

4.3 Recycle of the heterogeneous catalytic system (both Pd catalyst and ionic liquid)

Diethyl ether was applied to extract the organic components in the [emim][NTf_2] , obtaining the purified [emim][NTf_2].

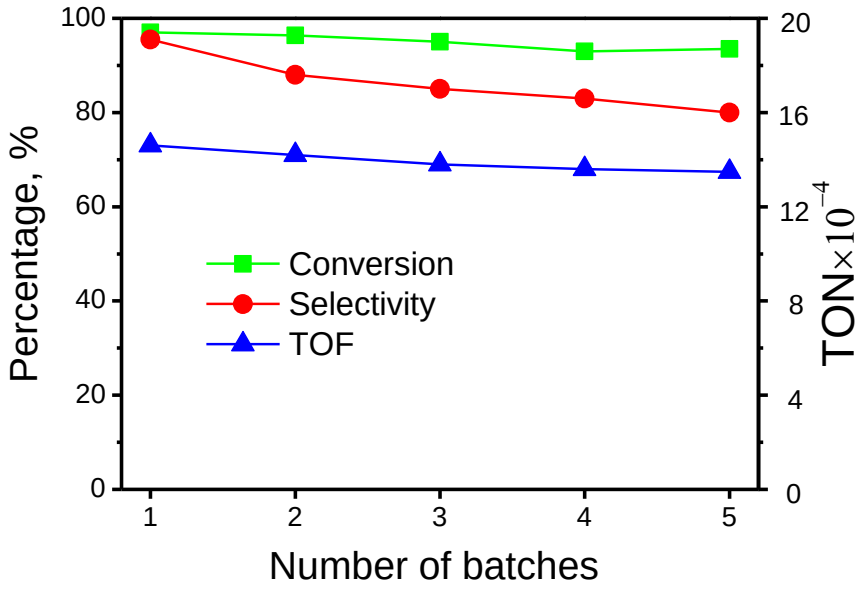

Fig.4.3 Recyclability of Pd/CNT. Run conditions: see footnote of Table 4.1.

Other than recycling the [emim][NTf_2] additive (Table 1,entry 9), the [emim][NTf_2] can be easily recovered after reaction and re-use in the next run,

showing a high TON of 135 000 (entry 9).

The recyclability of a Pd/CNT catalyst was also investigated (Fig. 4.3). There is only a slight deterioration for both catalytic activity and acetophenone selectivity during the repeated use of catalyst for 5 cycles, which can be contributed by the partial loss of catalysts during the recovery. Therefore, [Emim][NTf_2] not only promotes the catalytic performance but also enhances the resistance against deactivation. It has been verified that no observable leaching of the Pd catalyst occurs. Negligible conversion is observed when the liquid filtrate is used as catalyst for further reaction. It is suggested that metal is more resistant against leaching in a less polar solvent [25] which accounts for the catalyst stability in [emim][NTf_2].

4.4 The effect of temperature

The effect of reaction temperature was also examined (Fig. 4.4). The acetophenone selectivity is well maintained above 95% in the studied temperature range. The activity is hardly detectable at low reaction temperatures, whereas shows a sharp step increase above 100^{o}C. Despite the increased O_2 solubility, the rate of alcohol dehydrogenation decreases remarkably at low temperatures [24]. The high activation energy barrier (71.9 kJmol^{-1}) to initiate the reaction implies the absence of mass-transfer limitation in this catalytic system.

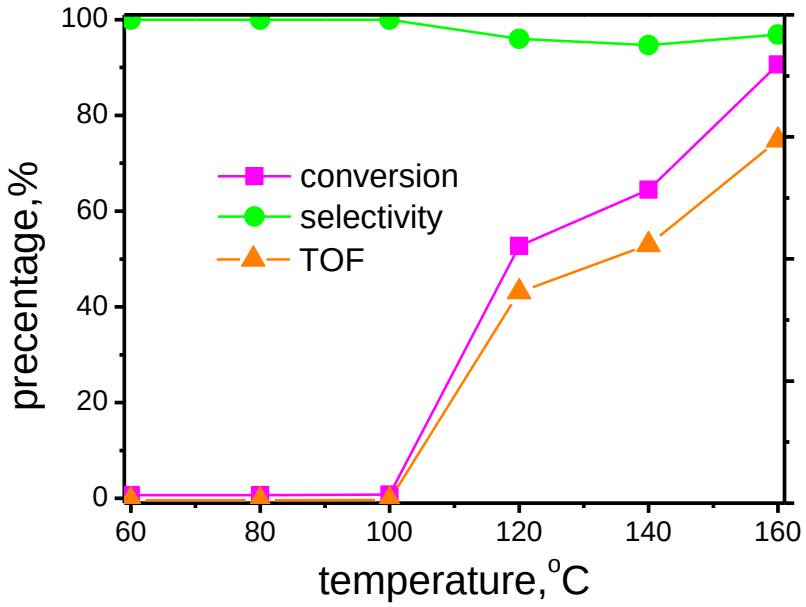

Fig.4.4 The effect of temperature. Run conditions: see footnote of Table 4.1.

4.5 The effect of oxygen pressure

N_2 and air were employed as alternatives of O_2 (Table 4.1, entries 10 and 11), showing that the catalytic activity increases with a higher O_2 partial pressure. When using N_2, the low alcohol conversion corresponds to the dehydrogenation mechanism where β-H elimination occurs upon dissociative adsorption of the substrate on active sites even in the absence of O_2 but suffers a fast catalyst deactivation due to product deposition on the Pd surface [2, 22].

The considerably low acetophonone selectivity is contributed by the C–O bond hydrogenolysis, affording the formation of ethylbenezne due to the abundant hydride species covered on the Pd surface and consequent catalyst deactivation [24].

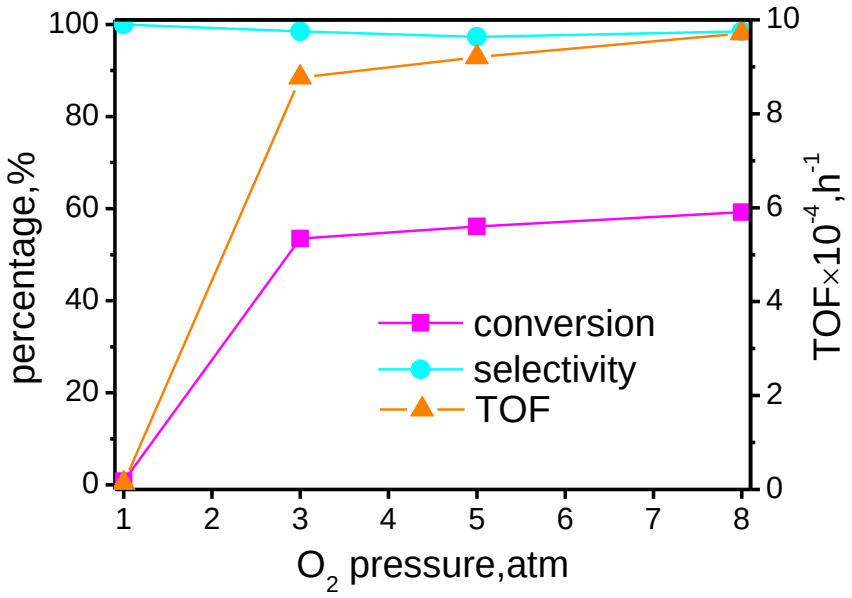

Fig.4.5 The effect of oxidaiton pressure. Run conditions: see footnote of Table 4.1.

Therefore, sufficient O_2 is essential to maintain the reaction in the kinetic region where the dehydrogenation but not the mass-transport is the rate-limitting step and to continuously consume surface Pd–H species. Elevating the O_2 total pressure from the atmosphere pressure to 3 atm leads to a drastically increased activity due to the enhanced solubility of O_2 (Fig. 4.5). Nonetheless, the activity reaches a plateau when further increasing the O_2 pressure, implying that the reaction is of zero order in O_2.1 Meantime, it is also speculated that abundant PdO phases may be formed concomitantly in the presence of excess O_2, resulting in the loss of metallic Pd active sites and consequently suppressed dehydrogenation step [24].

4.6 The improved catalytic activity due to the nature of ILs

Considering the similarity of cations in both ILs, the inferiority of [bmim]Br to [emim][NTf_2] can be addressed by the different nucleophilicities of two anions.[NTf_2]$^-$ is considered as a non-nucleophilic and innocent anion, i.e., more electrophilic compared to Br^- [21] In Pd-catalyzed alcohol oxidation following a dehydrogenation mechanism, electrons are transferred through a consecutive cycle from alcohol to H-acceptor (i.e., molecular O_2 via Pd active species [22]. When Pd nanoparticles are surrounded by an electrophilic enviroment, the electron transfer is accelerated due to the decreased electron density on Pd, leading to an enhanced catalytic activity. The electrophilicity of [NTf_2] also accounts for the moderate activity in the absence of a Pd/CNT catalyst (Table 4.1, entry 8). However, acetophenone and ethyl-benzene were produced in approximately equal amounts, suggesting that Pd/CNT can effectively suppress the hydrogenolysis of 1-phenylethanol. Furthermore, in addition to the better solubility of O_2 in IL, the remarkably improved catalytic rate in the [emim][NTf_2]-mediated reaction can be attributed to the hydrophobicity of [emim][NTf_2], which enriches the alcohol concentration at the catalyst–liquid inter-face where the reaction occurs and facilitates the desorption of hydrophobic ketone from catalyst surfaces [23]. On the contrary, the hydrophilic [bmim]Br is prone to adsorb on the catalyst surfaces which are

also hydrophilic after acid-pretreatment, thus poisoning the active sites and suppressing the reaction.

4.7 The effect of IL on the Pd/CNT catalyst

The effects of ILs on Pd/CNT, including both the Pd active sites and the CNT supports are further investigated by XPS, TEM and Raman characterizations of fresh Pd/CNT and spent catalysts collected after reaction without any post-treatment.

In Fig. 4.6 (a), fresh Pd/CNT shows two chemical states: metallic Pd and $Pd^{\delta+}$ assigned to PdO which is due to incomplete reduction or exposure in air.

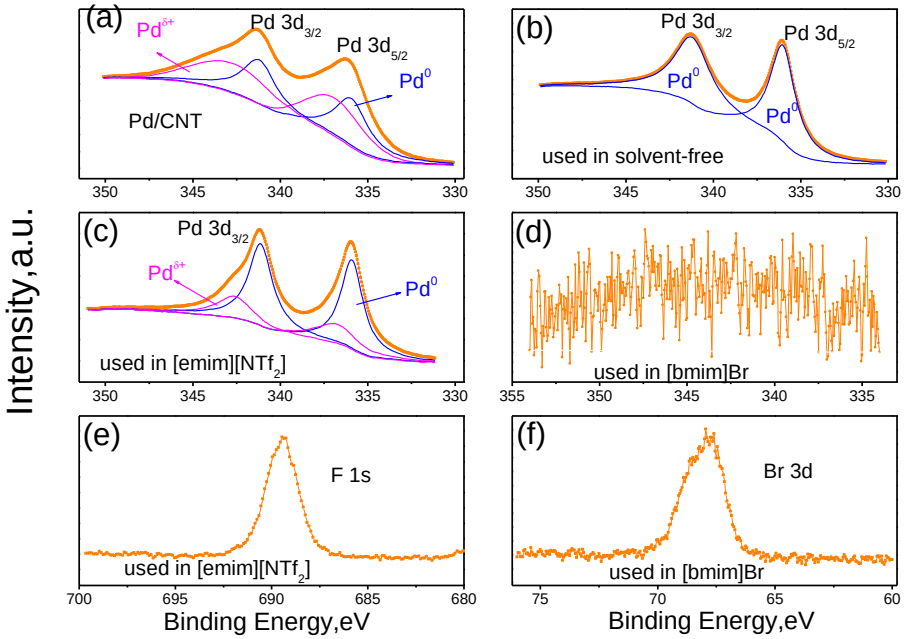

Fig.4.6 XPS spectra: (a) fresh Pd/CNT; (b) Pd/CNT used under solvent-free conditions; (c) Pd/CNT used in [emim][NTf_2]; (d) Pd/CNT used in [bmim]Br ((a)–(d): Pd 3d region); (e) Pd/ CNT used in [emim] [NTf_2] (F 1s region); (f)

Pd/CNT us ed in [bmim]Br (Br 3d region).

Nonetheless, Pd $^{\delta+}$ disappears after reaction under solvent-free conditions due to the reduction by an alcohol substrate. Considering the presence of F (Fig. 4.6 (b)), Pd $^{\delta+}$ which is ca. 28% of Pd surfaces in Pd/CNT used in [emim][NTf_2] is attributed to Pd–F bonds, indicating the interaction of [NTf_2]$^-$ and Pd active sites during thereaction.26 Surprisingly, no Pd signal is detectable in Pd/CNT used in [bmim]Br while the existence of Br has been verified (Fig. 4.6 (f)).

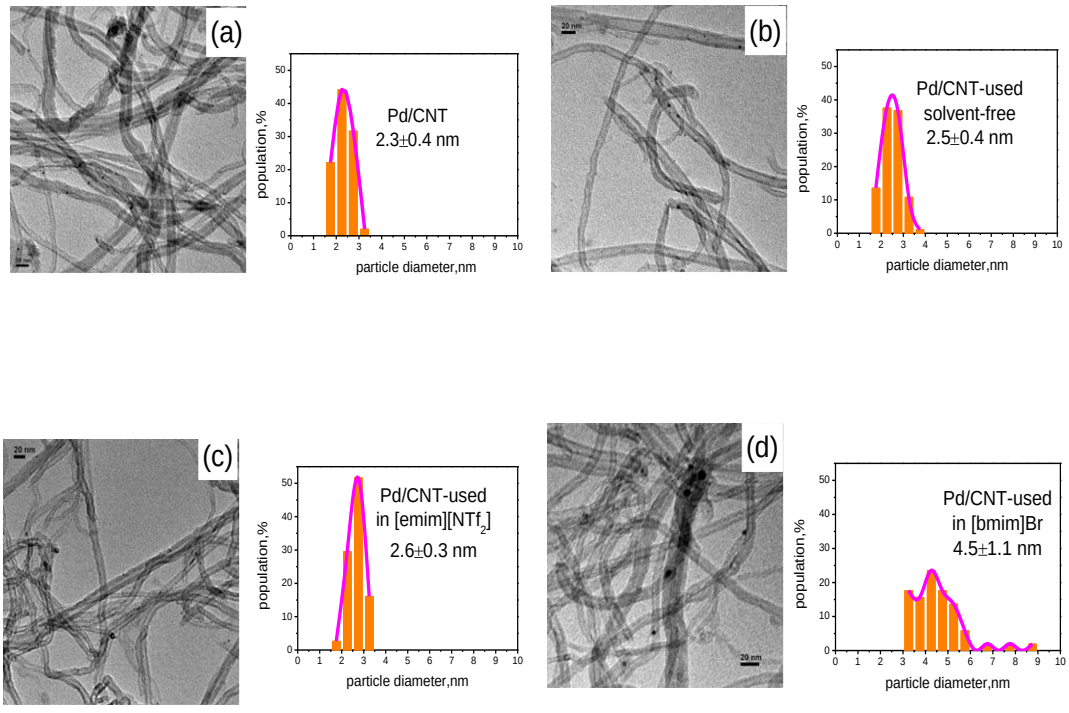

Fig. 4.7 TEM micrographs and size distribut ions: (a) fresh Pd/CNT; (b) Pd/CNT used under solvent-free condition; (c) Pd/CNT used in [emim][NTf_2]; (d) Pd/CNT used in [bmim]Br.

TEM observation shows Pd nanoparticles for this particular spent catalyst (Fig.4.7 (d)) and no Pd leaching occurs during the reaction. We suggest that Pd was covered by a thick layer of [bmim]Br. Two control experiments were carried out to verify this speculation (Table 1, entries 12 and 13).

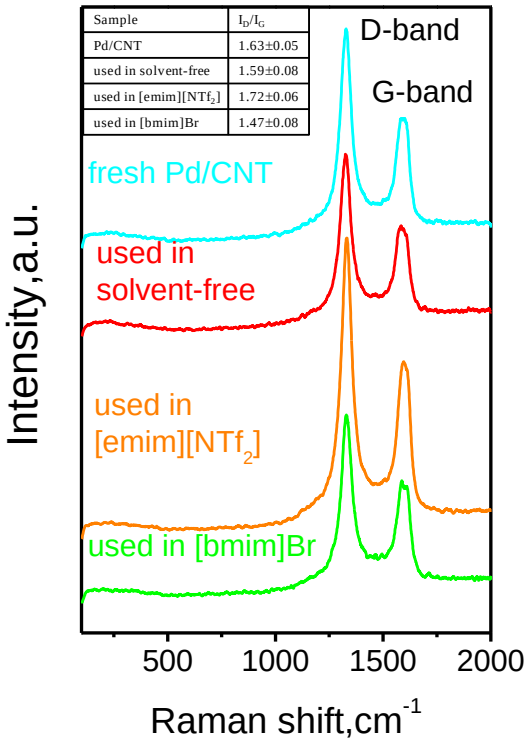

Fig. 4.8 Raman spectra of fresh and used Pd/CNT catalysts. [Bmim]Br alone shows no activity in the oxidation. After the catalyst in [bmim]Br was recovered by washing with acetone and re-used in a new reaction without any additive, comparable activity was observed with the solvent-free condition (entry 2). Therefore, when employed as an additive, hydrophilic [bmim]Br quickly adsorbs and accumulates on catalyst surfaces, resulting in catalyst

deactivation. This can be also confirmed by the decreased I_D/ I_G ratio in the Raman spectrum, which implies the diminished CNT defects due to [bmim]Br coverage (Fig. 4.8).

4.8 Catalytic performance of the heterogeneous catalytic system with [emim][NTf$_2$] as co-solvent on various alcohols

The aerobic oxidation of various alkene substrate scopes was also carried out and the results are summarized in Table 4.2.

For the aromatic alcohols with electron donating groups, such as 4-methylbenzyl alcohol, the catalytic system with [emim][NTf_2] involved still showed rather good activity, while for the ones with the electron-withdrawing groups and the aliphatic alcohols, limited activity was obtained.

Table 4.3. Oxidation of various alcohols by Pd/CNT in [emim][NTf_2] ionic liquid[a].

Entry	Substrate	Product	Conv. (%)	Select.[b] (%)	TON ×10[4b](h^{-1})
1	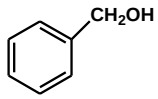	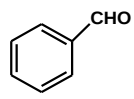	60.8	94.9	10.0
2	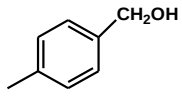	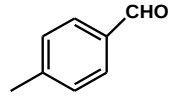	71.5	94.8	11.7

3	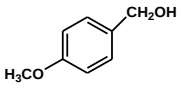	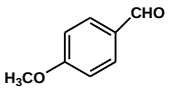	12.1	100	2.0
4	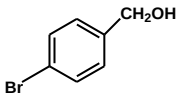	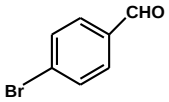	2.9	100	0.5
5	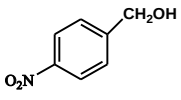	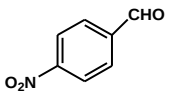	1.0	100	0.2
6	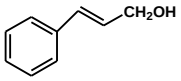	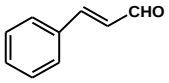	36.5	100	6.0
7	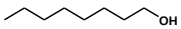		0.3	100	0.05
8	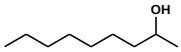	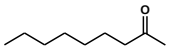	11.5	100	1.9

a.Reaction conditions: 25 mmol of substrate, 5 mg of Pd/CNT, 4 mL of [emim][NTf_2], 20 mL/min of O_2, 160 ^oC, 1h. Uncertainties: conv. ±0.15%, select. ± 0.35%, TON ±0.08%. b. TON was calculated based on D_{Pd} obtained from CO-stripping. c. byproduct: toluene (2.2%) and benzoic acid (2.9%). d. byproduct: p-xylene (5.2%)

4.9 Comparison of the catalytic performance with the present heterogeneous Pd catalyzed aerobic oxidation of 1-phenylethanol

The catalytic performance of the IL involved catalytic system including Pd/CNT is compared with those catalyzed by the representative heterogeneous Pd catalysts for the aerobic oxidation of 1-phenylethanol as shown in Table 4.4. The comparison result indicate that with IL involved the catalytic system is superior among the present catalytic systems of Pd catalysts.

Table 4.4. Aerobic oxidation of 1-phenylethanol catalyzed by a series of heterogeneous catalytic systems with Pd catalysts.

Catalytic System	Conversion (%)	Selectivity (%)	TOF[a] (h^{-1})	Ref.
Pd/CNT	67.6	90.8	111000	this work
Pd/CNT+[emim][NTf_2]	90.6	96.9	149000	this work
0.05-Pd-M41-AE	8.4	97.2	8637	[27]
Pd/NaX	66	97	626	[28]
0.5%Pd@C-Glu_A-550	-	80	157747	[29]

4.10 Conclusion

The aerobic oxidation of 1-phenylethanol over a carbon nanotube supported palladium catalyst was improved with an ionic liquid additive [emim][NTf_2], showing an excellent TON of149 000 which can be maintained for 5 recycle

runs.

Reproduced from Chem. Commun., 2011, 47, 6452–6454 with permission from Royal Society of Chemistry.

References

[1] D. I. Enache, J. K. Edwards, P. Landon, B. Solsona-Espriu, A. F. Carley, A. A. Herzing, M. Watanabe, C. J. Kiely, D. W. Knight and G. J. Hutchings, Science 311 (2006) 362–365.

[2] T. Mallat and A. Baiker, Chem. Rev. 104 (2004) 3037-3058.

[3] R. A. Sheldon, I. W. C. E. Arends, G.-J. ten Brink and A. Dijksman, Acc. Chem. Res. 35 (2002) 774–781.

[4] T. F. Blackburn and J. Schwartz, J. Chem. Soc., Chem. Commun. (1977) 157-158.

[5] K. Mori, T. Hara, T. Mizugaki, K. Ebitani and K. Kaneda, J. Am.Chem. Soc. 126 (2004) 10657-10666.

[6] F. Li, Q. H. Zhang and Y.Wang , Appl. Catal., A 334 (2008) 217-226 .

[7] Y. T. Chen, Z. Guo, T. Chen and Y. H. Yang, J. Catal. 275 (2010) 11-24.

[8] J. S. Wilkes and M. J. Zaworotko, J. Chem. Soc., Chem. Commun. (1992) 965-967.

[9] T. Welton, Coord. Chem. Rev. 248 (2004) 2459-2477.

[10] L. Rodrı´guez-Pe´rez, C. Pradel, P. Serp, M. Go´mez and E. Teuma, ChemCatChem 3 (2011) 749-754.

[11] L. Rodriguez-Perez, E. Teuma, A. Falqui, M. Gomez and P. Serp, Chem. Commun. (2008) 4201-4203.

[12] R. Singh, M. Sharma, R. Mamgain and D. S. Rawat, J. Braz. Chem. Soc. 19 (2008) 357-379.

[13] R. A. Brown, P. Pollet, E. McKoon, C. A. Eckert, C. L. Liotta and P. G. Jessop, J. Am. Chem. Soc. 123 (2001) 1254-1255.

[14] F. Favre, H. Olivier-Bourbigou, D. Commereuc and L. Saussine, Chem. Commun. (2001) 1360-1361.

[15] C. J. Mathews, P. J. Smith and T. Welton, Chem. Commun. (2000) 1249-1250.

[16] K. R. Seddon and A. Stark, Green Chem. 4 (2002) 119-123.

[17] Y. S. Chun, J. Y. Shin, C. E. Song and S. G. Lee, Chem. Commun. (2008) 942-944.

[18] V. Farmer and T. Welton, Green Chem. 4 (2002) 97-102.

[19] R. Sheldon, Chem. Commun. (2001) 2399-2407.

[20] V. R. Choudhary, D. K. Dumbre, V. S. Narkhede and S. K. Jana, Catal. Lett. 86 (2003) 229-233.

[21] R. Bini, C. Chiappe, E. Marmugi and D. Pieraccini, Chem. Commun. (2006) 897-899.

[22] J. Muzart, Tetrahedron 59 (2003) 5789-5816.

[23] Y. Chen, W. Chen, Q. Tang, Z. Guo, Y. Yang and F. Su, Catal. Lett. 141 (2010) 149-157.

[24] C. Keresszegi, J. D. Grunwaldt, T. Mallat and A. Baiker, J. Catal. 222 (2004) 268-280.

[25] A . Abad, A. Corm a and H . G arcia, Chem. Eur. J. 14 (2008) 212-222 .

[26] A. P. Umpierre, G. Machado, G. H. Fecher, J. Morais and J. Dupont, Adv. Synth. Catal. 347 (2005) 1404-1412.

[27] B. Qi, YB. Wang, LL. Lou, LY. Huang, Y. Yang, SX. Liu, J. Mol. Catal. A. 370 (2013) 95.

[28] F. Li, QH. Zhang, Y. Wang, Appl.Catal.A. 334(2008) 217.

[29] PF. Zhang, YT. Gong, HR. Li, ZR. Chen, Y. Wang, Nat. Commun. 4 (2013) 1593.

Chapter 5 Catalytic epoxidation of cis-cyclooctene over vanadium-exchanged faujasite zeolite catalyst with ionic liquid as co-solvent

Epoxidation of alkenes plays important roles in synthetic chemistry, allowing the hydrocarbon substrate converted to valuable precursors in the synthesis of fine chemicals [1]. Formulating highly efficient catalysts for alkene epoxidation therefore becomes a vital area in catalysis research. In recent years, a number of transition metal complexes have been reported to be effective in the homogeneous catalytic epoxidation of alkenes [2-4]. Nevertheless, homogeneous catalytic processes suffer the drawbacks such as the complication of metal complex synthesis and metal leaching during the reaction. In addition, it is rather difficult to retract the catalyst from reaction mixture for recycling purposes and the catalyst/product isolation generates large amounts of organic/inorganic wastes. Therefore heterogeneous catalysts which can overcome the above-mentioned problems of homogeneous catalysts are strongly desired. Tang et al. reported the epoxidation of styrene catalyzed by cobalt(II)-containing molecular sieves [5]. Iron-based solid catalysts were also attempted [6]. Our group showed the liquid phase *trans*-stilbene epoxidation over catalytically active cobalt substituted TUD-1 mesoporous materials (Co-TUD-1) using molecular oxygen [7]. Recently, a readily synthesized vanadium-exchanged faujasite zeolite catalyst (V-X) has been reported by our

group, which exhibited a reasonably good catalytic activity in the epoxidation of alkenes using *tert*-butyl hydroperoxide (TBHP) as the oxidant and dimethylformamide (DMF) as the solvent [8].

Ionic liquids (ILs) as 'green' solvents have attracted rapidly increased attention during the last few years. Interests in conducting catalytic processes in ILs have experienced a tremendous growth, and a variety of catalytic reactions have been successfully carried out in such neoteric media [9]. Indeed, many advantages of applying ILs as solvents are mainly due to their physical properties such as extremely low vapor pressure. In addition, IL is often referred to as 'designable solvent' because of their physical properties, such as melting point, viscosity, density, and solubility can be precisely tuned. As the investigation goes further more and more studies highlighted the importance of chemical nature of these unusual IL solvents that obviously affects the catalytic reactions through interaction with the catalyst or the components in the liquid phase. Srinivasan et al. proposed the formation of hydrogen bonding between IL cation and the carbonyl group of anhydrides as reactant [10]. The anions of IL possessing coordination atoms such as N, O, F were also proposed to be able to coordinate with the metallic active sites [11]. Moreover, it is generally accepted that the ionic characters of ILs provide the catalysts a unique ionic

environment that plays an important role in stabilizing the catalytically active species or the reaction intermediates [12, 13].

Up to now, the study of alkene epoxidation with ILs applied as solvent/co-solvent is mainly focused in the homogeneous catalytic processes. For instance, Anil et al. studied the tungstate complex in ILs [14]. Rhenium(VII) and molybdenum(VI) complexes in IL were investigated in the alkene epoxidation [15]. Manganese porphyrins in IL was also reported [16]. Nonetheless, the heterogeneous catalytic process with ILs as solvent/co-solvent for alkene epoxidation is rarely investigated; no detailed mechanistic study on the specific interaction between ILs and active sites/support/substrate was reported. In this work, the epoxidation of *cis*-cyclooctene over V-X catalyst with TBHP as oxidant and a representative IL 1-ethyl-3-methylimidazolium bis (trifluoromethylsulfonyl) imide ([emim][NTf_2]) as the co-solvent (along with DMF) was studied.. In addition, the IL 1-butyl-3-methylpyrrolidium bis (trifluoromethylsulfonyl) imide ([bmpy][NTf_2]) were also examined as co-solvent for comparison.

5.1 The catalytic performance of the heterogeneous catalytic system with ionic liquid [emim][NTf_2] involved as co-solvent for the epoxidation of cis-cyclooctene

Epoxidation of *cis*-cyclooctene is challenging mainly due to the weak nucleophilicity and rigid substrate structure [8]; and it was chosen as the chemically probed reaction in this study. [Emim][NTf_2] was introduced into DMF as co-solvent, and the catalytic results are summarized in Table 5.1. In the absence of catalyst, low *cis*-cyclooctene conversion and epoxide selectivity are observed in DMF solvent due to the non-catalytic epoxidation (entry 1). Epoxidation of *cis*-cyclooctene over V-X catalyst exhibits the conversion of 44.0% and selectivity of 94.0% towards epoxide in pure DMF accompanying small amounts of 2-cycloocten-1-one and cyclooctane-1, 2-diol as by-products (entry 2). Solvent has been reported to play a crucial role in the epoxidation: the solvent with low polarity such as chlorobenzene exhibits low *cis*-cyclooctene conversions while highly polar solvent may promote the activity [6].

Table 5.1. Epoxidation of *cis*-cyclooctene over V-X catalyst in different solvents[a].

Entry	Solvent	Co-solvent	R[b]	Conversion (%)	Selectivity[c] (%)
1	DMF[d]	-	-	5.3	34.6
2	DMF	-	-	44.0	94.0
3	[emim][NTf_2]	-	-	94.1	94.6
4	DMF	[emim][NTf_2]	4:1	54.4	96.8
5	DMF	[emim][NTf_2]	3:2	66.8	96.5
6	DMF	[emim][NTf_2]	2:3	90.0	93.0
7	DMF	[emim][NTf_2]	1:4	94.6	91.0

8	DMF[d]	[emim][NTf_2]	2:3	12.7	90.4
9	DMF	[bmpy][NTf_2]	2:3	85.4	90.9
10	DMF[e]	-	-	8.3	80.0
11	[emim][NTf_2][e]	-	-	92.6	93.7

a. Reaction conditions: 1mmol *cis*-cyclooctene, 0.2g V-X catalyst, 10 mmol TBHP, 80^{o}C, 24h. b. Molar ratio between [emim][NTf_2] and DMF in the mixed solvent. c. The main by-product is 2-cycloocten-1-one. d. no catalyst. e. 1 ml *t*-butanol is added.

Entries 3-7 show that [emim][NTf_2] distinctly promotes the catalytic performance: as the molar fraction of [emim][NTf_2] increases in the mixed solvent, *cis*-cyclooctene conversion remarkably increases and the selectivity towards epoxide remains constantly high. The best catalytic activity is obtained in pure [emim][NTf_2] solvent, showing the conversion of 94.1% and the selectivity of 94.6% towards epoxide (entry 3). A control experiment shows a considerable conversion of 12.3% (entry 8) in the mixed solvent (DMF and [emim][NTf_2]) in the absence of catalyst, implying that [emim][NTf_2] itself may facilitate the epoxidation of *cis*-cyclooctene as a catalyst. In addition, 2-cycloocten-1-one is the only by-product, which is distinct from the reaction in pure DMF. As shown in Table 5.1, the best catalytic activity is obtained in pure [emim][NTf_2] solvent. Nonetheless, due to the sticky nature of [emim][NTf_2] and economical consideration, a mixed DMF-[emim][NTf_2] solvent

(DMF:[emim][NTf_2] molar ratio 2:3) denoted as DMF-[emim][NTf_2] was chosen in the following studies.

5.2 Examination of reaction parameters for cis-cyclooctene epoxidation in DMF-[emim][NTf_2]

The kinetics results in DMF-[emim][NTf_2] solvent were benchmarked against those inpure DMF and pure [emim][NTf_2]. Fig. 5.1(a) shows the correlation between reaction time duration and catalytic conversions in DMF, DMF-[emim][NTf_2] and [emim][NTf_2]. In general, the *cis*-cyclooctene conversions in three reaction mixtures increase with the reaction time. In the entire reaction time range, the *cis*-cyclooctene epoxidation shows great advantages in the [emim][NTf_2]-involved solvents compared to pure DMF. For instance, after 6 hours of reaction, the conversions in both [emim][NTf_2]-involved reaction mixtures are remarkably higher than the conversion of 19.2% in pure DMF. After 30 hours of reaction, the conversions are around 96.0%in DMF-[emim][NTf_2] and [emim][NTf_2]. Further increasing the reaction time does not improve the conversion significantly. As shown in Fig. 5.1(b), the selectivity towards epoxide remains high in three reaction mixtures in the entire reaction time range and shows slight increase with the reaction time, which is due to the increased amounts of peroxo species with time. In the epoxidation of *cis*-cyclooctene, the allylic

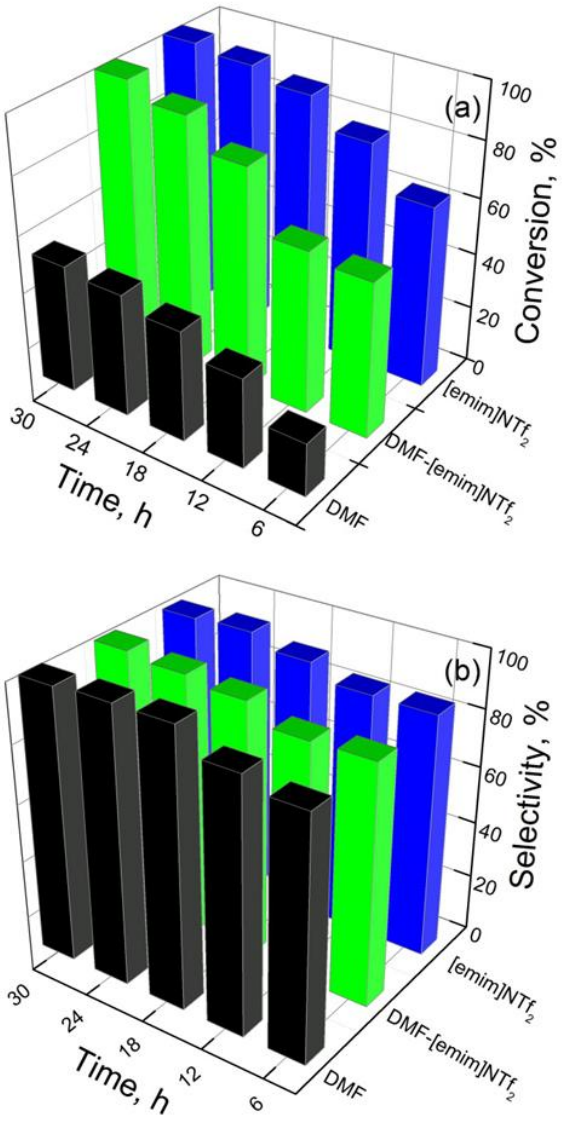

Fig.5.1. Kinetic profiles of *cis*-cyclooctene epoxidation at different reaction time. (a) conversion, (b) selectivity towards epoxide.

by-products (allylic alcohol and allylic aldehyde) are produced through the abstraction of allylic H atoms by radicals, while the epoxide is produced by the unimolecular Twigg re-arrangement after adding radical to the C=C bond.

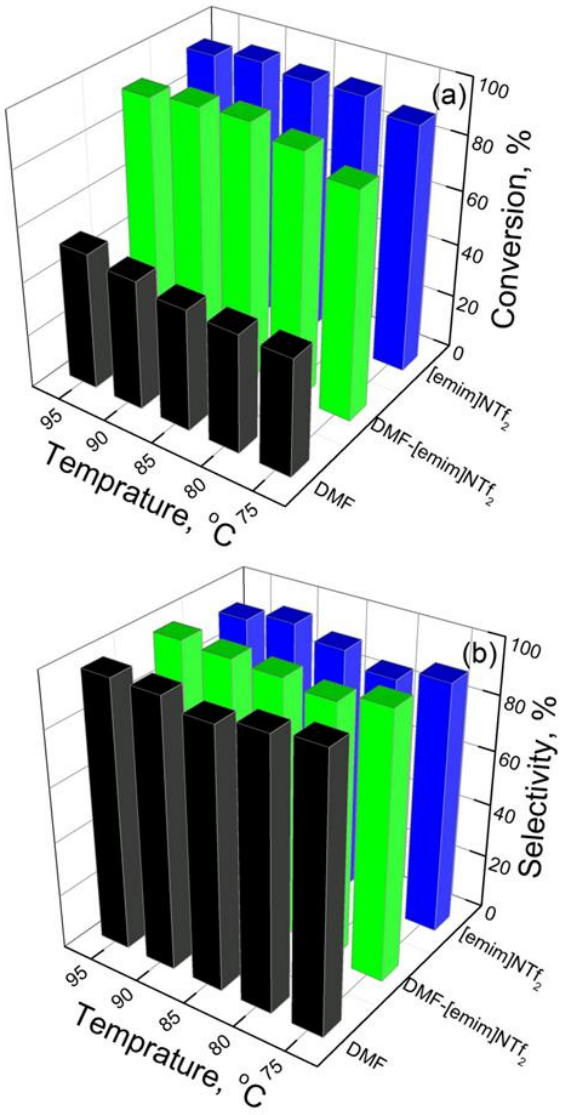

Fig. 5.2(a) shows the influence of reaction temperature on the epoxidation of *cis*-cyclooctene in three reaction solvents. *cis*-Cyclooctene conversion increases with the temperature in DMF.

The activation energy barrier of the abstraction step is higher than that of the addition step [17], therefore, the epoxidation of *cis*-cyclooctene favors the high epoxide selectivity.

While in DMF-[emim][NTf_2] and [emim][NTf_2], the conversion slightly increases with reaction temperature followed by slight decrease after 90 ^oC, which is attributed to the decomposition of TBHP at high temperature. The highest *cis*-cyclooctene conversion of 96.2% is obtained in [emim][NTf_2] at 90 ^oC.

Fig. 5.2(b) shows the correlation between reaction temperature and epoxide selectivity. In three mediums, the epoxide selectivity remains higher than 90% during the entire temperature range, showing no obvious change as the temperature increases.

5.3 Recycle of the heterogeneous catalytic system with ionic liquid [emim][NTf_2] as co-solvent

The recyclability of V-X catalyst in DMF-[emim][NTf_2] solvent was tested and the results are shown in Fig.5.3.

The spent V-X catalyst was collected by hot filtration after each reaction run, washed with acetone, dried, and re-used in the next reaction.The conversion of *cis*-cyclooctene gradually decreases after each testing run, which can be partially attributed to the vanadium active sites leached out during reaction because we noticed that the filtrate possessed a vague yellowish color while conducting the hot filtration.

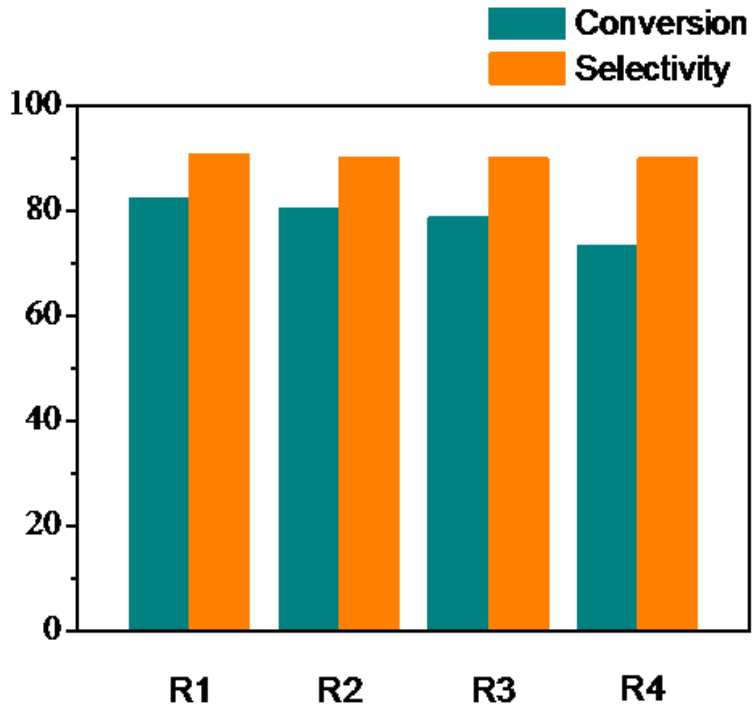

Fig. 5.3. The recycle of the V-X catalyst in the mixed solvent of DMF and [emim][NTf_2] (the molar ratio of DMF and [emim][NTf_2] is 2:3).

However, even recycled for four times, the V-X catalyst in the DMF-[emim][NTf_2] mixed solvent still shows a superior catalytic performance to that in DMF.

5.4 Characterizations of the spent V-X catalyst after reaction

Fig. 5.4 shows the XRD spectra of fresh and spent V-X catalysts. All samples show the diffraction patterns that are identical to pristine faujasite ($Na_2Al_2Si_2.5O_9$ $6.2H_2O$ XRD PDF card #00-038-0237), suggesting that the zeolitic crystalline structures of V-X catalysts were preserved during the

reaction. For the spent catalysts in IL mixed solvents, the intensity of XRD signal decreases due to the structure factors changed during the reaction [8].

SEM images in Fig. 5.5 show the morphology of both fresh and spent V-X catalysts (washed with acetone then dried for a clearer view).

The parent zeolite particles exhibit mono-dispersed nearly spherical morphology with diameter ranging from 2.0 to 2.5 μm.

Fresh V-X catalyst shows no obvious morphology change compared to the pristine zeolite.

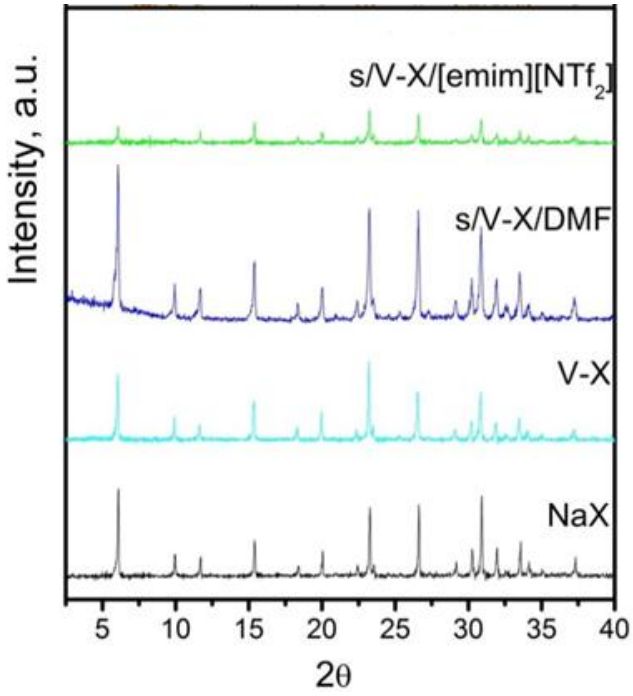

Fig. 5.4. XRD patterns of the fresh and spent V-X catalyst after reaction in different solvents.

The spent V-X catalysts show some morphology changes to different extents. The particle diameter of spent V-X catalyst in DMF clearly decreases

due to the cracking. For the particles of spent V-X catalyst in [emim][NTf_2], in addition to the diameter decrease and cracking, lumpy heaps are also observed.

Fig. 5.6 shows the UV-vis and UV-Raman spectra of fresh and spent V-X catalysts. For fresh V-X catalyst, the strong peak at 218 nm in the UV-vis spectrum has no distinct difference compared to the parent faujasite zeolite.

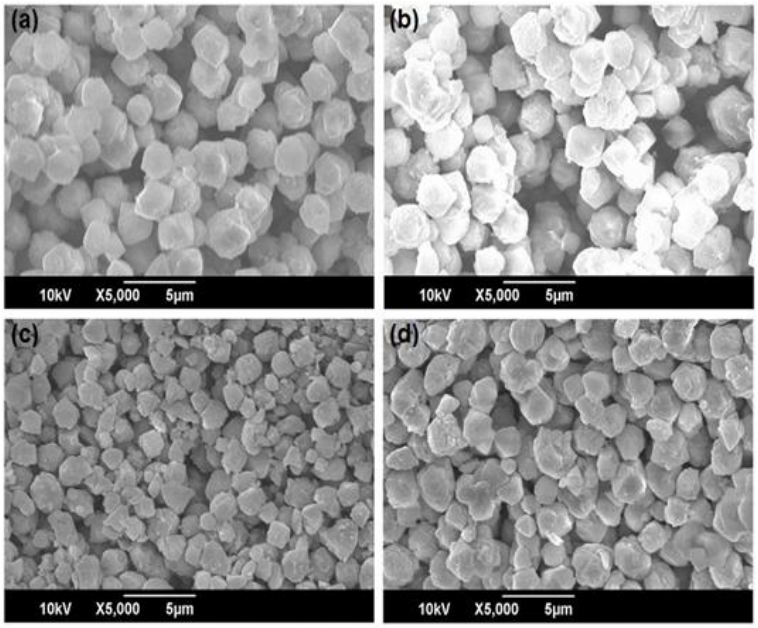

Fig. 5.5. SEM of the V-X catalyst after reaction in different solvents. (a) NaX, (b) V-X, (c) s/V-X/DMF (short for the spent V-X in DMF,), (d) s/V-X/ [emim][NTf_2]

The peak at 273 nm is attributed to V^{5+} in tetrahedral coordination [18-21]. The Raman bands at 294, 384 and 517 cm^{-1} are assigned to the parent faujasite zeolite. The 968 cm^{-1} band is due to V–O stretching [22, 23]. The sample is easily hydrated under ambient conditions, thus the V=O-H resonance under a

UV excitation causes the disappearance of the terminal V=O stretching bands in the range of 990–1050 cm^{-1}. From UV-vis and UV-Raman results, we conclude that the vanadium species of V-X catalyst is in V^{5+} valance and a distorted tetrahedral coordination [8]. The conclusion is consistent with the earlier-proposed tetrahedral model for the molecular structure of VO_4, which specifically has one short terminal and three long basal plane vanadium-oxygen bonds. The tetrahedral structure of vanadium species is generally considered to be responsible for the catalytic performance of the vanadium oxide catalysts [22-24].

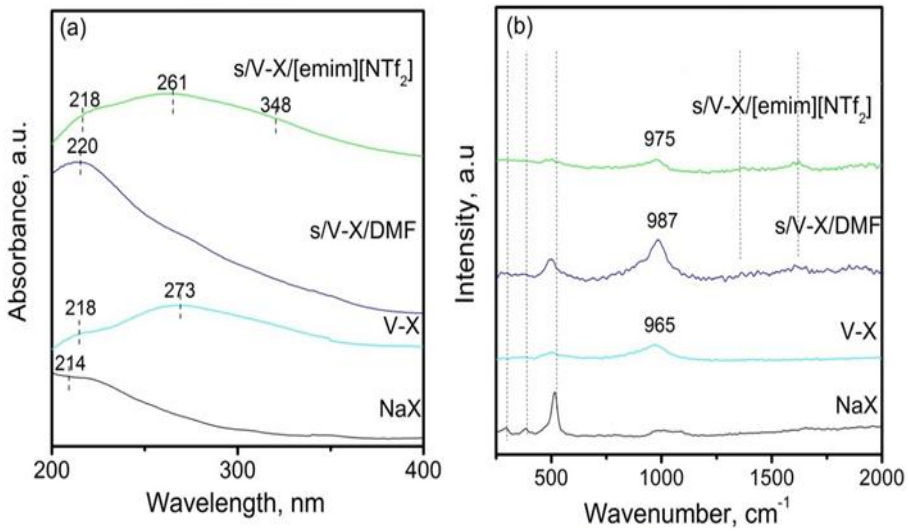

Fig.5.6. (a) UV-vis spectra of the spent V-X catalyst in different solvents; (b) UV-Raman spectra of the spent V-X catalyst in different solvents.

For the spent V-X catalyst in DMF, the UV-vis spectrum shows only one absorbance peak at 220 nm attributed to the zeolite support. Compared to the fresh catalyst, the peak at 273 nm disappears, implying the destructive

tetrahedral structure of vanadium species during the reaction. For the spent catalyst V-X in [emim][NTf_2], the peak at 261 nm assignable to V^{5+} in tetrahedral coordination is still retained [18-21]. The peak shows a bathochromic shift compared to the corresponding peak of fresh V-X catalyst at 273 nm. The higher energy band implies that a greater distortion of tetrahedral structure has been developed along with the decrease of coordination number [25, 26]. In addition, another broad peak appears at about 348 nm that can be assigned to the polyvanadate species in either tetrahedral or pentahedral coordination [18-21].

The fingerprint Raman bands for spent V-X catalysts in DMF and in [emim][NTf_2] are 987 and 975 cm^{-1}, respectively, both due to the V-O stretching [22, 23]. Compared with the band at 965 cm^{-1} for fresh V-X catalyst, a blue shift appears for both spent catalysts to different extents. The Raman shift of V-O stretching is often due to the coordination environment change of vanadium, leading to the steric change of mole structure of vanadium species, which induces the stretching energy change of V-O bond. For spent catalyst in [emim][NTf_2], the broad band in the range of 1350-1600 cm^{-1}, which is often assigned to alkenes and aromatic complexes [27], is due to the adsorbed organics (such as the reactant and IL) in the zeolite pores.

5.5 Discussion

XRD results along with the SEM images show the changes of zeolite structure and morphology, implying the interaction between the IL and zeolite. Further investigation is performed to study this specific interaction. The zeolite support (0.1 g) in the absence of vanadium active sites was soaked in the [emim][NTf_2] (5 ml) and stirred for 24 h under reaction condition, followed by filtrating, washing with acetone and drying overnight at 383 K. The treated zeolite with IL was denoted as d/X/IL and characterized by ^{29}Si MAS NMR. As shown in Fig. 5.7, the parent NaX shows chemical shifts at -83.5, -87.9, -92.4, -97.3 and -101.4 ppm that are respectively assigned to Q^4(4Al), Q^3 (3Al), Q^2 (2Al), Q^1 (1Al) and Q^0 (0Al) (Q^n (nAl) represents a Si atom bound to n-O-Al groups and 4-n-O-Sit groups [28]). Compared to the pristine NaX, the IL-treated zeolites show displaced Q^4 (4Al) and Q^3 (3Al) peaks and the peaks broaden to a different extend. The distortion of the corresponding tetrahedrons implies the interaction between IL cations and Na^+ [29]. Strong interaction between ILs and zeolite leads to the vanishing of Q^2 (2Al), Q^1 (1Al) and Q^0 (0Al) peaks. A certain amount of Na^+ is detected in the residue liquid after treating zeolite by IL as indicated by the ICP, which further supports the results.

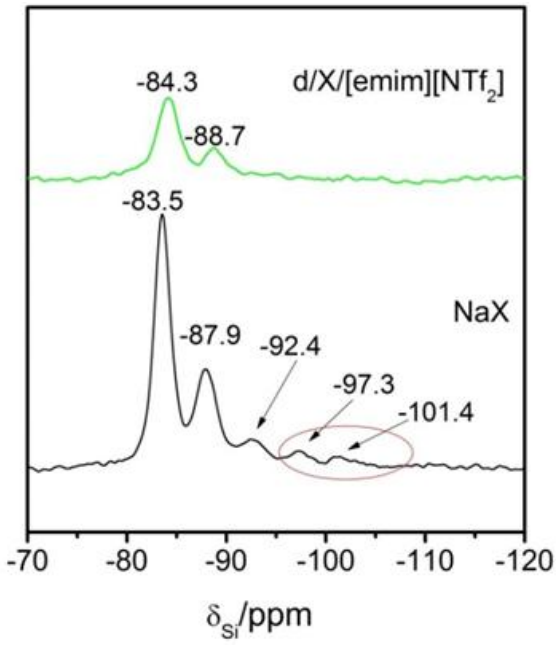

Fig. 5.7. The ^{29}Si MAS NMR spectra of the IL-treated NaX with IL.

The UV-*vis* and the UV-Raman results imply the coordination structures of vanadium active center are better preserved in IL-mixed solvent than in pure DMF. It is reasonable to assume that IL may interact with vanadium sites during the reaction. To investigate the possible interaction between IL and the vanadium active center, further control experiment and characterization were carried out: following similar procedures as the treatment of zeolite for the characterization of ^{29}Si MAS NMR, the V-X catalyst was treated, denoted as d/V-X/IL and characterized by XPS. As shown

in Fig. 5.8, the V $2p_{3/2}$ peak of d/V-X/IL catalyst at 517.8 eV shifts to a lower binding energy compared to that of the pristine V-X catalyst at 518.1 eV, indicating the slight increase of electron density of the vanadium center with

[emim][NTf_2] adsorbed. The binding energies of N 1s and F 1s for adsorbed [emim][NTf_2] shows no shift comparing to those of pristine [emim][NTf_2] as shown in Fig. 5.8.

The interaction between IL and heterogeneous catalyst, especially the metal oxide catalyst is complex. It was reported that the liquid–phase oxidation of pyrimidine thioether on Ti-SBA-15 with [emim][NTf_2] as the solvent showed superior catalytic activity [30].

The acidic C-H group (the carbon between two nitrogen atoms) of the imidazolium cation as hydrogen bonding donator is proposed to interact with the oxygen in the Ti-O bond, resulting in the increased Lewis acidity of the catalytic sites. However, the XPS spectra of pristine V-X and d/V-X/IL in this study indicate that the electron density of vanadium sites increases or rather the Lewis acidity of the catalytic site decreases when adsorbing ILs; furthermore, the binding energies of N 1s and F 1s for adsorbed [emim][NTf_2] of the d/V-X/IL do not shift compared to those of pristine [emim][NTf_2], therefore, the interaction between the IL and catalyst cannot be well correlated with the improved catalytic activity.

It is speculated that the catalytic performances of vanadium sites are affected through the cation exchange between the IL and the zeolite indirectly. Another aspect of the complexity in an IL-involved catalytic system is that

except for the interaction between IL and the catalyst, the interaction between IL and the substrate in the liquid phase also matters.

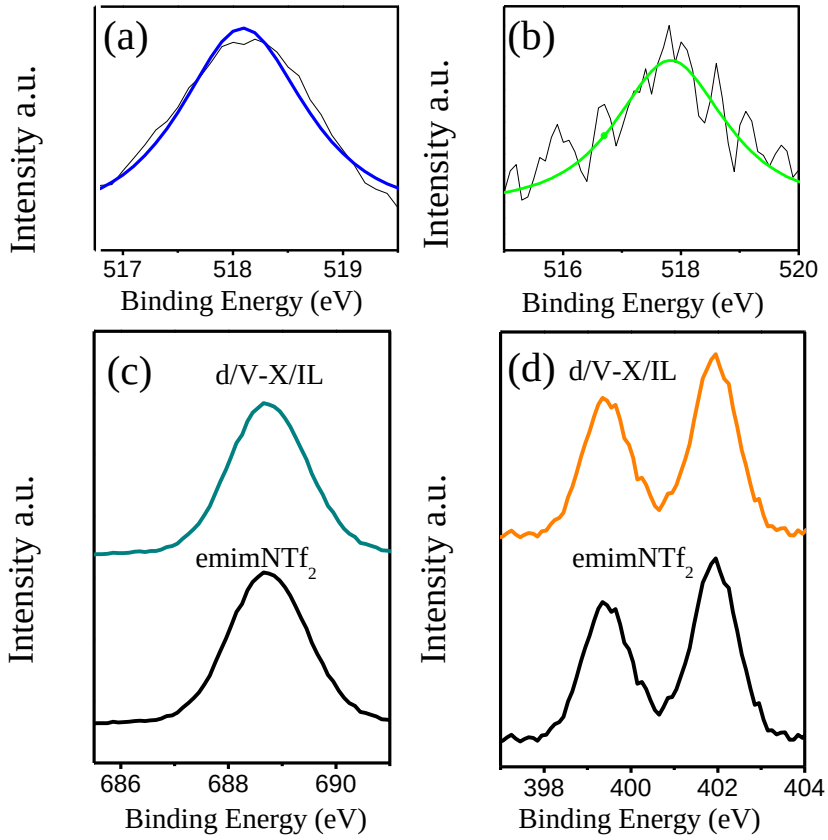

Fig. 5.8. (a) The V $2p_{3/2}$ spectra of V-X; (b) the V $2p_{3/2}$ spectra of the IL-treated V-X; (c)the comparison of N 1s spectra of V-X and the IL-treated V-X; (d) the comparison of F 1s spectra of V-X and the IL-treated V-X.

During the epoxidation, the by-product *t*-butanol and a small amount of water also form complexes with the catalytic sites; therefore compete the adsorption with TBHP to hinder the reaction [31]. Recently IL has continued to attract considerable interest in catalysis due to its capability of hydrogen

bonding [32]. Different from organic solvents, IL solvent may coordinate with *t*-butanol through hydrogen bonding [33] [34] and pull the *t*-butanol by-product away from the active sites, which in turn free the active site for adsorbing substrate and oxidant. In this regards, the anion of IL is proposed to play the main role to form hydrogen bonds [34]. To further verify the hypothesis mentioned above, additional *t*-butanol was introduced in the reaction. As shown in Entry 10 in Table 1, the reaction was obviously inhibited in pure DMF solvent due to the addition of *t*-butanol, while adding *t*-butanol does not affect the catalytic activity in IL-involved solvent as shown in Entry 11. Therefore, the improved catalytic performance in the presence of IL as co-solvent or solvent in epoxidation might be attributed to the specific hydrogen bonding interaction between the IL with *t*-butanol as well as water. Having the same anion with [emim][NTf_2], the reaction with [bmpy][NTf_2] as the co-solvent for comparison has shown similar catalytic activity (Entry 9), which agrees well with the hypothesis described above.

Iglesia et al. have addressed the importance of support acidity in the epoxidation of alkene with TBHP as oxidant over the Ti oxide catalyst [35]. Strong Brønsted acids open epoxide rings rapidly in the presence of trace amounts of water and lead to low epoxide yields. The catalyst will also be deactivated via chelation of Lewis acid active sites by the alkane diols. While

the density functional theory studies suggested that the formed hydrogen-bonded structures between the vicinal weakly acidic protons and the vanadium peroxo intermediate will decrease the activation barrier for the kinetically relevant step. In this study, the cation of IL may easily get exchanged with the Na^+ of NaX zeolite; hence the exchanged imidazolium cation capable of affording weak acidic proton might decrease the activation energy of the kinetically relevant step by H-bonding effect.

5.6 Catalytic performance of the heterogeneous catalytic system with [emim][NTf_2] as co-solvent on various alkenes

The epoxidation of various alkene substrate scopes was also carried out and the results are summarized in Table 5.2.

1-Heptene as a representative aliphatic alkene shows the increased conversion from 37.3% in DMF (entry 1) to 69.0% in DMF-[emim][NTf_2] (entry 2), with 2-heptenol as the only product instead of the corresponding epoxide. As shown in entry 3, the conversion of cyclohexene is only 5.6% in DMF, while the conversion is elevated to 73.2% in DMF-[emim][NTf_2] with 2-cyclohexen-1-one and cyclohexene epoxide as main products (entry 4). Styrene shows a high conversion of 98.0% as well as the epoxide selectivity of 53.4% in DMF (entry 5). In DMF-[emim][NTf_2] mixed solvent, not only the high conversion of 98.5% was maintained for styrene epoxidation, but also is

the epoxide selectivity greatly improved to 89.4%. For *trans*-stilbene, high conversion and epoxide selectivity have already been achieved in DMF (entry 7),

Table 5.2. Substrate scope of alkene epoxidation over V-X catalyst in mixed solvent[a].

Entry	Reactant	Solvent	Co-solvent	Conversion (%)	Selectivity[b] (%)
1	1-Heptene	DMF	-	37.3	0
2	1-Heptene	DMF	[emim][NTf_2]	69.0	0
3	Cyclohexene	DMF	-	5.6	66.7
4	Cyclohexene	DMF	[emim][NTf_2]	73.2	55.0
5	Styrene	DMF	-	98.2	53.4
6	Styrene	DMF	[emim][NTf_2]	98.5	89.4
7	*trans*-Stilbene	DMF	[emim][NTf_2]	96.5	86.3
8	*trans*-Stilbene	DMF	[emim][NTf_2]	100.0	83.5

a. Reaction conditions: 1mmol reactant, 0.2g V-X catalyst, 10 mmol TBHP, 80^{o}C, 24h, the molar ratio between DMF and [emim][NTf_2] in the mixed solvent is 2:3. b. The selectivity is towards corresponding epoxide. In supplement, for 1-heptene, the 1-hepten-3-ol is the main product; for cyclohexene, the main by-product is 2-cyclohexen-1-one; for styrene, the main by-products are benzaldehyde and benzoic acid; for trans-stilbene the main by-products are benzaldehyde and benzoic acid.

no remarkable improvement is observed when introducing [emim][NTf_2] to the solvent (entry 8).

5.7 Conclusion

The efficient selective epoxidation of *cis*-cyclooctene over V-X catalyst in DMF using TBHP as the oxidant has been reported in this work. The *cis*-cyclooctene conversion is greatly improved as well as the high epoxide selectivity is maintained in the presence of [emim][NTf_2] as co-solvent. In addition to the high polarity of IL, the superior catalytic activity with [emim][NTf_2]-involved solvent is summarized to be attributed to the following reasons. The vanadium active site shows improved stability in the [emim][NTf_2]-involved solvent, and the effective molecular structure of vanadium active site is well preserved. The hydrogen bonding between [emim][NTf_2] and by-product *t*-butanol prevents the coordination of *t*-butanol with vanadium center; hence improves the catalytic efficiency. Due to the weak acidity of the imidazolium cation, it is also proposed that the hydrogen bonding between the weak acidic protons with the vanadium peroxo intermediate may decrease the activation energy barrier of the kinetically relevant steps.

References

[1] Q.H. Xia, H.Q. Ge, C.P. Ye, Z.M. Liu, K.X. Su, Chemical Reviews 105 (2005) 1603-1662.

[2] M.H. Dickman, M.T. Pope, Chemical Reviews 94 (1994) 569-584.

[3] J.-M. Bregeault, Dalton Transactions (2003) 3289-3302.

[4] K.A. Joergensen, Chemical Reviews 89 (1989) 431-458.

[5] Q. Tang, Q. Zhang, H. Wu, Y. Wang, Journal of Catalysis 230 (2005) 384-397.

[6] J. Liang, Q. Zhang, H. Wu, G. Meng, Q. Tang, Y. Wang, Catalysis Communications 5 (2004) 665-669.

[7] X.-Y. Quek, Q. Tang, S. Hu, Y. Yang, Applied Catalysis A: General 361 (2009) 130-136.

[8] S. Hu, D. Liu, C. Wang, Y. Chen, Z. Guo, A. Borgna, Y. Yang, Applied Catalysis A: General 386 (2010) 74-82.

[9] J.P. Hallett, T. Welton, Chemical Reviews 111 (2011) 3508-3576.

[10] A.R. Gholap, K. Venkatesan, T. Daniel, R.J. Lahoti, K.V. Srinivasan, Green Chemistry 5 (2003) 693-696.

[11] Y. Chen, L. Bai, C. Zhou, J.-M. Lee, Y. Yang, Chemical Communications 47 (2011) 6452-6454.

[12] M.-A. Neouze, Journal of Materials Chemistry 20 (2010) 9593-9607.

[13] J.W. Lee, J.Y. Shin, Y.S. Chun, H.B. Jang, C.E. Song, S.-g. Lee, Accounts of Chemical Research 43 (2010) 985-994.

[14] A. Kumar, Catalysis Communications 8 (2007) 913-916.

[15] D. Betz, W.A. Herrmann, F.E. Kühn, Journal of Organometallic Chemistry 694 (2009) 3320-3324.

[16] S. Tangestaninejad, M. Moghadam, V. Mirkhani, I. Mohammadpoor-Baltork, R. Hajian, Inorganic Chemistry Communications 13 (2010) 1501-1503.
[17] U. Neuenschwander, I. Hermans, The Journal of Organic Chemistry 76 (2011) 10236-10240.
[18] S. Ferdov, Z. Lin, R.A. SáFerreira, Microporous and Mesoporous Materials 96 (2006) 363-368.
[19] B. Solsona, T. Blasco, J.M. López Nieto, M.L. Peña, F. Rey, A. Vidal-Moya, Journal of Catalysis 203 (2001) 443-452.
[20] Z. Wu, H.-S. Kim, P.C. Stair, S. Rugmini, S.D. Jackson, The Journal of Physical Chemistry B 109 (2005) 2793-2800.
[21] S. Hu, D. Liu, L. Li, A. Borgna, Y. Yang, Catal Lett 129 (2009) 478-485.
[22] K. Tran, M.A. Hanning-Lee, A. Biswas, A.E. Stiegman, G.W. Scott, Journal of the American Chemical Society 117 (1995) 2618-2626.
[23] H.-S. Kim, P.C. Stair, The Journal of Physical Chemistry A 113 (2009) 4346-4355.
[24] M. Huang, S. Shan, C. Yuan, Y. Li, Q. Wang, Zeolites 10 (1990) 772-777.
[25] G. Catana, R.R. Rao, B.M. Weckhuysen, P. Van Der Voort, E. Vansant, R.A. Schoonheydt, The Journal of Physical Chemistry B 102 (1998) 8005-8012.
[26] S. Dzwigaj, Current Opinion in Solid State and Materials Science 7 (2003) 461-470.
[27] Z. Wu, P.C. Stair, Journal of Catalysis 237 (2006) 220-229.
[28] E. Lippmaa, M. Maegi, A. Samoson, M. Tarmak, G. Engelhardt, Journal of the American Chemical Society 103 (1981) 4992-4996.
[29] A.N. Fitch, H. Jobic, A. Renouprez, The Journal of Physical Chemistry 90 (1986) 1311-1318.

[30] V. Cimpeanu, A.N. Pârvulescu, V.I. Pârvulescu, D.T. On, S. Kaliaguine, J.M. Thompson, C. Hardacre, Journal of Catalysis 232 (2005) 60-67.

[31] R.A. Sheldon, J.A. Van Doorn, Journal of Catalysis 31 (1973) 427-437.

[32] A. Aggarwal, N.L. Lancaster, A.R. Sethi, T. Welton, Green Chemistry 4 (2002) 517-520.

[33] J.L. Anderson, J. Ding, T. Welton, D.W. Armstrong, Journal of the American Chemical Society 124 (2002) 14247-14254.

[34] L. Cammarata, S.G. Kazarian, P.A. Salter, T. Welton, Physical Chemistry Chemical Physics 3 (2001) 5192-5200.

[35] J.M. Notestein, L.R. Andrini, F.G. Requejo, A. Katz, E. Iglesia, Journal of the American Chemical Society 129 (2007) 15585-15595.

Chapter 6 One-pot production of bio-derived chemicals from renewable resources: Transformation of cellobiose into formic acid and levulinic acid over ionic liquid-based polyoxometalate composites.

Biomass has been extensively discussed as one of the alternatives for energy and chemical production due to its abundance, high energy content, sustainability and biodegradability. As compared with existing techniques (enzymatic fermentation, high-temperature pyrolysis and thermal gasification), aqueous phase catalytic transformation of non-edible biomass resources (e.g. cellulose) with high efficiency and selectivity to valuable chemicals or bio-fuels is more desirable [1-3]. Although various routes for the catalytic conversion of biomass resources have been explored [4–7], transformation of cellulose into valuable platform molecules in a one-pot approach is undoubtedly one of the most attractive routes for biomass utilization. Yan et al. reported the one-pot transformation of cellobiose (a model compound of cellulose) to C_6-alcohols on Ru-based catalyst by combining hydrolysis and hydrogenation in aqueous medium [8]. A high yield of 62.3% toward 5-hydroxymethyl furfural (5-HMF) from lignocellulosic biomass materials was obtained by using an ionic liquid as solvent and an inorganic salt of $CrCl_3$ as homogeneous catalyst [9]. Shunmugavel and co-workers also developed a catalytic transformation of disaccharides to ethyl levulinate that is the final product of 5-HMF rehydration

in the presence of a functionalized ionic liquid with strong Brønsted acidity [10].

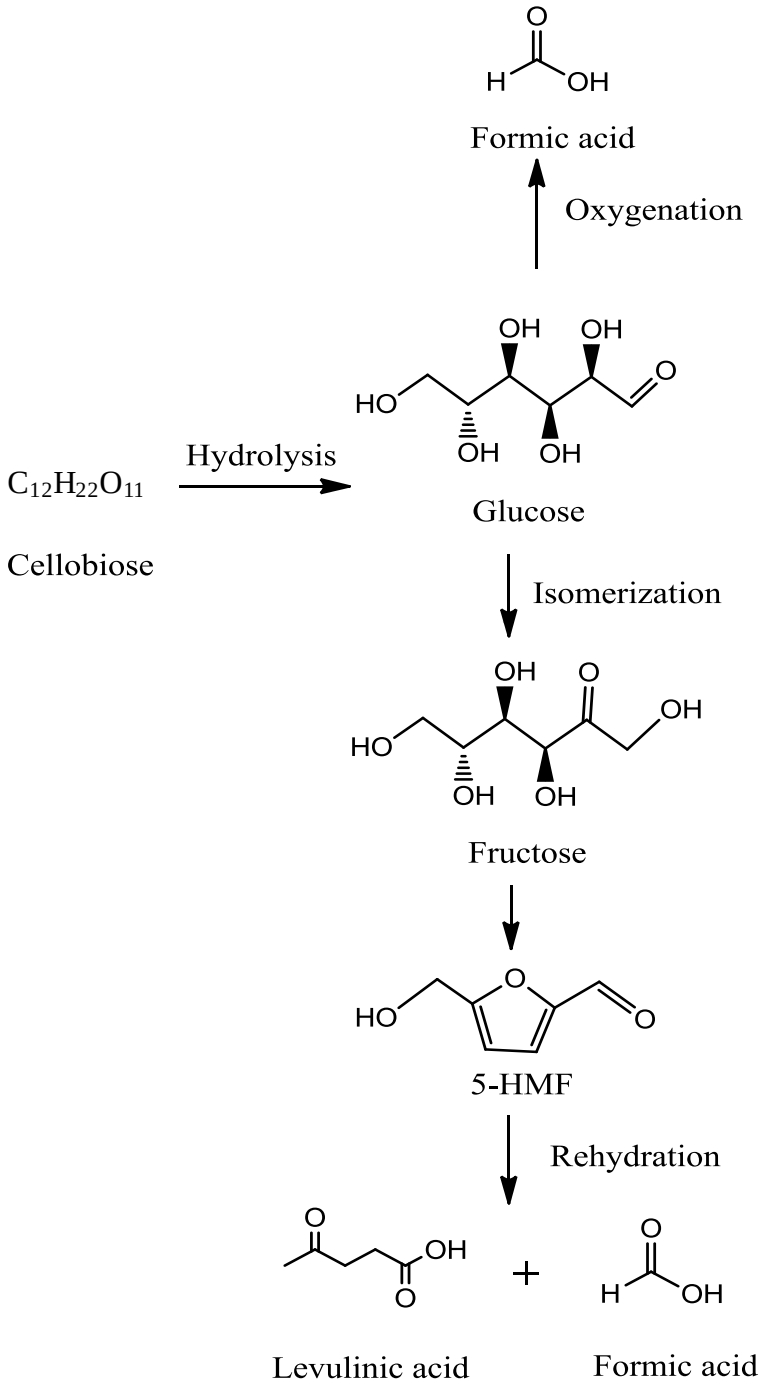

Scheme 6.1 Catalytic conversion of cellobiose to formic acid and levulinic

acid. In recent years, one-pot synthesis combining hydrolytic and oxidative degradation of biomass resources has been discerned to be an alternative route for efficiently producing valuable platform molecules. Catalyzed by gold nanoparticles loaded on nitric acid-pretreated carbon nanotubes, selective oxidation of cellobiose to gluconic acid proceeded efficiently in the aqueous solution with molecular dioxygen [11]. Recently, Wasserscheid et al. have reported a catalytic route to produce formic acid (FA) with extremely high selectivity in the conversion of biomass-based carbohydrates in the presence of $H_5PV_2Mo_{10}O_{40}$ as a bifunctional catalyst and molecular dioxygen. Although this catalytic system required a long reaction time and the detailed mechanism remained unclear, it provided a novel route for the sustainable production of FA that has been considered as an important commodity chemical and an energy carrier with high energy density [12]. Inspired by these great progresses in catalytic biomass transformation, it is believed that sustainable production of energy carriers and chemicals via the one-pot synthetic procedure will be realized by exploring multiple-functional catalysts.

Ionic liquid-heteropolyanion (IL-HPA) salts have been reported to show excellent catalytic performance and self-separation behavior in esterification process [13]. Due to its high melting point and polarity, IL-HPA salt dissolved in the polar solvent and acted as a homogeneous catalyst during the reaction at

high temperatures and precipitated as gelatinous solids at low temperatures, which made the catalyst recovery remarkably convenient [13]. In our previous work, the IL-HPA salts comprised of Keggin-type HPA and functionalized Brønsted acidic IL cation were found to afford similar catalytic performance and separation behavior in transesterification of trimethylolpropane [14]. Nonetheless, all these results about IL-HPA demonstrated that the HPA was primarily responsible for the self-separation rather than a catalytic active site carrier. In this study, a series of multi-functional ionic liquid based polyoxometalate (IL-POM) comprising IL cations with strongly acidic groups and POM anions containing various metal atoms (tungsten, molybdenum and vanadium) were designed, fabricated and employed in one-pot catalytic transformation of cellobiose to valuable chemicals in the presence of molecular dioxygen (Scheme 6.1). Both the Brønsted acidic sites in the IL cations and the redox catalytic sites in POM anions involved in the catalytic reaction. Upon the hydrolysis of cellobiose, subsequent oxygenation and rehydration led to selective C-C bond cleavage of the sugar intermediates. As a result, FA, formed by both oxygenation and rehydration, and Levulinic acid (LA), formed by rehydration, were found to be the dominant products. Moreover, the separation of IL-POM catalyst from the reaction mixture was simply achieved by filtration.

6.1 Structure characterization of as-synthesized IL-POM catalysts

FT-IR spectra of some representative as-synthesized IL-POM catalysts were collected and shown in Fig. 6.1. The IR bands at 1633 and 1486 cm^{-1}, which are observable for all $[PyBS]^+$ cation-based IL-POM catalysts, are attributed to the characteristics stretching vibrations modes of C-H and C=N, of pyridium ring, respectively. Characteristic IR bands at 794, 914, 976 and 1033 cm^{-1} were observed for $[PyBS]_4SiW_{12}O_{40}$ (Fig. 6.1c), indicating the Keggin structure is well preserved in the $[PyBS]_4SiW_{12}O_{40}$ catalyst.

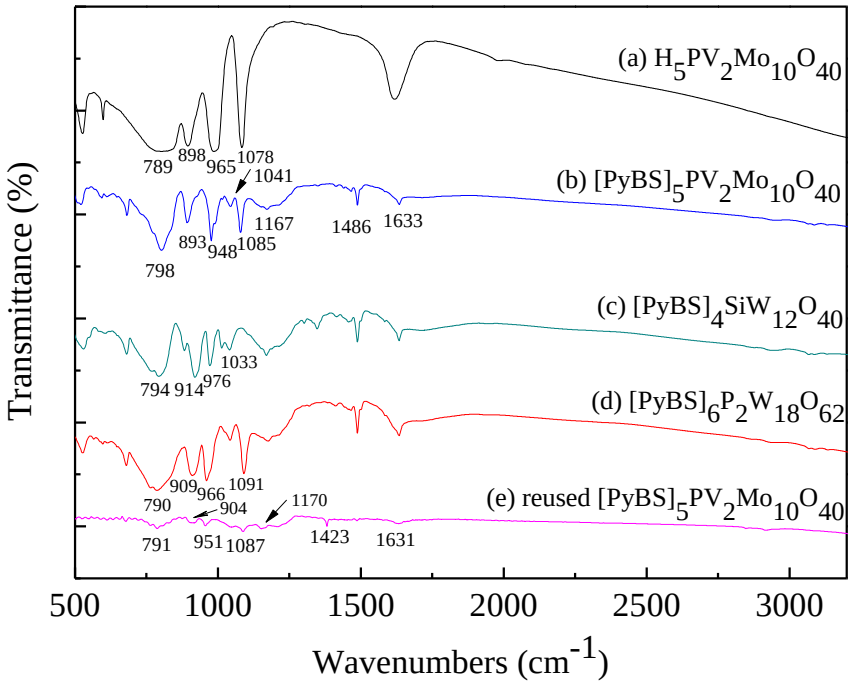

Fig. 6.1 FT-IR spectra of different catalyst (a) $[H_5PV_2Mo_{10}O_{40}$ (b) $[PyBS]_5PV_2Mo_{10}O_{40}$ (c) $[PyBS]_4SiW_{12}O_{40}$ (d) $PyBS]_6P_2W_{18}O_{62}$ (e) reused $[PyBS]_5PV_2Mo_{10}O_{40}$ after 4 runs

Similarly, the as-synthesized $[PyBS]_6P_2W_{18}O_{62}$ (Fig. 6.1d) possesses typical Dawson structure as evidenced by its characteristic IR bands at 790, 909, 966 and 1091 cm^{-1} attributed for ν(W-O_c-W), ν(W-O_b-W), ν_{as}(W=O_t) and ν(P-O), respectively.

The IR spectrum for Keggin-structured vanadium-containing $[PyBS]_5PV_2Mo_{10}O_{40}$ (Fig. 6.1b) shows slight difference in the characteristic bands for the POM anions from its parent molybdovanadophosphoric heteropoly acid ($H_5PV_2Mo_{10}O_{40}$, Fig. 6.1a) due to the structural distortion induced by the donation of conjugated π electrons of organic cations to inorganic anions [15,16]. Moreover, the IR band at 1078 cm^{-1} for ν(P-O) in $H_5PV_2Mo_{10}O_{40}$ is observed to split into two bands at 1085 and 1041 cm^{-1} after the protons are completely substituted by $[PyBS]^+$ cations, indicating the formation of extra hydrogen bonds between terminal oxygen atoms of POM anions and sulfate functional group in the IL cations [17-18]. Accordingly, it is speculated that the solid nature of these as-synthesized IL-POM composites at room temperature (melting points > 373 K) mainly arises from the existence of numerous extra hydrogen bonds and strong electrostatic interaction between the IL cations and the POM anions.

XRD patterns for $H_5PV_2Mo_{10}O_{40}$, $H_4SiW_{12}O_{40}$, $H_6P_2W_{18}O_{62}$, $[PyBS]_4SiW_{12}O_{40}$, $[PyBS]_5PV_2Mo_{10}O_{40}$, and $[PyBS]_6P_2W_{18}O_{62}$ are also

collected and shown in Fig. 6.2. The measured XRD patterns of both Keggin-structured $H_5PV_2Mo_{10}O_{40}$ and $H_4SiW_{12}O_{40}$ and Dawson-structured $H_6P_2W_{18}O_{62}$ are in good consistence with reported diffraction patterns in literature [18].

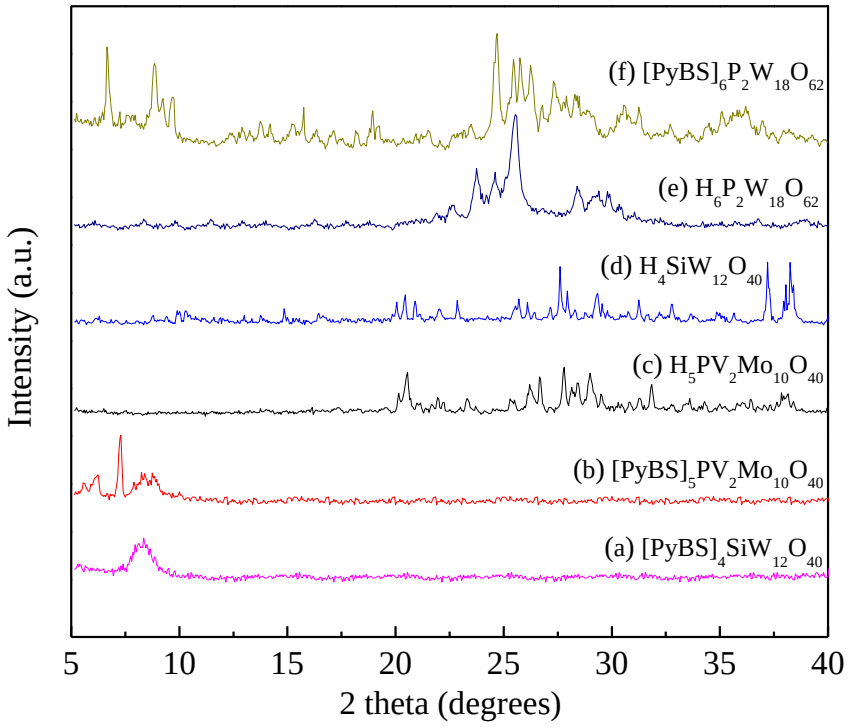

Fig. 6.2 XRD patterns of (a) $[PyBS]_4SiW_{12}O_{40}$ (b) $[PyBS]_5PV_2Mo_{10}O_{40}$ (c) $H_5PV_2Mo_{10}O_{40}$ (d) $H_4SiW_{12}O_{40}$ (e) $H_6P_2W_{18}O_{62}$ (f) $[PyBS]_6P_2W_{18}O_{62}$.

Moreover, the diffraction peaks for these three proton-type heteropoly acids are distinct and sharp, indicating the high crystallinity. After the protons in Keggin-structured $H_5PV_2Mo_{10}O_{40}$ and $H_4SiW_{12}O_{40}$ are completely replaced by $[PyBS]^+$ cations, characteristic XRD peaks in the range of 15~40° almost completely disappear, suggesting the low crystallinities of $[PyBS]_4SiW_{12}O_{40}$

and $[PyBS]_5PV_2Mo_{10}O_{40}$. Introducing organic $[PyBS]^+$ cations greatly influences the crystallization of POM anions and then results in the formation of a semi-amorphous structure.

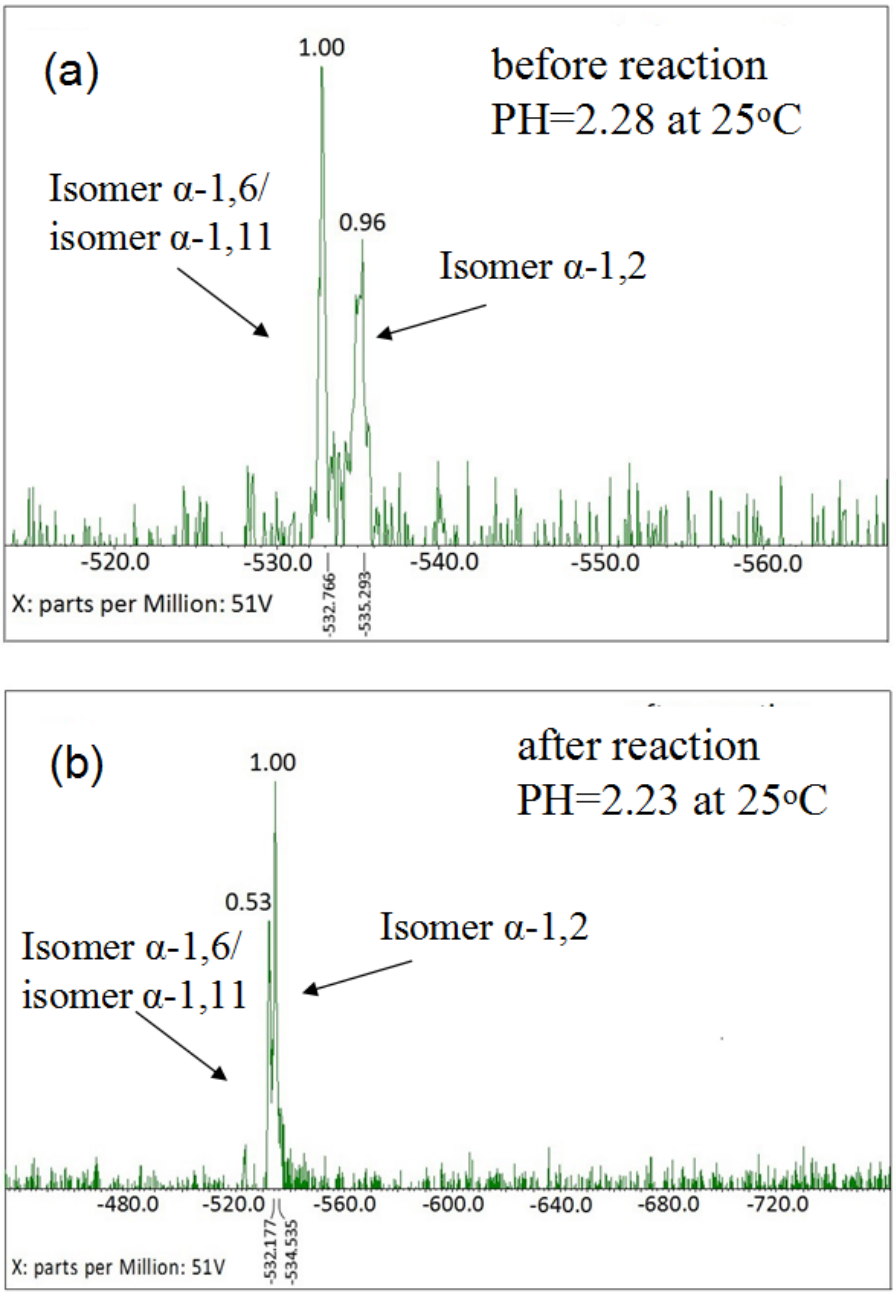

Fig. 6.3 ^{51}V NMR spectrum of $[PyBS]_5PV_2Mo_{10}O_{40}$ before and after reaction.

However, some diffraction peaks in the range of 5~10 ° emerge and they cannot be observed for parent heteropoly acids ($H_5PV_2Mo_{10}O_{40}$ and $H_4SiW_{12}O_{40}$). These low angle diffractions indicate the existence of facets with large inter-planar spacing according to the Bragg equation. Therefore, it is deduced that a unique inorganic-organic hybrid material with relatively large cavities is formed as Keggin structured POM anions combine with organic $[PyBS]^+$ cations. Differently, Dawson-structured POM based IL-POMs ($[PyBS]_6P_2W_{18}O_{62}$) reserve XRD diffractions clearly in the range of 15~40 °. Nonetheless, those peaks in the range of 5~10 °, which cannot be found in the XRD pattern of proton-typed Dawson heteropoly acids, is still clearly observed.

In brief, the characterization results reveal that Keggin or Dawson type IL-POM catalysts synthesized in this study retain the typical POM structural features of particular combination of oxygen with metals and non-metals while POM anions bond with the organic IL cations, as confirmed by the preservation of characteristic IR bands. However, various factors, such as supercritical electrostatic interactions between organic cations and inorganic anions, hydrogen bonding, Van der Waals forces, etc., greatly influence the crystallization behavior of the IL-POM compounds in atypical XRD patterns [19].

The vanadium-containing IL-POMs are further characterized by ^{51}V-NMR

spectrometry to gain information on the local symmetry of vanadium site.

According to the previous result [21], there are five possible Keggin structures for $[PV_2Mo_{10}O_{40}]^{5-}$, and they are identified by different rotated degrees on their X-O axis of edge-sharing M_3O_{13} group in the Keggin structure.

The ^{51}V-NMR chemical shift of these five positional isomers significantly varies with different pH values of medium in the range of 0-2, whereas changes smoothly when the pH value is above 2. According to the abundance and chemical shift ($\delta_{3\sigma}$) in a ^{51}V-NMR spectrum reported by Pettersson et al. [20], the chemical shift of ~-532 ppm shown in Fig. 6.3 is assigned to isomer α-1, 2 and the chemical shift of ~-534 ppm is assigned to isomer α-1,6 and isomer α-1,11. Moreover, these two chemical shifts are within ~2 ppm range, which is consistent well with the data reported by Pettersson and co-workers. Quantitative analysis shows that the molar ratio of isomer α-1, 2 to isomer α-1,6 / isomer α-1,11 is approximately 1:1 for as-synthesized catalyst before reaction (Fig. 6.3a).

6.2 One-pot transformation of cellobiose over different IL-POM catalysts

Cellobiose is a disaccharide consisting of two glucose molecules linked by a glycosidic bond and represents the simplest model molecule for cellulose, and it was chosen as the model substrate to facilitate the evaluation of different IL-POM catalysts. The catalytic performances these IL-POM catalysts with

different IL cations and POM anions are listed in Table 6.1. The blank experiment in the absence of any catalyst reveals that nearly no cellobiose is converted to valuable hydrolytic or oxidized products, such as saccharides and carboxylic acids (entry 1), implying that acid and redox sites of catalyst are important in the catalytic transformation of cellobiose. Adding IL-POMs promotes significantly the degradation of cellobiose, showing remarkably high conversions in the range of 83.6~100% under the relatively mild reaction conditions. The C-C bond cleavage of sugar intermediates was demonstrated by the appearance of FA and LA as the primary products. These results demonstrate the multi-functional roles of IL-POM in accelerating the transformation of cellobiose including the hydrolysis of cellobiose and C-C bond cleavage of sugars intermediates. According to the proposed mechanism for LA and FA formation via hydrolytic pathways [10, 21], the rehydration of 5-HMF affords equimolar FA and LA simultaneously (n(C-atoms of FA): n(C-atoms of LA) = 1:5). The evidence for the existence of hydrolytic transformation of cellobiose in this study is the presence of trace amounts of fructose and 5-HMF in the reaction products. In the acidic environment mainly originated from the sulfonic group in the IL cations, the catalytic hydrolysis of cellobiose to glucose and the isomerizaiton of glucose to fructose proceeds more rapidly than in a neutral environment without catalyst, consequently leading to almost complete

conversion of cellobiose and rehydration of 5-HMF to LA and FA. The strong Brønsted acidic sites of these IL-POMs are responsible for their catalytic activity in the hydrolytic degradation of cellobiose, which is consistent with our previous results [14]. The influence of cation of IL-POM on the catalytic activity is in the following sequence: [PyBS] >[MIMBS] > [TEABS] (entry 2-4), as evidenced by the conversion of cellobiose and selectivity toward LA and FA.

The structures of POM anions may also influence the hydrolysis of cellobiose and subsequent reactions. As compared to Keggin-structured IL-POMs (entry 2-6), Dawson-structured IL-POMs (entry 12-13) afford higher cellobiose conversion with primary products of glucose and subsequent transformations of glucose to fructose, 5-HMF. The formation of LA and FA over these Dawson-structured IL-POM catalysts is significantly inhibited, implying the superior catalytic activity of Keggin type POM-s to Dawson type POMs in isomerization of glucose to fructose and subsequent hydrolytic degradations. Notably, under the similar reaction conditions, the selectivity toward FA sharply increases in the degradation of cellobiose catalyzed by vanadium-containing IL-POMs, concurrently with a significant decline of selectivity toward glucose and increase of selectivity of gaseous products (entry 7-9). Introducing vanadium into the IL-POMs markedly promotes the catalytic oxidation of sugar intermediates with molecular oxygen after hydrolyzing

cellobiose, leading to FA formation and deep oxidation products. A stepwise Mars-van Krevelen-type mechanism is proposed to be involved in such catalytic oxidation reactions, in which the valence alternation of V atom between V^{5+} and V^{4+} in catalytic cycles is responsible for the redox transformations of substrates [22]. In order to confirm the hypothesis of oxidative transformation of cellobiose, two comparative experiments on $[PyBS]_5PV_2Mo_{10}O_{40}$ are conducted by changing the reaction atmosphere from dioxygen to hydrogen and nitrogen (entry 10-11). No obvious increase of FA and a similar product distribution to that under IL-POMs without vanadium (entry 2-6) are found in the absence of molecular dioxygen as the oxidant for formaldehyde, which is the first product due to the initial oxidative C-C bond scission [23]. Furthermore, three vanadium-containing IL-POMs with different exchange degrees between proton and $[PyBS]^+$ afford dissimilar cellobiose conversion and selectivities toward LA, FA and gaseous product. As the molar ratio of cellobiose /IL-POM is kept at a constant of 20:1 for all catalytic runs, the amount of $[PyBS]^+$ in the reaction mediums varies in an order of $[PyBS]_5PV_2Mo_{10}O_{40}$ > $[PyBS]_4HPV_2Mo_{10}O_{40}$ > $[PyBS]_3H_2PV_2Mo_{10}O_{40}$. This decrease in the concentration of $[PyBS]^+$ substantially hinders the reaction rates of cellobiose catalytic degradation and reduces the yields of LA and FA, indicating that the protons from the sulfonic groups in $[PyBS]^+$ are more

beneficial for promoting cellobiose transformation via hydrolytic pathways than that from parent heteropolyacids.

Table 6.1 Catalytic performances of different IL-POM catalysts in cellobiose degradation in the presence of molecular dioxygen [a].

Entry	Catalyst	Conversion (%)	Selectivity (%)						
			Glucose	Sorbitol	Fructose	Levulinic acid	Formic acid	5-HMF	Gaseous product (mainly CO_2)
1	□	7.8	0	0	0	0	0	0	7.8
2	$[TEABS]_3PW_{12}O_{40}$	83.6	47.1	0	17.6	25.6	5.1	2.5	2.1
3	$[MIMBS]_3PW_{12}O_{40}$	88.8	45.2	0	16.0	29.2	5.9	3.1	0.6
4	$[PyBS]_3PW_{12}O_{40}$	90.1	44.1	0	10.4	35.8	7.3	2.2	0.2
5	$[PyBS]_3PMo_{12}O_{40}$	90.5	41.3	0	11.7	32.1	6.6	2.4	5.9
6	$[PyBS]_4SiW_{12}O_{40}$	98.9	36.9	0	10.0	40.8	8.2	1.1	3.0
7	$[PyBS]_5\ PV_2Mo_{10}O_{40}$	100.0	5.6	0	2.1	48.3	26.1	0.2	17.7
8	$[PyBS]_4HPV_2Mo_{10}O_{40}$	99.7	11.6	0	4.5	40.7	24.1	3.2	15.9
9	$[PyBS]_3H_2PV_2Mo_{10}O_{40}$	98.8	13.9	0	5.9	34.8	23.6	5.0	16.8
10[b]	$[PyBS]_5PV_2Mo_{10}O_{40}$	89.1	39.1	0	13.4	31.5	9.3	3.1	3.6
11[c]	$[PyBS]_5PV_2Mo_{10}O_{40}$	88.2	34.4	0	11.4	38.9	10.8	0.8	3.7
12	$[PyBS]_6P_2W_{18}O_{62}$	100.0	82.4	0	3.1	10.2	2.0	1.7	0.6
13	$[PyBS]_6P_2Mo_{18}O_{62}$	100.0	79.0	0	1.8	8.5	1.6	0.1	9
14	$H_3PW_{12}O_{40}$	95.0	56.8	0	0.4	2.6	0.5	0	39.7
15	$[PyBS]HSO_4$	100.0	47.0	0	1.0	0	0	0	52.0
16[d]	$[PyBS]_5PV_2Mo_{10}O_{40}$	34.6	30.7	3.6	2.3	21.5	8.6	0.8	32.5

a. reaction condition: 0.125 g cellobiose,423K, 3MPa O_2,catalyst amount= 5 mol% (based on the mole of cellobiose), 10ml H_2O, 3 h.

b. under 3MPa H_2; c. under 3MPa N_2; d. reaction conditions: 0.1g cellulose, 423K,3 MPa O_2, 3 h, catalyst amount = 5wt% (base on the total weight of mixture).

A pure heteropolyacid catalyst of $H_3PW_{12}O_{40}$ is examined in the reaction (entry14). A small amount of FA and LA are found, implying that the cation of IL-POM is responsible for the rehydration of 5-HMF to LA and FA. The IL without heteropolyanion is also tested (entry 15). Surprisingly, 47.0% selectivity of glucose is obtained and no other side-product is detected, implying that the acid strength of the IL is insufficient to rehydrate 5-HMF to form LA and FA.

In order to explore the practical application of IL-POM catalysts in the biomass transformation to valuable chemicals, the optimal catalyst of $[PyBS]_5PV_2Mo_{10}O_{40}$ is employed in the cellulose degradation at 423 K. Upon 3 MPa pressure and 5 wt.% catalyst amount, 34.6 % conversion is obtained with considerable selectivities toward FA and LA (entry 16). The lower conversion compared with cellobiose transformation is due to the robust crystalline structure and water-insolubility of cellulose.

6.3 Recovery and reusability of IL-POM catalysts

One of the outstanding advantages of as-synthesized IL-POMs in catalyzing one-pot transformation of cellobiose is the convenient recovery of catalysts. Since

these IL-POMs possess relatively high melting points and low solubility in water, they can recrystallize into solid state, and then be easily recycled for the next catalytic run. A four-run recycling test of $[PyBS]_5PV_2Mo_{10}O_{40}$ for the transformation of cellobiose is conducted and the results are shown in Fig. 6.4.

Only a slight decline in cellobiose conversion and FA selectivity is observed after four successive recycling tests. The stable performance of this catalyst is consistent with the characterization results. Compared with the fresh catalyst, the recovered one shows similar IR bands at 1087, 951, 904 and 791 cm^{-1} for POM-anion along with the bands at 1170, 1631 and 1423 cm^{-1} for IL-cation (curve *e* in Fig. 6.1). ^{51}V NMR result of spent catalyst (Fig. 6.3b) does not show any evidence of impurities and degradation, further suggesting the durable structure of 2 to isomer α-1,6/ isomer α-1,11 becomes 2:1 according to their relative intensities shown in Fig. 6.3b. $[PyBS]_5PV_2Mo_{10}O_{40}$ during the catalytic cycle. After the reaction, the molar ratio of isomer α-1, The alternation of relative intensities is probably due to the decreased pH in the reaction mixture as LA and FA are accumulated during the reaction, which is consistent well with the conclusion

proved by Pettersson and co-workers that the relative abundance of these isomers changes when part of them become mono-protonated resulted from the decline of pH in the system [20].

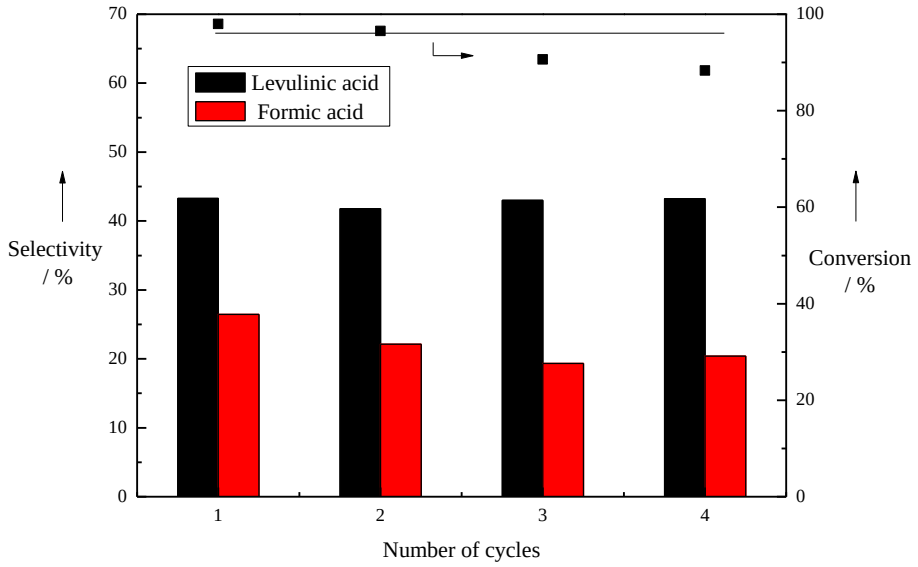

Fig. 6.4 Cellobiose and cellulose conversion and selectivity for levulinic acid and formic acid for four recycling runs on $[PyBS]_5PV_2Mo_{10}O_{40}$ (Reaction conditions: 0.125 g cellobiose, 423K, 3 MPa O_2,catalyst amount = 5 mol% base on the mole of substrate, 10ml H_2O, 3 h).

6.4 Exploration of catalytic reaction mechanism

Catalytic degradation of cellobiose catalyzed by IL-POM catalyst in the

presence of molecular dioxygen comprises a series of successive hydrolysis, isomerization and oxidation reactions. In order to probe into the catalytic mechanism, several compounds including glucose, sorbitol, xylitol, erythritol, glycerol and ethylene glycol, which are possible reaction intermediates, are employed as substrates in the presence of $[PyBS]_5PV_2Mo_{10}O_{40}$ under identical reaction conditions, and the results are shown in Table 6.2.

Table 6.2 Selectivity of final product in reactions of different sugar intermediates[a].

Entry/substrate		Selectivity			
		Fructose	Levulinic acid	Formic acid	Gaseous product (mainly CO_2)
1[b]	Glucose	5.7	47.1	9.6	36.8
2	Glucose	4.8	50.8	27.3	17.1
3[c]	Glucose	1.8	5.4	48.1	44.5
4	Sorbitol	0	0	65.8	34.2
5	Xylitol	0	0	61.2	38.8
6	Erythritol	0	0	49.5	50.5
7[d]	Glycerol	0	0	67.8	32.2
8[d]	Ethylene glycol	0	0	99.1	0.9

a. Reaction conditions: 423 K, 3h, 3 MPa O2, 10 ml H_2O, 0.125 g sugars

intermediates, catalyst amount of $[PyBS]_5PV_2Mo_{10}O_{40}$= 3 mol% (based on the mole of substrate), sugar intermediates conversions are all 100%.

b. The reaction was catalysed by $[PyBS]_4SiW_{12}O_{40}$.

c. The reaction was catalysed by $H_5PV_2Mo_{10}O_{40}$.

d. Conversion of glycerol and ethylene glycol was 49.2% and 58.3%, respectively.

As compared with the glucose conversion catalyzed by $[PyBS]_4SiW_{12}O_{40}$ in the absence of vanadium active sites incorporated in the POM anion (entry 1), the selectivity toward FA increases sharply over the $[PyBS]_5PV_2Mo_{10}O_{40}$ catalyst. The amount of gaseous products significantly decreases while the LA yield only slightly changes(entry 2). Glucose is converted to LA and FA with relatively high selectivities of 50.8% and 27.3%, respectively. It is assumed that the oxidative C-C bond cleavage of glucose, which is the first product derived from the hydrolysis of cellobiose, dominates the transformation of cellobiose to FA and CO_2 over the active species of vanadium [12, 24], the FA/CO_2 ratio in the products of glucose degradation should be close to that for cellobiose degradation, after subtracting the FA yielded from rehydration of 5-HMF. The oxidative C-C bond cleavage of organics in the presence of molecular dioxygen and vanadium-containing POMs

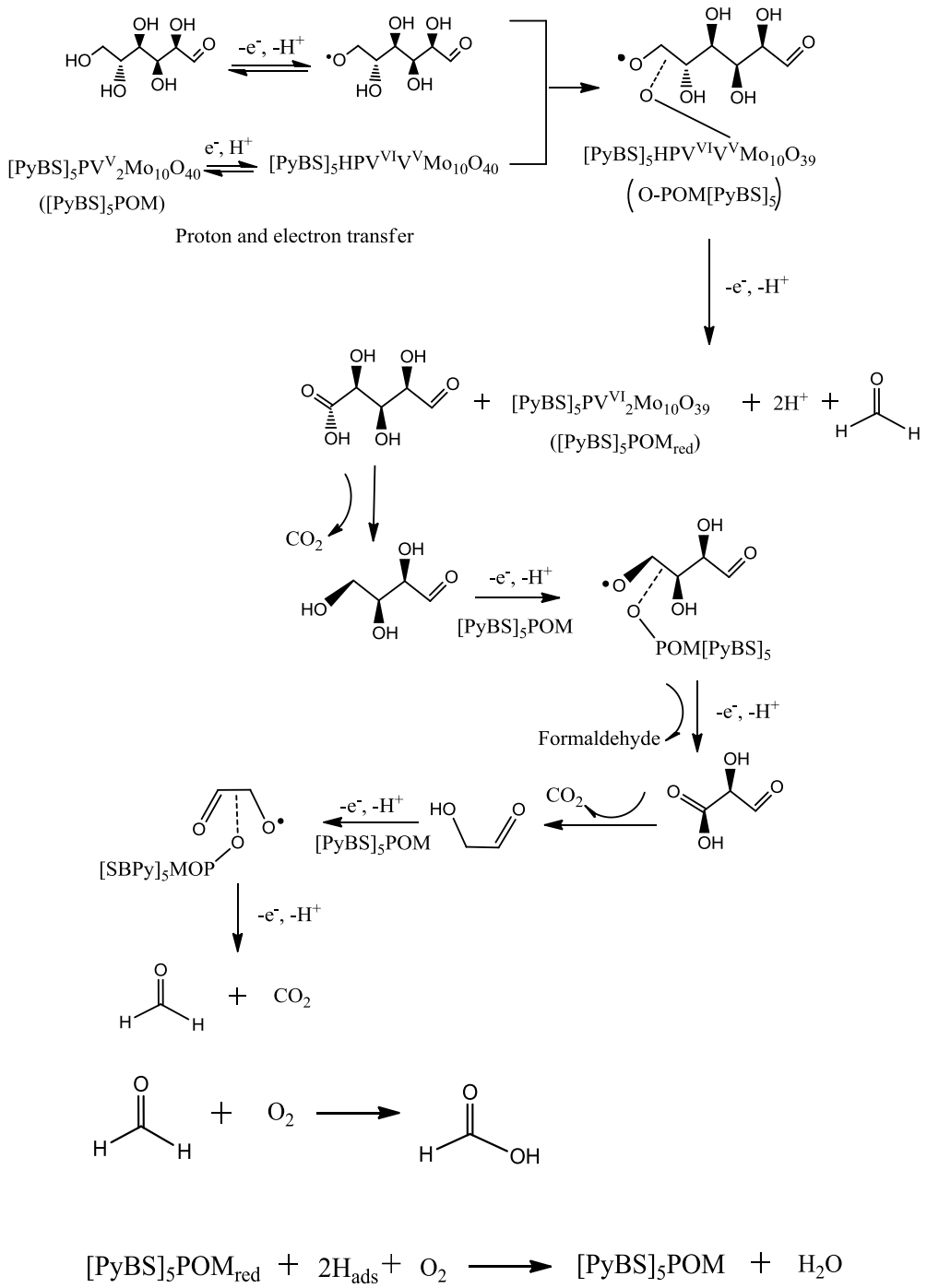

$$[PyBS]_5POM_{red} + 2H_{ads} + O_2 \longrightarrow [PyBS]_5POM + H_2O$$

Scheme 6.2 Pathway for the oxidation of glucose to formic acid and carbon oxide.

has been proposed to follow an electron-oxygen transfer (ET-OT) mechanism [12, 22-24], as depicted in Scheme 6.2 for oxidative degradation of glucose. Initially, a POM-substrate complex is formed after electron and proton transfer from glucose to IL-POM, and then this complex undergoes C-C bond cleavage after the oxygen transfer from the IL-POM to the substrate, followed by an additional electron and proton transfer.

Finally, the ET-OT reactions lead to the formation of final products and the reduced and deoxygenated IL-POM, which can be easily re-oxidized by molecular dioxygen to restore their catalytically active structure. This is a two-electron oxidation coupled with one molecular oxygen transfer and two protons release. According to this mechanism and the study on oxidation of glucose and C2-substrates to FA and CO_2 by Wasserscheid et al. [12], one can expect that the ratios of FA/CO_2 in products for glucose, sorbitol, xylitol, erythritol, glycerol and ethylene glycol should be 1/1, 2/1, 3/2, 1/1, 2/1 and 1/0, respectively. In this study, the FA/CO_2 ratios in all these substrates are consistent with the proposed molar ratios except glucose transformation (entry 2). This exception for glucose reaction

becomes more understandable when taking into account that part of FA coming from rehydration of 5-HMF. $H_5PV_2Mo_{12}O_{40}$ is employed to confirm this hypothesis since the rehydration of 5-HMF to LA and FA is significantly inhibited in the absence of IL-cation. 1/1 of FA/CO_2 is obtained (entry 3), which is similar to the result in the glucose reaction reported by Wasserscheid.

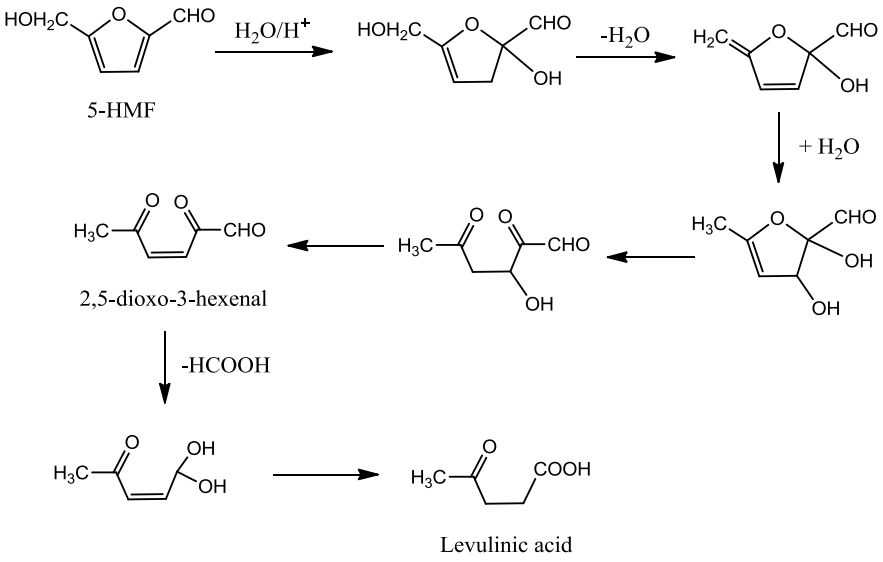

Scheme 6.3 Pathway for the rehydration of 5-HMF to formic acid and levulinic acid.

These results strongly support the validity of degradation of polyols and saccharides via ET-OT oxidation. 5-HMF and LA cannot be found in the transformation of C2~C5 alcohols (sorbitol, xylitol, erythritol, glycerol and

ethylene glycol), which further supports the standpoint that LA originates from the rehydration of 5-HMF via a series of hydrolysis and isomerization steps of saccharides. Accordingly, a possible reaction pathway for Brønsted acid catalyzed rehydration of 5-HMF is proposed in Scheme 6.3 [11].

The rehydration of 5-HMF undergoes a series of hydrolysis and isomerization steps, leading to a variety of intermediates, and finally forms LA and FA. It is worth noting that 1) LA and FA molecules, which are all terminal carboxylic acid without oxygen-containing functional group on the α-carbon atom, are remarkably more stable than glucose, fructose and 5-HMF in the presence of vanadium-containing POM-IL catalyst and molecular dioxygen; 2) equimolar LA and FA, which is corresponding to 5/1 of n (C-atoms of LA)/n(C-atoms of FA), is always obtained through hydrolysis and isomerization pathways.

6.5 Conclusion

A series of multiple-functional ionic liquid-based polyoxometalate (IL-POM) catalysts were synthesized and applied for transformation of cellobiose in the presence of molecular dioxygen. Some of the POM-IL catalysts are very efficient

and easily recyclable for the catalytic transformation of cellobiose/ cellulose to valuable chemicals, such as FA and LA. This approach combines successfully two different reaction pathways, which are the formation of LA and FA via acid catalyzed hydrolysis and isomerization under the IL functional groups and also the oxidative degradation of carbonoxygenates to FA and CO_2 under the active vanadium species, to provide a green and efficient synthesis of LA and FA from biomass materials.

The content in Chapter 6 has been published ChemsusChem and the DOI : 10.1002/cssc.201402157.

References

[1] D. Klemm, B. Heublein, H. Fink, A. Bohn, Angew. Chem. 2005, 117, 3422 -3458; Angew. Chem. Int. Ed. 2005, 44, 3358 -3393.

[2] J. Zakzeski, B.M. Weckhuysen, ChemSusChem 4 (2011) 369.

[3] S. van de Vyver, J. Geboers, P. A. Jacobs, B. F. Sels, Recent Advances in the Catalytic Conversion of Cellulose, ChemCatChem 2011, 3, 82-94.

[4] S. Biella, L. Prati and M. Rossi, J. Catal., 2002, 206, 242-247.

[5] Y. Önal, S. Schimpf and P. Claus, J. Catal., 2004, 223, 122-133.

[6] X. S. Tan, W. P. Deng, M. Liu, Q. H. Zhang and Y. Wang, Chem. Commun., 2009, 7179-7181

[7] C. Baatz and U. Prüße, J. Catal., 2007, 249, 34-40.

[8] N. Yan, C.Zhao, C. Luo, P. J. Dyson, H. Liu, Y. Kou, J. Am. Chem. Soc. 2006, 128, 8714-8715

[9] Wang P, Yu H, Zhan S, Wang S. Catalytic hydrolysis of lignocellulosic biomass into 5-hydroxymethylfurfural in ionic liquid.2011,102, 4179-4183.

[10]Shunmugavel Saravanamurugan, Olivier Nguyen Van Buu, and Anders

Riisager. Conversion of Mono- and Disaccharides to Ethyl Levulinate and Ethyl Pyranoside with Sulfonic Acid-Functionalized Ionic Liquids[J]. ChemSusChem 2011, 4, 723-726

[11] J. Zhang, X. Liu, M. N. Hedhili, Y. Zhu and Y. Han, ChemCatChem, 2011, 3, 1294-1298.

[12] Rene W ̈olfel, Nicola Taccardi, Andreas B ̈osmann and Peter Wasserscheid. Selective catalytic conversion of biobased carbohydrates to formic acid using molecular oxygen. Green Chem., 2011, 13, 2759-2763

[13] Y. Leng, J. Wang, D.R. Zhu, X.Q. Ren, H.Q. Ge, L. Shen, Heteropolyanion-based ionic liquids: reaction-induced self-separation catalysts for esterification, Angew. Chem. Int. Ed. 2009, 48, 168-171.

[14] K.X. Li ,L. Chen, H.L. Wang, W.B. Lin, Z.C. Yan, Heteropolyacid salts as self-separation and recyclable catalysts for transesterification of trimethylolpropane, Appl catal a-gen. 2011, 392, 233-237.

[15] L.S. Felices, P. Vitoria, J.M. Gutierrez-Zorrilla, S. Reinoso, J. Etxebarria, L. Lezama, A novel hybrid inorganic−metalorganic compound based on a polymeric

polyoxometalate and a copper complex: Synthesis, crystal structure and topological studies, Chem. Eur. J. 2004, 10, 5138.

[16] A.M. Douvas, K. Yannakopoulou, P. Argitis, Thermally induced acid generation from 18-molybdodiphosphate and 18- tungstodiphosphate within poly (2-hydroxyethyl methacrylate) films, Chem. Mater. 2010, 22, 2730.

[17] K. Y. Lee, N. Mizuno, T. Okuhara and M. Misono, Bull. Chem. Soc. Jpn. 1989, 62, 1731;

[18] S. Bareyt, S. Piligkos, B. Hasenknopf, P.Gouzerh, E. Lacote, S. Thorimbert and M. Malacria, Efficient Preparation of Functionalized Hybrid Organic/Inorganic Wells−Dawson-type Polyoxotungstates, J. Am. Chem.Soc. 2005, 127, 6788.

[19] X. Yan, P. Zhu, J. Fei, J. Li, Self-assembly of peptide-inorganic hybrid spheres for adaptive encapsulation of guests, Adv. Mater. 22 (2010) 1283-1287.

[20] Lage Pettersson, Itn gegard Andersson, Anna Selling,and John H. Grate. Multicomponent Polyanions. 46. Characterization of the Isomeric Keggin Decamolybdodivanadophosphate Ions in Aqueous Solution by ^{31}P and ^{51}V NMR[J]. Inorg. Chem. 1994, 33, 982-993

[21] Weiping Deng, Qinghong Zhang and Ye Wang. Polyoxometalates as efficient catalysts for transformations of cellulose into platform chemicals [J]. DaltonTransactions, 2012, 41, 9817

[22] R. Neumann, Inorg. Chem., 2010, 49, 3594-3601.

[23] A. M. Khenkin and R. Neumann, J. Am. Chem. Soc., 2008, 130, 14474-14476

[24] A. M. Khenkin, G. Leitus and R. Neumann, J. Am. Chem. Soc., 2010, 132, 11446-1144

Chapter 7 Conclusions and Future Perspectives

7.1 Conclusions

In this thesis, the IL involved heterogeneous catalytic systems were successfully designed and performed on several oxidative transformations with particular highlights on how specifically IL benefits the oxidation in the catalytic systems. The primary results and findings are summarized in this chapter.

The aerobic oxidation of 1-phenylethanol over a carbon nanotube supported palladium catalyst was improved by adding small amount of IL [emim][NTf_2], showing an excellent TON of 149 000. The increased concentration of reactant and the oxygen in [emim][NTf_2] are partially responsible for the improve effect of IL. Moreover, the electrophilic environment conferred by the anion NTf_2^- is proposed to accelerate the electron transfer hence accelerate the reaction. Besides the instrinsic properties conferred by IL itself, the characterization of both the pristine and spent Pd catalysts indicate the stability of both the Pd metal and the carbon nanotube support with the existence of IL. Especially, the XPS results showed the the existence of the Pd speices in the status of $Pd^{\delta+}$, which may imply the interaction between the F atom in the IL anion and the Pd metal resulting in stabilizing the catalyst. The heterogeneous catalytic system consisting of IL [emim][NTf_2] and Pd/CNT catalyst shows good activity in the

aerobic oxidation of a series of phenylic alcohols, which can even maintain for 5 runs.

Starting the point of cutting down the usage of traditional organic solvent, [emim][NTf_2] was introduced as a second solvent to mixed with dimethylformamide (DMF) whereby the alkene epoxidation was significantly improved over vanadium-exchanged faujasite zeolite catalysts (V-X), using *tert*-butyl hydroperoxide (TBHP) as the oxidant. The *cis*-cyclooctene conversion is greatly improved as well as the high epoxide selectivity is maintained in the presence of [emim][NTf_2]. In addition to the high polarity of IL, the superior catalytic activity with [emim][NTf_2]-involved solvent is summarized to be attributed to the following reasons. The vanadium active site shows improved stability in the [emim][NTf_2]-involved solvent, and the effective molecular structure of vanadium active site is well preserved. The hydrogen bonding between [emim][NTf_2] and by-product *t*-butanol prevents the coordination of *t*-butanol with vanadium center; hence improves the catalytic efficiency. Due to the weak acidity of the imidazolium cation, it is also proposed that the hydrogen bonding between the weak acidic protons with the vanadium peroxo intermediate may decrease the activation energy barrier of the kinetically relevant steps.

From the economic view the strategy of reducing the using amount of IL

meanwhile maintaining its unique properties to obtain effective heterogeneous catalysis is urged to be developed. To integrate IL directly with the heterogeneous catalyst, IL-based polyoxometalate (IL-POM) composites were synthesized by ion exchange method. A series of multiple-functional ionic liquid-based polyoxometalate (IL-POM) catalysts were synthesized and applied for transformation of cellobiose in the presence of molecular dioxygen. Some of the IL-POM catalysts are very efficient and easily recyclable for the catalytic transformation of cellobiose/ cellulose to valuable chemicals, such as FA and LA. This approach combines successfully two different reaction pathways, which are the formation of LA and FA via acid catalyzed hydrolysis and isomerization under the IL functional groups and also the oxidative degradation of carbonoxygenates to FA and CO_2 under the active vanadium species, to provide a green and efficient synthesis of LA and FA from biomass materials. The heterogeneous

7.2 Future perspectives

Basing on the results of Chapter 4, we have discovered and primarily investigated the involvement of imidazolium ionic liquid [emim][NTf_2] leading to an enhanced conversion of the aerobic oxidation of benzyl alcohol. The improve effect of IL was explained from two aspects (1) the instrinsic properties of IL, mainly the anion (2) the interaction between IL and the Pd

catalyst which is mainly supported by the comparison of the XPS spectra of pristine and spent catalysts. However, the evidences are still not sufficient to clearly elucidate the specific effect of IL in the reaction course. It's found that the aerobic oxidation of a metal complex such as $(C_5Me_5)_2Fe(II)$ might also be promoted by employing imidazolium ILs [1]. In this work the importance of the imidazolium cation of ILs was highlighted and the imidazolium ILs accelerated

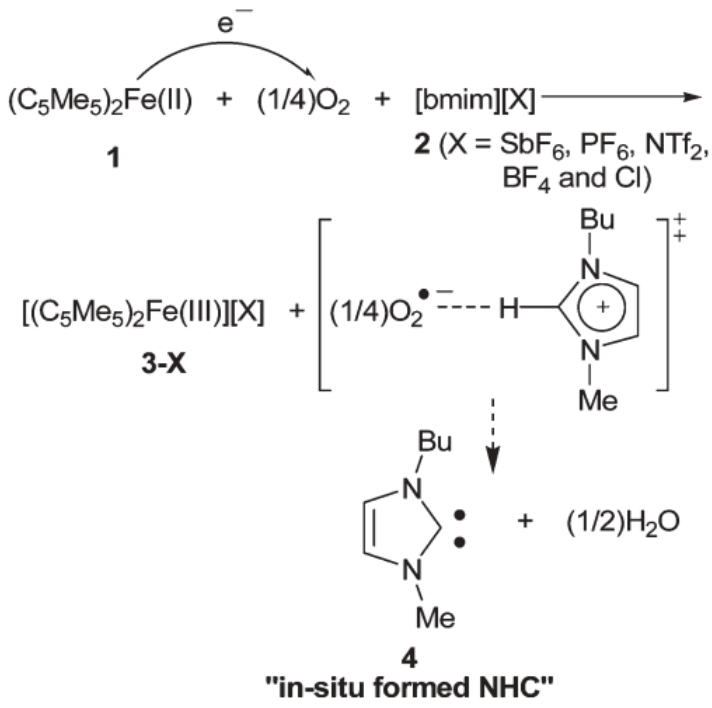

Scheme 7.1 Proposed mechanism for aerobic oxidation of the metal catalyst promoted by imidazolium ILs.

the one-electron mechanism as depicted in Scheme 7.1. The imidazolium cation of acidity might interact with anionic oxygen then generate the in-situ N-heterocyclic carbene (NHC). Considering the similarity of this work and our

one, we're obliged to examine the cation effect on the reaction. On one aspect, the hydrogen bonding ability of IL directly affects the interaction between IL and the alcohol substrate hence affects the reaction progress. Moreover, it's necessary to find out if the imidazolium cation anticipates the activation of O_2 and if the NHC appears as the reference work.

Basing on the content in Chapter 5, the introduction of IL [emim]NTf_2 significantly improved the epoxidation reaction. However the large amount of cost of IL as reaction solvent still becomes the obstacle of expanding the application. Hence basing on the present recognition that how IL benefited the epoxidation, to modify the zeolite support with imidazolium IL is planned in the future work. The Na^+ of zeolite support can be replaced by the imidazolium cation, which is called the IL-modified zeolite. Using the IL modified zeolite as support the vanadium exchanged catalyst is synthesized as the used method. As the primary investigation, a weak acidic environment due to the imidazolium cation may possibly improve the activity of the catalyst, where the IL amount will be significantly reduced. Additionally, other promising effective catalytic systems with IL will be tried and investigated as well in the future research plan.

Reference

[1] D.S. Choi, D.H. Kim, U.S. Shin, R.R. Deshmukh, S.G. Lee, C.E. Song, Chem Commun (Camb) (2007) 3467-3469.

Reproduced from Chem. Commun., 2007, 3467-3469 with the permission of The Royal Society of Chemistry.

Appendix

A1 $Co_6(\mu 3\text{-}OH)_6$ cluster based coordination polymer as an effective heterogeneous catalyst for aerobic epoxidation of alkenes

Catalytic epoxidation of alkenes takes a vital position in both organic synthesis and industrial processes for producing the highly reactive epoxides as one type of the most useful synthetic intermediates. Traditional epoxidation normally involves peroxide-oxidants such as H_2O_2, PHIO, ethylbenzene hydroperoxide, and *tert*-butyl hydroperoxide (TBHP), which are strongly oxidative, corrosive, toxic, and environmentally unfriendly [1]. As the increasing concerns on the development of green catalytic technology, directly employing free oxygen/air in the epoxidation (aerobic epoxidation) process is suggested to be the ideal oxidant choice and this process can contain the maximum content of active oxygen [2]. Nevertheless, without additional radical initiators and reducing reagents, maintaining high conversion and high selectivity at the same time for the application of oxygen in the alkene epoxidation is a big challenge [3].

Although the heterogeneous gold catalyst is reported to show promising behaviour in the aerobic epoxidation, its limited activity for several alkenes drives further investigation of other types of catalysts [4]. Coordination polymers (CPs) or metal-organic frameworks (MOFs) are rapidly emerging

class of multifunctional hybrid materials that have potential applcitaions in gas storage [5],5 separation [6], chemial sensors [7], nonlinear optics [8], magnets and biology [9]. CPs are also considered to be useful for diverse heterogeneous catalytic applications as either catalysts or catalyst supports [10]. Several works have already shown that CPs as catalysts in the alkene epoxidation give good acitivity and even asymmetric selectivity [11]. However, the very high turn-over frequencies (TOFs) and numbers (TONs) that required for industrial oxidation or oxygenation reactions are still not achieved. In addition, the CP catalyzed alkene epoxidation using molecular oxygen as the only oxidant without the assistance of any sacrificial reductant or additive is rarely reported [12].

Here, we report a newly synthesized hexaprismane Co(II)6(μ3-OH)6 cluster-based three-dimensional CP, noted as CO6-CP (Figure A.1) as an effective recyclable heterogeneous catalyst for the epoxidation of alkenes with oxygen as the only oxidant.

A1.1 Experimental

A1.1.1 Materials

All chemicals were purchased from Alfa Aesar, TCI chemical and Aldrich and used without further purification.

A1.1.2 Synthesis of compound Co(μ_3-OH)(HCOO)$_{0.72}$(CH3COO)$_{0.28}$ (Co$_6$-CP)

The Co6 cluster based CP (Co_6-CP) was synthesized by solvothermal method. $Co(NO_3)_{2.6}H_2O$ (86 mg, 0.5 mmol), NaOAc (82 mg, 1 mmol) and pyridine (0.5 ml) were added to a solution of DMF (3 ml) methanol (3 ml) and deionized water (0.5 ml). The mixture solution was sealed in a teflon-lined steel autoclave and heating at 110 ^oC for 5 days. Dark purple cubic crystals were isolated after filtration in 62% yield with respect to cobalt.

A1.1.3 Characterization

Crystallographic measurements: data collection of crystals was carried out on Bruker APEX II CCD diffractometer equipped with a graphite-monohromatized MoKα radiation source (λ=0.71073 Å). Empirical absorption was performed, and the structure was solved by direct methods and refined with the aid of a SHELXTL program package. All hydrogen atoms were calculated and refined using a riding model. CCDC number for Co6-CP is 915825.

Powder X-ray diffraction data were recorded on a Bruker D8 Advance diffractometer with a graphite-monochromatized Cu Ka radiation. FTIR spectra were recorded from KBr pellets by using a Perkin Elmer FTIR SpectrumGX spectrometer. Elemental analyses were obtained from a EuroVector Euro EA elemental analyzer. Thermogravimetric analysis (TGA) was carried out on a TA Instrument Q500 Thermogravimetric Analyzer at a heating rate of 10 ^oC/min up

to 800 ^{o}C.

ICP-MS analyses were performed on an ICP-MS Agilent 7700 spectrometer, before which the sample was obtained as the following procedures: a hot solution obtained after 8 h reaction time was filtered and 5.00 ml of this solution was used for further analysis. After evaporating the organic solvent in vacuum over night the residual was digested assisted by the CEM MDS-5 microwave oven then diluted with double distilled water to 10.0 ml.

A1.1.4 Catalytic reaction

The epoxidation of various alkenes using molecular O_2 was carried out in a bath-type reactor operated under atmospheric conditions: a three-necked glass flask (50 ml) precharged with 2 mmol of alkenes, 2 mg of Co_6-CP, 20 ml of DMF as well as a stirring bar, was heated by a silicon oil bath, where a thermocouple was applied to control the temperature and a reflux condenser to condense the vapor of products. In each reaction run, the mixture was heated to the desired reaction temperature under vigorous stirring (stirring rate: 1000 rpm). Oxygen flow was bubbled at 30 ml/min controlled by a mass flow controller into the mixture to initiate the reaction.

To investigate the oxygen pressure effect, the reaction was alternatively carried out in a stainless steel reactor with Teflon liner (Parr 4950, controller 4843). The residual air inside the reactor was expelled by pressurizing and

releasing O_2 several times. The reaction was performed under the oxygen pressure of 20 bar, with the other reaction conditions unchanged.

The liquid mixture after reaction with Co_6-CP filtered was analyzed by Agilent gas chromatograph 6890 equipped with a HP-5 capillary column (30 m long and 0.32 mm in diameter, packed with silica-based supelcosil) and flame ionization detector (FID). Dodecane was the internal standard. The by-products were identified by a gas chromatography-mass spectrometry (GCMS, Agilent, GC 6890N, MS 5973 inert).

For reaction time effect examination, the reaction in the first 1h was performed from 15 min to 1 h with 15 min interval, next from 2 h to 6 h with 1 h interval.

A1.1.5 Recycle of catalyst

After each reaction cycle, the filtered catalysts were recovered by washing with plenty of acetone (>99%, Sigma–Aldrich) and dried in vacuum at 373 K. Then the recycled catalysts were reused under the same reaction condition as described above.

A1.2 Results and discussion

A1.2.1 Characterization of Co_6-CP

The detailed crystal analysis showed that Co_6-CP crystallized in the trigonal space group R-3. The structure of the Co_6-CP is shown in Figure A.1. Each

Co(II) octahedrally coordinates with three OH groups and three oxygen atoms from the carboxylate groups.

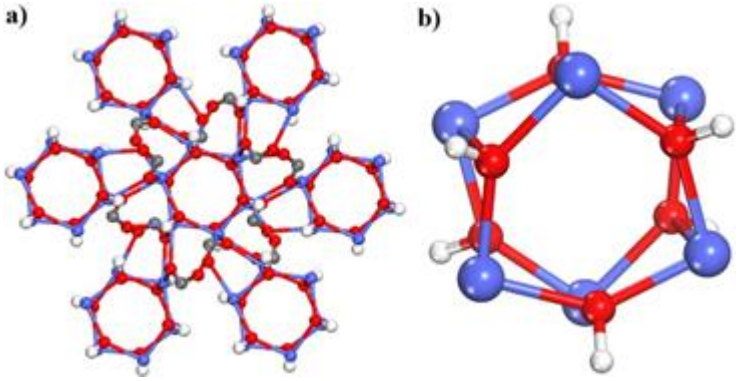

Figure A1.1 a) The 3D structure of Co_6-CP; b) The $Co_6(\mu 3\text{-}OH)_6$ cluster subunit in Co_6-CP. Color code: red ball, Oxygen; gray ball, Carbon; blue ball, Cobalt; white ball, hydrogen.

The oxygen atom in each OH group bridges with three different Co atoms to form a hexaprismane $Co_6(OH)_6$ cluster. Each Co_6 cluster is further connected with six neighbouring Co_6 clusters by edge sharing via the bidentate carboxylate groups to form a three-dimensional network.

The experimental powder XRD pattern for Co_6-CP matches very well with the simulated one generated on the basis of single crystal structure analysis, which confirms the phase purity of the bulk materials of Co_6-CP (Figure A1.2). The IR spectrum of pristine Co6-CP is shown in Figure A1.3. The strong peak at 3512 cm^{-1} could be assigned to the v(O-H). The v(C-H) of the methyl group is located at 2924 cm^{-1} and 2855 cm^{-1}. The peak at 747 cm^{-1} and 681 cm^{-1} could

be assigned to the Co-O stretching vibration for Co(μ3-OH) group, confirming the existence of Co-hydroxide cluster in the crystal [13].

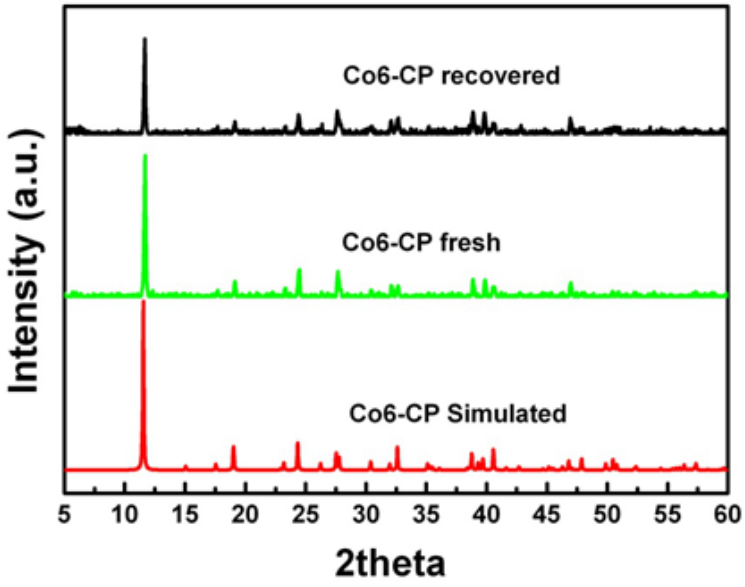

Figure A1.2. The simulated and experimental powder XRD patterns of Co6-CP.

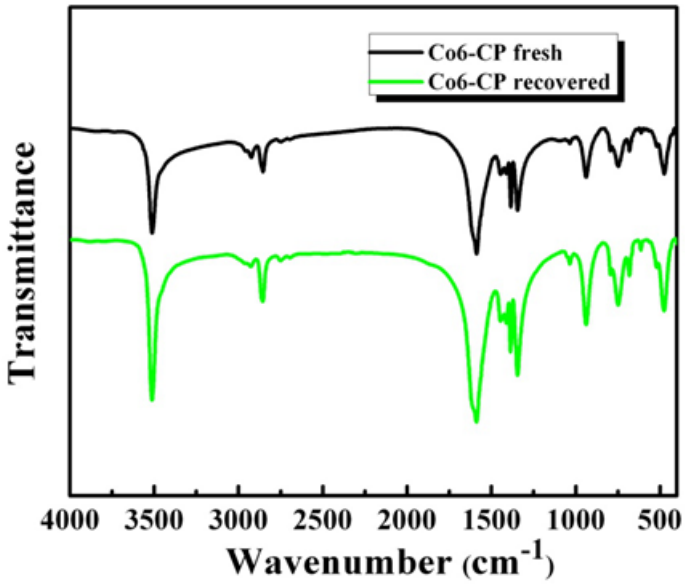

Figure A1.3. The IR spectra of pristine and recovered Co_6-CP.

The thermal stability of Co_6-CP was investigated by thermogravimetric (TG) (Figure A1.4). The decomposition temperature of Co_6-CP is about 290 ^oC

and almost no weight loss happened when heating to 270 ^{o}C, which indicates the quite good thermal stability of the crystal.

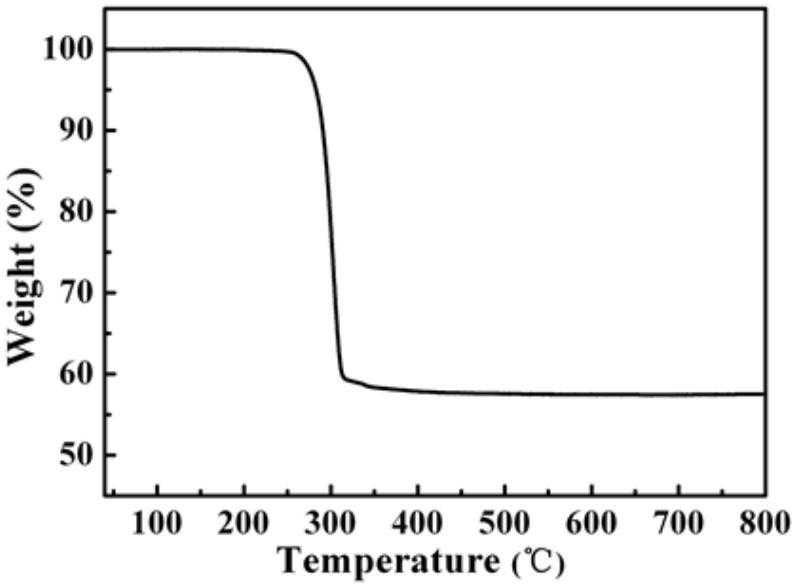

Figure A1.4. The TGA spectra of fresh and recovered Co_6-CP

A sharp weight loss (40%) occurred in the temperature range of 290-330 ^{o}C due the decomposition of the organic ligand. Then, there was no further weight loss till 800 ^{o}C.

A1.2.2 Aeroataic epoxidation activity of Co_6-CP

The activity of Co_6-CP was studied with the epoxidation of *trans*-stilbene as the test reaction with molecular oxygen as the oxidant and N,N-Dimethylformamide (DMF) as solvent. Figure A1.2 shows the time course of the epoxidation of the trans-stilbene. After reaction for 6 hours, the conversion and the selectvity towards the epoxide reached 98.6% and 98.0%,

respectively.

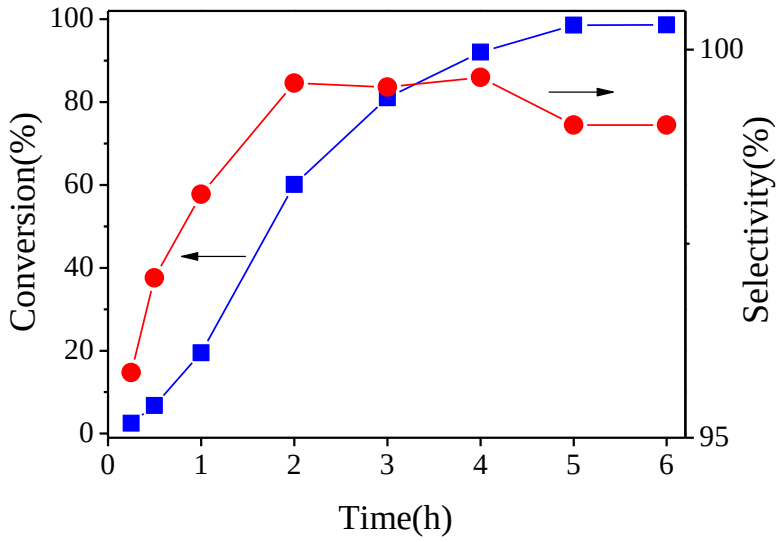

Figure A1.6. The epoxidation of *trans*-stilbene catalyzed by Co6-CP. The reaction conditions refer to the foot note of Table A.1.

The average TOF of 22 h^{-1} was obtained for the reaction lasting for 6 hours. The high TOF value and excellent conversion along with the epoxide selectivity surpass all the ones reported with CP materials as heterogeneous catalyst for converting *trans*-stilbene to corresponding epoxide [11a, 11f, 12a, 14] and rival those of the traditional heterogeneous catalysts [15]. Moreover, most of these works involving CP catalysts are required to employ either peroxides or co-catalysts due to the limited catalytic activity of CPs. From the aspect of catalytic ability, the Co_6-CP catalyst takes the lead among the CP materials to have achieved good activity which does not fade next to the traditional heterogeneous catalysts of good activity. Except for trans-stilbene, the Co_6-CP

was found to be capable of catalyzing the epoxidation of other various alkenes and the results were summarized in Table A1.1.

Table A1.1. Epoxidation of various alkenes over Co_6-CP.[a]

Entry	Substrate	Conversion (%)	Selectivity[b] (%)	Turnover number[c]
1	*trans*-Stilbene	98.6	98.0	133.1
2	*cis*-Stilbene	66.2	84.3	89.4
3	Styrene	94.2	76.8	127.2
4	*cis*-Cycloocten e	16.5	97.5	22.3
5	1-Decene	14.0	83.4	18.9
6	*trans*-Stilbene[d]	0.2	100.0	0.3
7	*trans*-Stilbene[e]	22.6	76.7	30.5

a. Reaction conditions: substrate, 2mmol; Co_6-CP, 2mg; solvent, dimethylformamide 20ml; oxygen flow rate 30ml/min, reaction time 6h, reaction temperature 120 ^oC.

b. The selectivity is towards corresponding epoxide for each substrate: for *trans*-stilbene the by-product is benzaldehyde; for *cis*-stilbene the by-products are trans-stilbene and benzaldehyde; for styrene the by-products are benzaldehyde and benzoic acid; for *cis*-cyclooctene the by-products are

2-cyclooctene-1-one.and 4-cyclooctene-1-one; for 1-decene the by-product is 3-decanone.

c. TON is calculated by mmol of substrate converted to corresponding epoxide/mmol of cobalt in the Co6-CP.

d. Radical scavenger 0.02 mmol butyl hydroxy toluene (BHT) is added.

e. The epoxidation of *trans*-stilbene was performed in a closed reaction system with the oxygen pressure of 20 bar instead of the oxygen flow.

As shown in Table A1.1, no matter for the cyclo-alkene (cis-cyclooctene)of rigid structure and weak nucleophilicity (entry 4) or the alphalic alkene (1-decene) (entry 5) Co_6-CP shows quite good catalytic activity during the conversion to corresponding epoxide. The excellent catalytic behavior for the aerobic epoxidation reaction raises the prospect of using the CP material for the green industrial epoxidation process.

A1.2.3 Examination of reaction parameters

As the next step, the effects of temperature, oxygen flow rate, catalyst amount and the initial substrate concentration were studied in detail for the aerobic epoxidation of trans-stilbene. As shown in Figure A1.7, higher temperatures improved the reaction rate. The conversion was very low at 90 ^{o}C (40.9 %) while at 110 ^{o}C the reaction reaches a higher conversion (larger than 95%). The selectivity increased from 97.0 % to 99.1 % when the reaction

temperature raised from 90 °C to 100 °C; then, a slight decrease of selectivity was displayed with the further increase of reaction temperature.

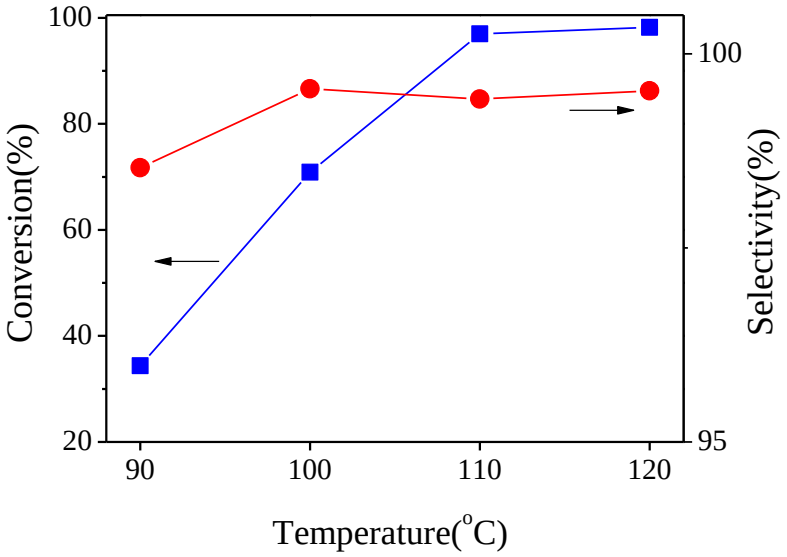

Figure A1.7. The reaction temperature effect on the epoxidation of *trans*-stilbene over Co_6-CP. The reaction conditions refer to the foot note of Table A1.1.

The oxygen flow rate also has obvious influnce on the reaction rate. As shown in Figure A1.8, only a conversion of 60.8 % was achieved when the oxygen flow rate is 10 ml/min while the epoxidation conversion was efficiently improved to 92.7 % at a flow rate of 60 ml/min. Note that the selectivity (above 97.0 % all the time) showed a small change. This phenomenon is quite consistent with the results obtained by W. Kleist et al., indicating that high oxygen availability is crutical to the aerobic epoxidation [12a].

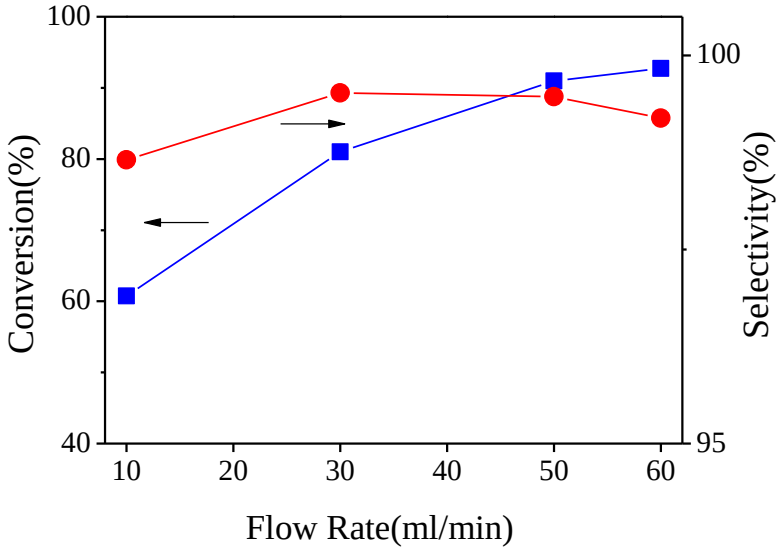

Figure A1.8. The oxygen flow rate effect on the epoxidation of *trans*-stilbene over Co6-CP. The reaction time is 3h and other conditions refer to the footnote of Table A1.1

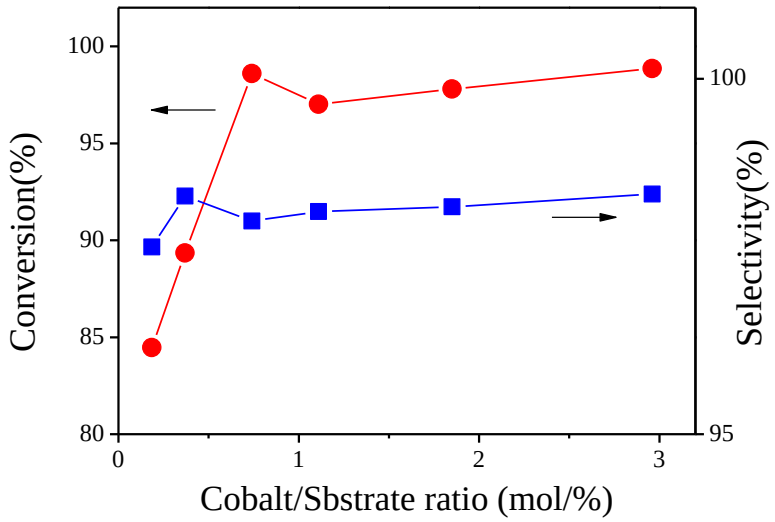

Figure A1.9. The catalyst amount effect on the epoxidation of *trans*-stilbene.

The reaction conditions refer to the foot note of Table A1.1. This indicates that the mass transfer effect might not majorly limit the reaction

The reaction rate increases with the amount of catalyst (Figure A1.9) till which reaches 2 mg since the conversion of the reactant has reached its limitation. rate.

Furthermore, the initial substrate concentration effect is examined keeping the constant cobalt/substrate ratio by adjusting the volume of the solvent. It's found that within limits a higher initial concentration gave a higher conversion as shown in Figure A1.10.

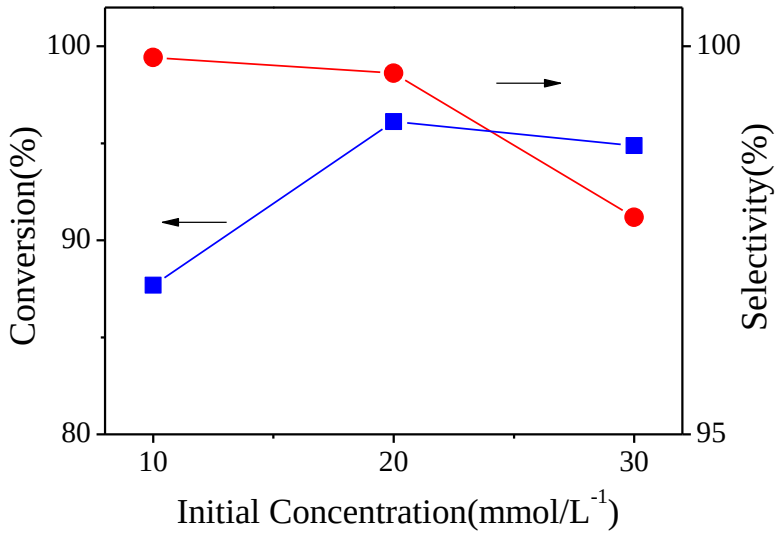

Figure A1.10. The initial concentration effect on the epoxidation of *trans*-stilbene over Co_6-CP.The reaction conditions refer to the foot note of Table A1.1.

The solvent plays vital role for the epoxidation reaction. The use of

Dimethyl sulfoxide (DMSO) and 1,2-Dichlorobenzene did not yield any epoxidation products. On the other hand cyclohexanone and N,N-Dimethylacetamide (DMA) proved to be suitable solvents, affording rather high reaction rate, as shown in Table A1.2.

Table A1.2. Solvent effect on the epoxidation over Co_6-CP[a].

Entry	Substrate	Conversion (%)	Selectivity (%)
1	DMF	98.6	98.0
2	DMSO	-	-
3	1,2-Dichlorobenzene	-	-
4	DMA	97.1	73.4
5	Cyclohexanone	98.0	90.8

a. Reaction conditions: *trans*-stilbene, 2mmol; Co_6-CP, 2mg; solvent, 20ml; oxygen flow rate 30ml/min, reaction time 6h, reaction temperature 120 ^oC.

A1.2.4 Recyclability and stability of Co_6-CP

An important issue of coordination polymer material as solid catalyst is if the catalysis proceeds mainly heterogeneously [10c], [16]. In our research, the catalyst was removed by hot filtration to examine the nature of the catalysis. As shown in Figure A1.11, the reaction proceeds after the removal, but with an obvious reduce of reaction rate.

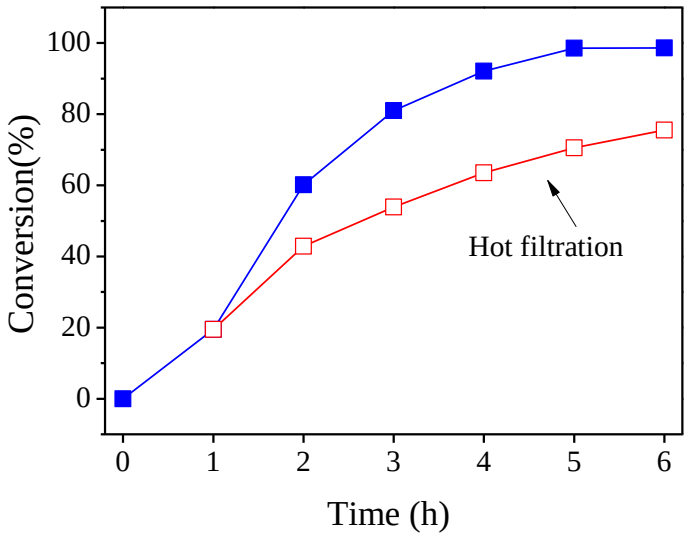

Figure A1.11. The comparation of the epoxidation of *trans*-stilbene with and without catalyst removal after 1h. The reaction conditions refer to the foot note of Table A1.1.

Indeed after the whole reaction duration for 6h, the residue liquid solution was obtained by removing the catalyst and characterized by ICP-MS. The cobalt amount in the liquid is only 1.00 ppm, amounting to approximately 1% of the employed Co, indicating limited amount of cobalt of Co_6-CP leached out. To exclude the possibility that the catalytic activity were attributed to the leached-out homogeneous cobalt species, the Co_6-CP was pretreated in DMF at the reaction temperature for 6h before reaction, and then, the catalytic result was examined with the reactant added as shown in Figure A1.12.

Comparing with the reaction without the pretreated process, however, a higher reaction rate was not observed. Basing all above, it's reasonable to

attribute the excellent catalytic activity mainly to the heterogeneous route with Co_6-CP.

After confirming the heterogeneity of the Co6-CP, the stability as an essential property to assess a heterogeneous catalyst was carefully examined.

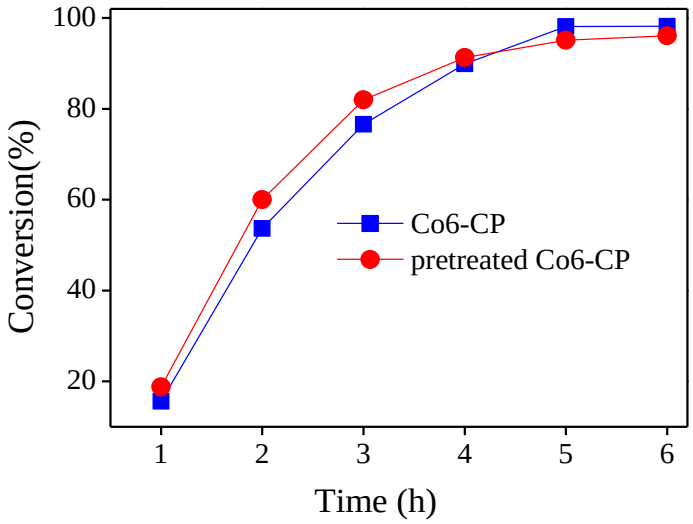

Figure A1.12. The comparison of the epoxidation of *trans*-stilbene with Co6-CP and pretreated Co_6-CP in DMF. The reaction conditions refer to the footnote of Table A1.1.

The recycle usage of the Co_6-CP was shown in Figure A1.13. In the second-run and third-run test, the selectivity showed almost no change while the conversion was slight reduced, which indicated the good stability of the catalyst except for the excellent catalytic activity.

The stability of Co6-CP was further examined by powder XRD and IR spectra. The XRD pattern of the Co_6-CP after reaction (Figure A1.2&1.3) didn't

show obvious changes. In addition, IR spectra of both pristine and spent Co_6-CP have been studied and no obvious peak-shifts were observed. This result together with the XRD result could furthermore support the recycle usage result and indicate the excellent stability of the Co_6-CP.

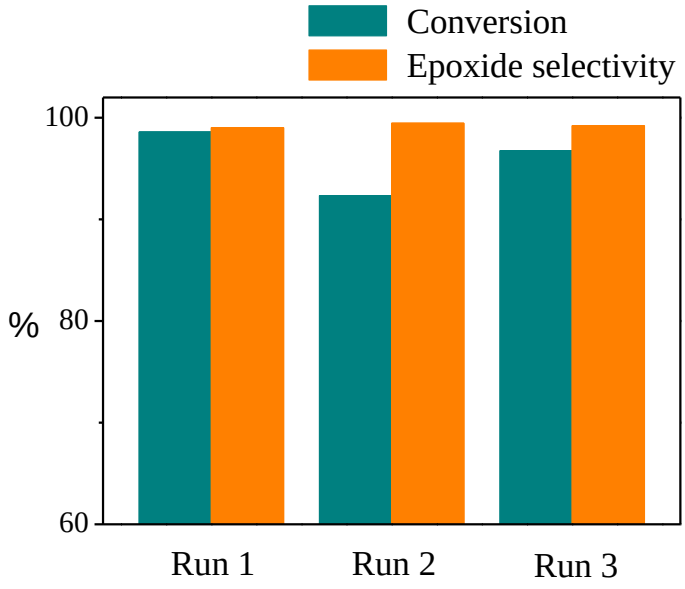

Figure A1.13 The recycle of Co_6-CP for the epoxidation of *trans*-stilbene.

A1.3 Disscussion

To uncover the epoxidation with Co_6-CP as a primary catalyst, the reaction was performed with the addition of a very small amount of free radical scavenger butylhydroxytoluene (BHT) while keeping all other reaction conditions same. As shown in entry 6 of Table A1.1, the conversion of *trans*-stilbene decreased almost to zero. This observation indicates the radical nature of the active oxygen species. As shown in Figure A1.5, an obvious induction period appeared in the beginning of the epoxidation. In addition,

trans-stilbene oxide has been observed as the main product in the epoxidation of *cis*-stilbene. Furthermore, we have confirmed that the isomerization of *cis*-stilbene to *trans*-stilbene and that of *cis*-stilbene oxide to *trans*-stilbene oxide do not take place in the absence of O_2 under the same reaction conditions. Thus radical intermediate formed after the attack of the active oxygen may have a long enough lifetime to rotate around the single carbon–carbon bond to undergo isomerization, which is also due to the larger thermodynamical stability of trans-isomer than that of *cis*-isomer. Considering that the induction period is a typical feature of the radical reactions along with the retarded epoxidation when radical scavenger exists and the isomerization of the *cis*-stilbene to *trans*-stilbene during the epoxidation as described above, it can be obviously concluded that the Co_6-CP catalyzed epoxidation of alkene to be the radical chain reaction [12a], [16b].

It is well known that many Co (II) complexes can bind O_2 and activate it to form complexes (e.g. Co(III)-(O_2-)) [17]. Therefore, we proposed that a similar binding of O_2 to the Co (II) sites may also occur in the initial step. The intermidiate Co(III)-(O_2-) species might undergo further reactions to generate an active oxygen species with a radical nature responsible for the epoxidation. To confirm if the oxidation state change of cobalt appears during the reaction, the pristine Co_6-CP and spent one were carefully characterized by UV-vis

(Figure A1.14).

The UV/Vis spectrum of the pristine Co_6-CP is in complete agreement with the coordination environment revealed by X-ray single-crystal structure analysis: each Co(II) is octahedrally coordinated by three OH groups and three oxygen atoms from the carboxylate groups. The broad band at 450 nm is assigned to the transition $^4T_{1g}(P) \rightarrow {}^4T_{1g}(F)$ [18]. The bands at 475 and 510 nm characteristic of high-spin Co^{2+} ions in octahedral coordination, which can be assigned to the transitions $T_{1g}{}^4 \rightarrow {}^2{}_aT_{1g}$ and $^4A_{2g}$ respectively [19].

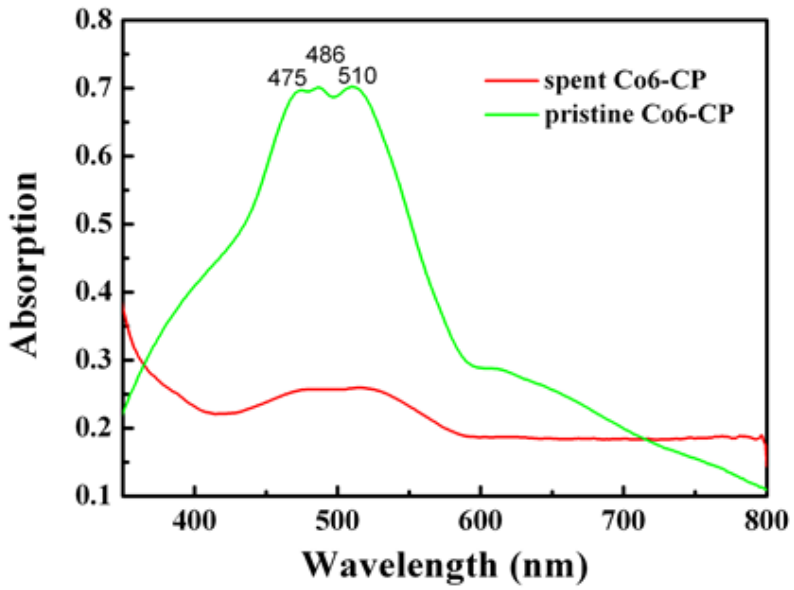

Figure A1.14. The UV-vis spectra of the Co_6-CP: the pristine one (green), the spent one (red).

The band at 486 nm arises from the d→d transition according to Hitchman [20]. For contrast, in the spectra of the spent Co_6-CP, the bands at 450 and 475 nm disappeared while the bands at 486 nm and 510 nm shift slightly to 487 nm

and 515 nm, respectively, indicating a slight change of the coordination between the ligands and cobalt. This small change cannot be detected by the XRD spectrum of the spent Co_6-CP. The adsorption of the Co (III) was negligible, however this isn't sufficient to exclude the possibility of the formation of active Co(III)-(O_2-) specie because of the possible reduction by the reaction mixture. On the other hand, in the transition-metal-catalyzed aerobic epoxidation of alkenes, the concomitant by-product alhydes are often considered to act as sarcrificant reductants to interact with the Co (III)-(O_2^-) specie and result in the formation of peroxide oxygen species. However, it's noteworthy that the Co_6-CP catalyzed epoxidation of *trans*-stilbene gives a very high epoxide selectivity with only trace amount of benzylalhyde as the by-product. Since several works reported the succesful heterogeneous cobalt-catalyzed alkene epoxidation involving the amide solvent, the epoxidation process has been proposed that the the olefin transformation is accompanied by significant DMF oxidation to N-formyl-N-methylformamide (FMF) [21]. Thus, we believe that the epoxidation mechanism involving the solvent (DMF) as co-oxidation may account for the negligible UV-vis spectral change of the spent catalyst. The mechanism was further confirmed by that FMF was detected in after-reaction mixture through GC-MS.

A1.4 Conclusion

In conclusion, we have demonstrated that the new hexaprismane $Co_6(\mu 3\text{-}OH)_6$ cluster based three-dimensional CP can efficiently catalyze the epoxidation of alkenes with molecular oxygen as the oxidant, which is a green route to obtain epoxides. In the catalytic epoxidation of the *trans*-stilbene, the conversion and the selectivity towards the epoxide reached 98.6% and 98.0%, respectively. The average TOF of 22 h^{-1} was obtained for the reaction lasting for 6 hours. The high TOF value and excellent conversion and selectivity are among the most efficient catalytic activities in all reported CP materials. The excellent catalytic behavior for the aerobic epoxidation reaction raises the prospect of using the CP material as green epoxidation catalysts for industrial process.

Reproduced from Dalton Trans., 2014, 43, 2559. with permission from Royal Society of Chemistry.

References

[1] (a) H. M. Neu, M. S. Yusubov, V. V. Zhdankin and V. N. Nemykin, Adv. Synth. Catal. 351 (2009) 3168; (b) J. T. Groves and R. Quinn, J. Am. Chem. Soc. 107 (1985) 5790; (c) S. T. Oyama, Mechanisms in homogeneous and heterogeneous expxidation catalysis, Elsevier B. V., Amsterdam (2008).

[2] (a) G. J. ten Brink, I. W. C. E. Arends and R. A. Sheldon, Science, 2000, 287, 1636; (b) R. A. Sheldon, Chem. Soc. Rev. 41 (2012) 1437; (c) M. Shibuya, Y. Osada, Y. Sasano, M. Tomizawa and Y. Iwabuchi, J. Am. Chem. Soc. 133 (2011) 6497; (d) A. F. Lee, C. V. Ellis, J. N. Naughton, M. A. Newton, C. M. A. Parlett and K. Wilson, J. Am. Chem. Soc.133 (2011) 5724.

[3] (a) H. Tanaka, H. Nishikawa, T. Uchida and T. Katsuki, J. Am. Chem. Soc. 132 (2010) 12034; (b) D. Gajan, K. Guillois, P. Delichere, J. M. Basset, J. P. Candy, V. Caps, C. Coperet, A. Lesage and L. Emsley, J. Am. Chem. Soc. 131 (2009) 14667; (c) C. Aprile, A. Corma, M. E. Domine, H. Garcia and C. Mitchell, J. Catal. 264 (2009) 44; (d) G. Jiang, J. Chen, H. Y. Thu, J. S. Huang, N. Zhu and C. M. Che, Angew. Chem. Int. Ed. 47 (2008) 6638; (e) K. Guillois, L. Burel, A. Tuel and V. Caps, Appl. Catal. A 415 (2012) 1; (f) P. A. Shringarpure and A. Patel, Ind. Eng. Chem. Res. 50 (2011) 9069.

[4] (a) M. Kotobuki, R. Leppelt, D. A. Hansgen, D. Widmann and R. J. Behm, J. Catal. 264 (2009) 67; (b) M. Ojeda and E. Iglesia, Chem. Commun. (2009) 352;

(c) M. Ojeda, B. Z. Zhan and E. Iglesia, J. Catal. 285 (2012) 92; (d) J. H. Huang, T. Akita, J. Faye, T. Fujitani, T. Takei and M. Haruta, Angew. Chem. Int. Ed. 48 (2009) 7862.

[5] (a) M. P. Suh, H. J. Park, T. K. Prasad and D. W. Lim, Chem. Rev. 112 (2012) 782; (b) K. Sumida, D. L. Rogow, J. A. Mason, T. M. McDonald, E. D. Bloch, Z. R. Herm, T. H. Bae and J. R. Long, Chem. Rev. 112 (2012) 724; (c) H. X. Deng, S. Grunder, K. E. Cordova, C. Valente, H. Furukawa, M. Hmadeh, F. Gandara, A. C. Whalley, Z. Liu, S. Asahina, H. Kazumori, M. O'Keeffe, O. Terasaki, J. F. Stoddart and O. M. Yaghi, Science 336 (2012) 1018; (d) X. J. Wang, P. Z. Li, Y. F. Chen, Q. Zhang, H. C. Zhang, X. X. Chan, R. Ganguly, Y. X. Li, J. W. Jiang and Y. L. Zhao, Sci. Rep. 3 (2013) 921.

[6] (a) E. D. Bloch, W. L. Queen, R. Krishna, J. M. Zadrozny, C. M. Brown and J. R. Long, Science 335 (2012) 1606; (b) J. R. Li, J. Sculley and H. C. Zhou, Chem. Rev., 112 (2012) 869; (c) M. C. Das, S. C. Xiang, Z. J. Zhang and B. L. Chen, Angew. Chem. Int. Ed. 50 (2011)10510; (d) S. C. Xiang, Z. J. Zhang, C. G. Zhao, K. L. Hong, X. B. Zhao, D. R. Ding, M. H. Xie, C. D. Wu, M. C. Das, R. Gill, K. M. Thomas and B. L. Chen, Nat. Commun. 2 (2011) 204; (e) J. K. Sun, M. Ji, C. Chen, W. G. Wang, P. Wang, R. P. Chen and J. Zhang, Chem. Commun., 49 (2013) 1624.

[7] (a) L. E. Kreno, K. Leong, O. K. Farha, M. Allendorf, R. P. Van Duyne and J.

T. Hupp, Chem. Rev. 112 (2012) 1105; (b) Y. J. Cui, Y. F. Yue, G. D. Qian and B. L. Chen, Chem. Rev. 112 (2012) 1126; (c) Y. J. Cui, H. Xu, Y. F. Yue, Z. Y. Guo, J. C. Yu, Z. X. Chen, J. K. Gao, Y. Yang, G. D. Qian and B. L. Chen, J. Am. Chem. Soc. 134 (2012) 3979; (d) Y. Kang, F. Wang, J. Zhang and X. H. Bu, J. Am. Chem. Soc. 134 (2012) 17881.

[8] (a) J. C. Yu, Y. J. Cui, C. D. Wu, Y. Yang, Z. Y. Wang, M. O'Keeffe, B. L. Chen and G. D. Qian, Angew. Chem. Int. Ed. 51 (2012) 10542; (b) Q. Huang, J. F. Cai, H. Wu, Y. B. He, B. L. Chen and G. D. Qian, J. Mater. Chem. 22 (2012) 10352; (c) Q. A. Huang, J. C. Yu, J. K. Gao, X. T. Rao, X. L. Yang, Y. J. Cui, C. D. Wu, Z. J. Zhang, S. C. Xiang, B. L. Chen and G. D. Qian, Cryst. Growth Des. 10 (2010) 5291; (d) O. R. Evans and W. B. Lin, Chem. Mater. 13 (2001) 3009; (e) C. Wang, T. Zhang and W. B. Lin, Chem. Rev. 112 (2012) 1084.

[9] (a) J. Gao, K. Ye, M. He, W.-W. Xiong, W. Cao, Z. Y. Lee, Y. Wang, T. Wu, F. Huo, X. liu and Q. Zhang, J. Solid State Chem. 206 (2013) 27; (b) P. Horcajada, R. Gref, T. Baati, P. K. Allan, G. Maurin, P. Couvreur, G. Ferey, R. E. Morris and C. Serre, Chem. Rev. 112 (2012) 1232; (c) A. C. McKinlay, R. E. Morris, P. Horcajada, G. Ferey, R. Gref, P. Couvreur and C. Serre, Angew. Chem. Int. Ed. 49 (2010) 6260; (d) J. Gao, M. He, Z. Y. Lee, W. Cao, W.-W. Xiong, Y. Li, R. Ganguly, T. Wu and Q. Zhang, Dalton Trans. 42 (2013) 11367; (e) P. Horcajada, T. Chalati, C. Serre, B. Gillet, C. Sebrie, T. Baati, J. F. Eubank,

D. Heurtaux, P. Clayette, C. Kreuz, J. S. Chang, Y. K. Hwang, V. Marsaud, P. N. Bories, L. Cynober, S. Gil, G. Ferey, P. Couvreur and R. Gref, Nat. Mater. 9 (2010) 172.

[10] (a) H. L. Jiang and Q. Xu, Chem. Commun., 2011, 47, 3351; (b) M. Yoon, R. Srirambalaji and K. Kim, Chem. Rev. 112 (2012) 1196; (c) J. Lee, O. K. Farha, J. Roberts, K. A. Scheidt, S. T. Nguyen and J. T. Hupp, Chem. Soc. Rev. 38 (2009) 1450; (d) P. Kaur, J. T. Hupp and S. T. Nguyen, Acs Catal. 1 (2011) 819; (e) T. Yang, H. Cui, C. Zhang, L. Zhang and C.-Y. Su, Inorg. Chem. 52 (2013) 9053; (f) X. M. Lin, T. T. Li, L. F. Chen, L. Zhang and C. Y. Su, Dalton Trans. 41 (2012) 10422.

[11] (a) A. Dhakshinamoorthy, M. Alvaro and H. Garcia, Catal. Sci. Technol. 1 (2011) 856; (b) S. H. Cho, B. Q. Ma, S. T. Nguyen, J. T. Hupp and T. E. Albrecht-Schmitt, Chem. Commun. (2006) 2563; (c) O. K. Farha, A. M. Shultz, A. A. Sarjeant, S. T. Nguyen and J. T. Hupp, J. Am. Chem. Soc. 133 (2011) 5652; (d) A. M. Shultz, O. K. Farha, J. T. Hupp and S. T. Nguyen, Chem. Sci. 2 (2011) 686; (e) A. M. Shultz, A. A. Sarjeant, O. K. Farha, J. T. Hupp and S. T. Nguyen, J. Am. Chem. Soc. 133 (2011, 133) 13252; (f) F. J. Song, C. Wang, J. M. Falkowski, L. Q. Ma and W. B. Lin, J. Am. Chem. Soc. 132 (2010) 15390; (g) M. Zheng, Y. Liu, C. Wang, S. B. Liu and W. B. Lin, Chem. Sci. 3 (2012) 2623; (h) M. Tonigold, Y. Lu, B. Bredenkotter, B. Rieger, S. Bahnmuller, J.

Hitzbleck, G. Langstein and D. Volkmer, Angew. Chem. Int. Ed. 48 (2009) 7546.

[12] (a) M. J. Beier, W. Kleist, M. T. Wharmby, R. Kissner, B. Kimmerle, P. A. Wright, J. D. Grunwaldt and A. Baiker, Chem. Eur. J. 18 (2012) 887; (b) S. Bhattacharjee, D. A. Yang and W. S. Ahn, Chem. Commun. 47 (2011) 3637; (c) Y. Nishiyama, Y. Nakagawa and N. Mizuno, Angew. Chem. Int. Ed. 40 (2001) 3639.

[13] (a) R. Chakrabarty, P. Sarmah, B. Saha, S. Chakravorty and B. K. Das, Inorg. Chem. 48 (2009) 6371; (b) R. Chakrabarty, S. J. Bora and B. K. Das, Inorg. Chem., 46 (2007) 9450.

[14] (a) A. Dhakshinamoorthy, M. Alvaro and H. Garcia, J. Catal. 289 (2012) 259; (b) X. Y. Quek, Q. H. Tang, S. Q. Hu and Y. H. Yang, Appl. Catal. A 361 (2009) 130; (c) A. Dhakshinamoorthy, M. Alvaro and H. Garcia, Acs Catal. 1 (2011) 48.

[15] (a) D. Farrusseng, S. Aguado and C. Pinel, Angew. Chem. Int. Ed. 48 (2009) 7502; (b) J. Jiang, R. Li, H. Wang, Y. Zheng, H. Chen and J. Ma, Catal. Lett. 120 (2008) 221; (c) D. Jiang, A. Urakawa, M. Yulikov, T. Mallat, G. Jeschke and A. Baiker, Chem. Eur. J. 15 (2009) 12255; (d) F. Gandara, A. de Andres, B. Gomez-Lor, E. Gutierrez-Puebla, M. Iglesias, M. A. Monge, D. M. Proserpio and N. Snejko, Cryst. Growth Des. 8 (2008) 378; (e) D. Jiang, T.

Mallat, D. M. Meier, A. Urakawa and A. Baiker, J. Catal. 270 (2010) 26; (f) H. Furutachi, S. Fujinami, M. Suzuki and H. Okawa, J. Chem. Soc. Dalton Trans. (1999) 2197; (g) M. D. Hughes, Y. J. Xu, P. Jenkins, P. McMorn, P. Landon, D. I. Enache, A. F. Carley, G. A. Attard, G. J. Hutchings, F. King, E. H. Stitt, P. Johnston, K. Griffin and C. J. Kiely, Nature 437 (2005)1132.

[16] (a) J. Q. Li, B. Marler, H. Kessler, M. Soulard and S. Kallus, Inorg. Chem. 36 (1997) 4697; (b) H. K. Lee, C. H. Lam, S. L. Li, Z. Y. Zhang and T. C. W. Mak, Inorg. Chem. 40 (2001) 4691; (c) D. M. Jiang, A. Urakawa, M. Yulikov, T. Mallat, G. Jeschke and A. Baiker, Chem. Eur. J. 15 (2009) 12255.

[17] (a) E. Giamello, Z. Sojka, M. Che and A. Zecchina, J. Phys. Chem. 90 (1986) 6084; (b) C. Comuzzi, A. Melchior, P. Polese, R. Portanova and M. Tolazzi, Inorg. Chem. 42 (2003) 8214.

[18] L. Poul, N. Jouini and F. Fievet, Chem. Mater. 12 (2000) 3123

[19] (a) A. A. Verberckmoes, B. M. Weckhuysen and R. A. Schoonheydt, Micropor. Mesopor. Mat. 22 (1998) 165; (b) Y. Okamoto, K. Nagata, T. Adachi, T. Imanaka, K. Inamura and T. Takyu, J. Phys. Chem. 95 (1991) 310; (c) M. G. F. da Silva, Mater. Res. Bull. 34 (1999) 2061.

[20] M. A. Hitchman, Inorg. Chem. 16 (1977) 1985.

[21] Z. Opre, T. Mallat and A. Baiker,J. Catal.245 (2007) 482.

A.2 Journal publications and conference presentations

Journal publications

1. Linlu Bai, Kaixin Li, Xinli Jia, Jongmin Lee*, Yanhui Yang*, Catalytic epoxidation of *cis*-cyclooctene over vanadium-exchanged faujasite zeolite catalyst with ionic liquid as co-solvent (submited).
2. Kaixin Li, Linlu Bai, Xinli Jia, CL Chen, SH Mushrif*, Yanhui Yang*, Highly efficient and easily recyclable ionic liquid-based polyoxometalate catalysts for bio-lubricant production: Experimental and theoretical studies (submited).
3. Hai-Sheng Lu, Linlu Bai (co-first), Wei-Wei Xiong, Peizhou Li, Junfeng Ding, Guodong Zhang, Tom Wu, Yanli Zhao, Jongmin Lee, Yanhui Yang*, Baoyou Geng*, Qichun Zhang*, Surfactant Media to Grow New Crystalline Cobalt-1, 3, 5-Benzenetricarboxylate Metal-Organic Frameworks, Inorganic Chemistry, 2014, 53(16), 8529–8537.

4. Kaixin Li, Linlu Bai, PN Amaniampong, Xinli Jia, Jongmin Lee*, Yanhui Yang*, One-pot production of bio-derived chemicals from renewable resources: Transformation of cellobiose to formic acid and levulinic acid over ionic liquid-based polyoxometalate hybrids, ChemsusChem, doi: 10.1002/cssc.201402157.

5. Junkuo Gao, Linlu Bai (co-first), Qian Zhang, Yongxin Li, Ganguly Rakesh, Jong-Min Lee, Yanhui Yang*, Qichun Zhang*, $Co_6(\mu_3\text{-}OH)_6$ cluster based coordination polymer as an effective heterogeneous catalyst for aerobic epoxidation of alkenes" Dalton Transactions, 2014, 43 (6), 2559 - 2565.
6. Kaixin Li, Linlu Bai, Yanhui Yang*, Xinli Jia*, Kinetics of ionic liquid-heteropolyanion salts catalyzed transesterification of oleic acid methyl ester: a study by sequential method, Catalysis Today, 2014, 233, 155-161;
7. Yuanting Chen, Linlu Bai, Chunmei Zhou, Jong-Min Lee, Yanhui Yang*, Palladium-catalyzed aerobic oxidation of 1-phenylethanol in an ionic liquid additive, Chemical Communications, 2011, 47(22), 6452-6454.

Conference presentations

1. Linlu Bai, Yanhui Yang*. Application of Ionic liquid in the Heterogeneous Catalytic Oxidation. *The 16th National Conference on Catalysis of China (16th NCC)*, Shenyang, China, Dec 2012 (Oral presentation).
2. Linlu Bai, Yanhui Yang*. Application of Ionic liquid in the alcohol oxidation and alkeneepoxidaiton, *5th Singapore Catalysis Forum*, Singapore, May 2012 (Poster presentation)